Universidade de Aveiro Departamento de Química
2017

Gabriela Vilaça Cruz Cerqueira dos Santos

Qual o papel das sinucleínas na neurodegeneração da retina?

Bringing light to darkness: What is the role of synucleins in retinal neurodegeneration?

Gabriela Vilaça Cruz Cerqueira dos Santos

Qual o papel das sinucleínas na neurodegeneração da retina?

Bringing light to darkness: What is the role of synucleins in retinal neurodegeneration?

Dissertação apresentada à Universidade de Aveiro para cumprimento dos requisitos necessários à obtenção do grau de Mestre em Biotecnologia, ramo de Biotecnologia Molecular, realizada sob a orientação científica da Doutora Sandra Vieira, Professora Auxiliar do Departamento de Ciências Médicas da Universidade de Aveiro e coorientação da Doutora Sandra Tenreiro e Doutora Gabriela Silva, do CEDOC Chronic Diseases FCM Nova.

This work was funded by iNOVA4Health Research Unit (UID/Multi/04462/2013), which is cofounded by Fundação para a Ciência e Tecnologia / Ministério da Ciência e do Ensino Superior, through national funds and by FEDER under the PT2020 Partnership Agreement.

Juri members

Presidente	Professor Doutor José António Teixeira Lopes da Silva Professor Auxiliar, Universidade de Aveiro
Vogal **Orientador**	Doutora Sandra Isabel Nogueira Tenreiro Bolseira de Investigação, Universidade Nova de Lisboa
Vogal **Arguente Principal**	Doutora Raquel Sarabando Santiago Bolseira de Investigação, Faculdade de Medicina da Universidade de Coimbra

Aknowledgments

I would like to thank the following people, without whom this would not have been possible. I am such a lucky girl for having you.

To my supervisor at University of Aveiro, **Doctor Sandra Vieira**. Thank you for accepting me with such short notice and for never letting me down. Even far away, you were able to mentor and help me with my every need.

To **Doctor Sandra Tenreiro,** how should I even thank you? For the warmest welcome one could expect, for all the guidance, support, trust, kindness and friendship you shared during this year. I could not have hoped for a better supervisor. From the bottom of my heart, thank you. **Doctor Gabriela Silva**, thank you for the amazing opportunity and for always sparing some of your very busy time whenever I needed help. To **Doctor Hugo Vicente Miranda**, thank you for all the support that came in many forms: suggestions, encouragement and cake. To **CEDOC - NOVA Medical School**, as an institution and as a community, thank you for for making me feel at home in such a motivational environment. A special thanks to **Doctor Telmo Pereira** and **Doctor Ana Farinho**, for all the patience and guidance, even after hours.

To **Morsos**. How should I even begin? You made Lisboa my home. To **Ana**, aka Avó Anita, aka Grande Bastarda, aka Miss Panqueca. I am already your favourite, so everything I say here you know it comes from the heart. To thank you is not good enough. During this year you became by role model, my friend, my family. I know just how tough, scary and mean you try to be (specially when you have a “colher de pau”. That damn thing hurts!) but you know what? You have the biggest, sweetest heart! Thank you for every phone call, every advice, every “raspanete”, every kind word. For showing me what kind of scientist and woman I want to be. For all the food and all the care, every special moment you made even more so, and for being there every single time I needed you. I want you to know that I admire and love you, with all my heart. To **Joana**, aka FlowJo, aka rainha da baba, aka roomie, aka half of my other mother, aka second-best-at-uno-stop-and-buzz. You know how cheesy this is going to be. Thank you being there from day one. For making our house a home, for reminding me how it feels like to laugh until you cry, for lighting up my world. For every time you have listened to my crazy dilemmas, every “beijinho na testa” and my special song. Thank you for every time you have shared a shoulder, a sock, a smile, a tear, a joy, even your drawling. I sure as hell will miss that. You are one of a kind, did you know that? And I know that not even the distance will keep us apart. I mean, Hakuna Makasa is forever right? Btw, thank you for every slap as well. I am sure that when you come back it will have stopped burning. Please don’t take too long. To **Bárbara**, aka Babs, aka the other half of my other mother. You have no idea how much you have warmed up my heart all this time with your songs, your amazing humour, the happiest and sweetest hug every time you saw me even if we have only been apart a day – it felt damn long! Thank you for every time you have cheered me up, for protecting against the world, for making sure I am never alone because you will be there with your camera recording the whole damn thing! You have coloured up my world. Thank you for always doing your best to make us feel special, for every

surprise, every “good-night kiss”. Please stop hurting yourself ok? I would like to keep you in my life a little longer, like forever! (apply an “awwww” here!). To **João**, aka morsito, aka Johny boy, my partner and mentor. Thank you for all the late nights and sunrises at the confocal that you made easier, for walking me home every single time, for teaching me that “mekié?” is not a question to be asked and that statistics can be cool when Whitney Houston is nearby. Thank you for all the patience, for everything you have taught me and for always being there for me, even though you are far away. To **Luis**, aka Lulu Pastelão. It took you only a week to get from colleague to friend. Thank you for all the inappropriate jokes, for taking forever to enter that huge fortress that you call “lunch box”, taking twice the time to eat, for ears dropping in every conversation and making sure your opinion is well understood. Above all, thank you for your kind heart, for listening, worrying and helping me so I could do a thousand things without panicking. To **Diogo Bitoque**, aka my dear Padawan. Thank you for always sparing 5 minutes of your very busy days to answer my million questions, for being my number one supplier (lab stuff of course!) and for one amazing prank war. Most importantly, thank you for sharing the amazing Star Wars world with me. You have made it even more amazing than it already was. Thank you for your everyday support and friendship. To **Rute Araujo**, you were able to make me feel strong and comfortable in the very beginning when everything was huge and scary and to calm me down at the very end. I will never forget how much you helped me taking my first steps. To **Daniela Santos**. In such a short time you became one of my favourite people at CEDOC. Thank you for all the times you have teamed up with me and defended me against the dark lord Bitoque. For all the encouragement and fun trips to Biotério. Sometimes you try to be mean and not lend me the material I need. But don’t bother. It really doesn’t suit you and I know you like me as much as I like you!

To all my friends in Peniche, with whom I started this whole adventure. To my dear **Claudia**, for every time you were my strength and warmed my heart. To **Pity**, for her very sweet being and the way she would bring light to the room. To **Bia**, for helping me to get out of my little shell with that amazing smile of hers. To **Paulo**, I better keep things to myself. Just so you know, you were one of the most special people I have met in my whole life. To **Carlinha**, one of the best people I know. Thank you for never leaving my side. For holding my hand when I needed, for keeping me strong.

To the best people Aveiro could have! **Inês, Mário and Simões**. If it weren’t for you I would not be here right now. Thank you for the incomparable friendship.

To **Raquelinha**, the other half of my orange, the salt in my potatoes, my favourite Capricorn, my partner in crime. I would have to right a whole thesis about our many adventures and it would still not be enough. You were there through my best and worst times and never left my side. From a night by the bathroom door, two crashed cars, hospital beds, several bottles of Rosé as well. I can honestly say that you are my favourite person in the whole planet. Thank you for this amazing adventure. “Uma amizade, uma família”.

To **Rui**. Where should I begin? Our story goes way back. I think I can say we have been through everything together. Ever since the beginning of time you were my safehouse, my home. There is so much to thank you for. For all the encouragement, all the late phone calls, for making distance

closer, for making me believe that I could do everything I set my mind on, for knowing that dessert is always the answer, for knowing that the best castle I could wish for is one made of “crepes”. For all the timings, all the words that didn’t need to be spoken, for every time you chose my world over yours even if you didn’t quite understand it. For being the half of a whole. I love you. And I always will.

Finally, and most importantly, to my family. To **my parents**, Gabriel and Felicidade, words aren’t enough. Everything I am is because of you. To my mother, thank you for being the best listener, my number one adviser, the one that turns our house into a home, that drives my demons away, that keeps my heart in a safe place. You are the strongest Woman I know and when I grow up, I want to be just like you. To my father, the man of my life, my hero. You gave me this world and the next one and never asked for anything in return. You taught me how to fly without ever being afraid, because you would always be there to catch me. “Nunca te vou deixar cair”, wasn’t it? Well let me tell you, I was never afraid. All because of you. To my **little brother**, Pedro. You are the most amazing person I know. Thank you for being my protector, my best friend, my superhero. Every hug, every laugh and all the love you’ve shared made me stronger. I don’t know if I chose you or if you chose me, but who ever did, did not think of our poor parents! I love you. To “vovó” Julieta.You have walked me to work every single day and every day you told me how much you loved me and how proud you were. Thank you for every letter, every hidden icecream, every story we’ve shared. Thank you for warming both my feet and my heart. Saying “I love you” will never be enough. To my dear avó Amélia. You have showed me what kind of woman I want to be. The one who conquers to world. You never seem to be afraid of anything, a neither will I. Thank you for always taking care of me in your own sweet way. I love you more than I can say. To the rest of my family, thank you to each and everyone of you for making me who I am. For all the love, all the care.

“Don’t tell me the sky is the limit, when there are footprints on the moon”

- Paul Brandt

Resumo

A retinopatia diabética é uma complicação progressiva da diabetes e é a principal causa de cegueira em adultos. Apesar de ter sido, por muitos anos, considerada uma doença microvascular, estudos recentes sugerem que há neurodegeneração da retina antes de ocorrerem danos a esse nível.

A família das sinucleínas é composta por três proteínas que partilham uma grande homologia, alfa-sinucleína (aSyn), beta-sinucleína (bSyn) e gama-sinucleína (gSyn), que estão associadas a doenças neurodegenerativas, tal como a doença de Parkinson. A agregação das sinucleínas foi descrita em pacientes com outras doenças neurodegenerativas, assim como ocorrendo com o envelhecimento. Estas proteínas são também expressas na retina, mas tanto a sua função fisiológica como possíveis papéis patológicos estão por estudar neste contexto.

Vários estudos sugerem um mecanismo de neurodegeneração comum entre a Doença de Parkinson e a Retinopatia Diabética. Nomeadamente, o facto da diabetes ser um fator de risco para a Doença de Parkinson; o facto da Diabetes promover a toxicidade e agregação da aSyn devido à possível glicação da mesma; O facto de L-DOPA levar à recuperação de danos visuais em ratinhos modelo da Retinopatia Diabética e drogas anti-diabéticas tecerem um efeito neuroprotetor em neurónios nigrostriatais e da retina em modelos de ratinho da Doença de Parkinson. Para além disso, o ambiente diabético do olho, onde se sabe ocorrer stress oxidativo, inflamação, aumento dos níveis de AGEs e debilitação na mitocôndria, apresenta semelhanças extraordinárias com elementos que se sabe estarem envolvidos na agregação da aSyn no cérebro de doentes de Parkinson.

O objetivo deste trabalho é estabelecer uma correlação entre o perfil das sinucleínas na retina e a progressão da retinopatia diabética, num modelo de ratinho diabético ($Ins2^{Akita}$) e em controlos, em vários estadios de desenvolvimento da doença.

Pretende-se caracterizar o padrão de distribuição das sinucleínas nas várias populações neuronais da retina de ratinhos $Ins2^{Akita}$ e 'Wild Type', por imunohistoquímica. Os níveis de expressão das proteínas sinucleínas vão ser também avaliados nestes mesmos animais por western-blot.

Os resultados obtidos indicam que a aSyn e a bSyn se encontram distribuídas pela camada plexiform interna (IPL), nos terminais pré-sinápticos das células amácrinas, assim como em corpos celulares da camada nuclear interna (INL).

Palavras-chave:

Retinopatia Diabética, Retina, Envelhecimento, Sinucleínas, $Ins2^{Akita}$

Para além disso, foi possível localizar a aSyn nas células amácrinas dopaminérgicas, considerando-se a possibilidade da aSyn levar à degeneração destas células com o envelhecimento, tendo em conta a sua co-localização e a diminuição das células dopaminérgicas nas retinas de ratinhos WT ao longo do envelhecimento. O aumento de co-localização entre a aSyn e a Syntaxina 1A na IPL pode sugerir alterações a nível das sinapses destas proteínas.

A bSyn encontra-se localizada em células bipolares na INL e a gSyn em células horizontais na INL e em corpos celulares da camada de células ganglionares (GCL). Outra observação interessante é o facto de ocorrer co-localização entre a aSyn e bSyn, e aSyn e gSyn em corpos celulares da INL. Um aumento da co-localização entre a aSyn e a bSyn nas células amácrinas poderá levar a danos nestas células devido a um aumento de toxicidade da aSyn e bSyn como descrito em levedura, indicando um possível papel destas proteínas na retinopatia diabética.

Estes resultados são promissores e podem sugerir alterações importantes destas proteínas no contexto da retinopatia diabética, mas especialmente com o envelhecimento. Apesar da função exata das sinucleínas na visão e na retinopatia diabética permanece por esclarecer, este trabalho contribuiu para o conhecimento da distribuição das sinucleínas na retina, assim como para a sua potencial contribuição no envelhecimento.

Abstract

Diabetic retinopathy is a progressive complication of diabetes and the leading cause of irreversible vision in adults. While it is considered a microvascular pathology, recent evidence suggests that neurodegeneration is an earlier event in diabetic retinopathy.

The synuclein family is composed of three proteins that share high homology, alpha-synuclein (aSyn), beta-synuclein (bSyn) and gamma-synuclein (gSyn), which have been associated with neurodegenerative diseases, such as Parkinson's disease. Aggregation of the synucleins was described in other neurodegenerative disorders as well as with ageing. These proteins are also expressed in the retina, but both its physiological function and its pathologic role are yet to be described in this context.

Several indications point to a shared mechanism of neurodegeneration in PD and DR. Namely, diabetes being a risk factor for Parkinson's disease; diabetes promoting aSyn toxicity and aggregation due to aSyn glycation; L-DOPA being observed to rescue visual impairment in a DR mouse model, and an antidiabetic drug demonstrating to have a neuroprotective effect on retinal and nigrostriatal neurons in a PD mouse model. Moreover, the environment of the diabetic eye where it is known to occur oxidative stress, inflammation, increased levels of AGE and mitochondrial impairment, has remarkable similarities with the features that are known to be involved in aSyn aggregation in the brain of PD patients.

The aim of this study is to establish a correlation between the retina profile of the synucleins and the progression of diabetic retinopathy, using diabetic model mice ($Ins2^{Akita}$) as well as Wild Type controls in different stages of the disease. We intended to characterize the distribution pattern of these proteins in the different neuronal populations of the retina in $Ins2^{Akita}$ and wild type mice, through immunohistochemistry. The synucleins proteins expression levels were also assessed in these animals by western blot techniques.

Our results show that aSyn and bSyn are pre-synaptic proteins in the Inner Plexiform Layer of the retina, and are localized in amacrine cells pre-synaptic terminals but also in amacrine cell bodies in the Inner Nuclear Layer (INL). aSyn is further localized in the dopaminergic amacrine cells, where aSyn might be leading to dopaminergic amacrine cells degeneration with ageing, considering its localization in those cells and a loss of dopaminergic amacrine cells.

Keywords: Diabetic Retinopathy, ageing, retina, synucleins, $Ins2^{Akita}$.

Moreover, the increased colocalization between aSyn and Syntaxin 1A in the might suggest alterations in amacrine cell synapses.

bSyn was found to be localized in bipolar cells in the INL and gSyn in horizontal cells in the INL but also in the Ganglion Cell Layer.

Another interesting observation is that co-localization between aSyn with bSyn and aSyn with gSyn might occur in the INL. The increased colocalization between aSyn and bSyn in amacrine cells of 9 months old $Ins2^{Akita}$ may lead to damages to amacrine cells due to exacerbation of cytotoxicity by aSyn and bSyn, similar to what is described in yeast, indicating that these proteins' colocalization may play a part in DR.

These results are promising and may suggest important alterations in these proteins, especially in ageing. Although the exact role of the synucleins in vision and in DR pathophysiology remains unclear, this work contributed to furthering the knowledge about the synucleins in the retina, by elucidating their special distribution in normal and diabetic retina, providing insights on their potential contribution in ageing.

Table of contents

Abbreviations

AD	Alzheimer's Disease
AGEs	Advanced Glycation Products
aSyn	Alpha-synuclein
ALP	Autophagy/Lysosomal Pathway
ATP	Adenosine Triphosphate
Bax	Bcl-2-associated X protein
BCA	Bicinchoninic Acid
BSA	Bovine Serum Albumin
bSyn	Beta-synuclein
CNS	Central Nervous System
CT	Camera Temperature
DAPI	4',6-diamidino-2-phenylindole
DDC	Dopa Decarboxilase
DLB	Dementia with Lewy Bodies
DM	Diabetes Mellitus
DME	Diabetic Macular Edema
DO	Dopamine
DR	Diabetic retinopathy
ER	Endoplasmic Reticulum
ERG	Eletroretinography
FELASA	Federation of European Laboratory Animal Science Associations)
GABA	γ-aminobutyric acid
GCL	Ganglion Cell Layer
GLUT2	Glucose Transporter 2
gSyn	Gamma-synuclein
IHC	Immunohistochemistry
INL	Inner Nuclear Layer
IPL	Inner Plexiform Layer
L-DOPA	L-3,4-dihydroxyphenylalanine
LB	Lewy bodies
MODY	Maturity-Onset Diabetes of the Young
MSA	Multiple System Atrophy
mtDNA	Mitochondrial DNA
NAC	Non-B-amyloid component
NPDR	Nonproliferative Diabetic Retinopathy
NSF	N-enthylmaleimide-Sensitive Factor
OCT	Optimal Cutting Temperature

O/N	Over night
ONL	Outer Nuclear Layer
OPL	Outer Plexiform Layer
OT	Object temperature
PBS	Phosphate-buffered saline
PBS-T	PBS-Tritton
PFA	Paraformaldehyde
PD	Parkinson's disease
PDD	Parkinson's Disease Dementia
PDR	Proliferative Diabetic Retinopathy
PKC	Protein kinase C
PNS	Peripheral Nervous System
REM	Rapid Eye Movement
ROS	Reactive oxygen species
RPE	Retinal Pigment Epithelium
RT	Room Temperature
SDS	Sodium Dodecyl Sulfate
SNARE	NSF-Attatchment Protein Receptor
SNAP-25	SynaptopSome-Associated Protein
STZ	Streptozotocin
syn	Synucleins
TBS	Tris-Buffered Saline
TBS-T	Tris-Buffered Saline – Tween 20
TFAM	Mitochondrial Transcription Factor A
TH	Tyrosine Hydroxylase
TUNEL	Terminal deoxynucleiotidyl transferase nick and labeling
UPS	Ubiquitin Proteasome System
VAMP 2	Vesicle-Associated Membrane Protein 2
VEGF	Anti-Vascular Endothelial Growth Factor
WB	Western Blot
WT	Wild type

Index of figures

Index of tables

1. Introduction

1.1. Diabetes mellitus

Diabetes mellitus (DM) is a chronic disease characterised by hyperglycaemia that is becoming a global issue mainly due to changes in people's alimentary and exercise habits as well as ageing. The World Health Organization estimated that the number of people with diabetes has risen from 108 million in 1980 to 422 million in 2014, mostly due to sedentary lifestyles, lack of physical activity and obesity (1).

Diabetes can be classically classified in type 1 DM and type 2 DM but there is also gestational diabetes, Latent Autoimmune Diabetes in Adults and Maturity-Onset Diabetes of the Young (MODY). Type 1 DM, known as the insulin-dependent type, is characterised by the deficient insulin production due to the destruction of the islets of Langerhans in the pancreas and requires insulin administration. Type 2 DM, on the other hand, is the most common type and results from hyperglycaemia and insulin resistance (2).

DM is responsible for significant macro- and microvascular complications. Macrovascular complications include cardiovascular disease, stroke, and peripheral vascular disease. Microvascular complications include damage in the nervous and renal systems (neuropathy and nephropathy, respectively) and eye damage including increased risk for glaucoma, cataracts and, the most threatening ocular implication, diabetic retinopathy (DR) (3,4).

1.2. Diabetic retinopathy

Diabetic retinopathy is a progressive complication of diabetes and the leading cause of irreversible vision loss in working age adults (20-70 years old) (5).

The onset of diabetic complications such as DR is directly related to the duration of diabetes and the quality of glycaemic control (6). Since it may be asymptomatic until vision loss occurs and its diagnostics is based on direct ophthalmoscopy analysis or medical history upon complaint, DR is usually late diagnosed. However by 20–25 years of diabetes almost 90% of patients present some forms of retinopathy (7,8).

1.2.1. Proliferative and non-proliferative DR

Diabetic retinopathy can be classified into two stages, according to its severity: a less-severe form is non proliferative DR (NPDR) and a severe-form proliferative diabetic retinopathy (PDR) (2).

Non proliferative DR shows as early signs microaneurisms that arise from the retinal capillaries, leading to haemorrhages caused by the release of erythrocytes from said microaneurisms (9). These can be visible through the observation of some leakage by fundus photography, documenting the retina, and fluorescein angiography, a technique that examines the circulation of the retina and the choroid using a fluorescent dye and special camera (10).

Proliferative DR, which may occur up to 50% of type 1 diabetes patients and up to 10% of type 2 diabetes ones (11,12), is characterized by further ischemia resulting in the formation of new blood vessels that, untreated, extend into the vitreous cavity of the eye with the possibility of haemorrhage and consequent tractional retinal detachment. Furthermore, the formation of new blood vessels in other chambers of the eye may lead to block the outflow of the aqueous humour causing neovascular glaucoma. Altogether, these events lead to vision loss (13,14).

Both non proliferative and proliferative DR can lead to another change: the diabetic macular edema (DME), that can affect up to 20% of type 1 diabetes patients and up to 25% of patients with type 2 diabetes (15). It is characterized by increased vascular permeability and breakdown of the blood-retinal barrier, culminating in leakage from plasma from the macula, responsible for the major part of visual function, causing the swelling of the central retina. This event is followed by the formation of exudates from deposition of the lipid and lipoprotein content from the plasma, disrupting the light path in the macula and, ultimately, vision loss (9,13,15).

1.2.2. Retinal microvascular dysfunction

Microvasculature of the retina is considered by many the main site of pathology associated with DR. Although its biochemical mechanisms are not fully elucidated, it is known that continuous exposure of the retina to hyperglycaemia leads to metabolic abnormalities, including the activation of several pathways, accumulation of advanced glycation end products (AGEs), protein kinase C (PKC) activation and increase in oxidative stress (16,17).

In DR, increased AGEs and PKC are reported within retinal capillaries. Increased AGEs are associated with increased inflammation while PKC activation leads to increased vascular permeability, alterations on blood flow and stimulation of neovascularization due to its relation with the vascular endothelial factor (VEGF) which is suspected to be a primary peon in the induction of vascularization in diabetes (Fig. 1.1) (18,19). Metabolic abnormalities combined with auto-oxidation of glucose and an impaired antioxidant defence system result in the production of reactive oxygen species (ROS) (Fig. 1.1) (20).

Under pathological conditions, the excessive bioavailability of ROS, as a result of increased production and/or decreased removal of ROS, will further increase the production of PKC and damage proteins, lipids and DNA (21). Mitochondria and its DNA (mtDNA) are one of the targets of its damaging effects (20,22).

ROS, by activating matrix metalloproteinases, damages the mitochondrial membrane changing its permeability allowing apoptotic induced factors to be released in the cytosol and subsequently activate the apoptosis machinery (Fig. 1.1). Thereby, retinal capillary and non-capillary cells undergo accelerated apoptosis. In early stages of DR, pericytes start to undergo accelerated death which is followed by the loss of endothelial cells resulting in pericyte ghosts, acellular capillaries and microaneurysms (23). Moreover, damages to the mtDNA impairs its transcription, further interfering with its homeostasis and compromising the mitochondrial machinery, namely the electron transport chain resulting in an increased ROS production (24).

Overall, microvascular complications result in an increase of vascular permeability, alterations of blood flow and neovascularization, which are the hallmarks of DR. This leads to edema, ocular haemorrhage and eventual retinal vessel closure (16,22).

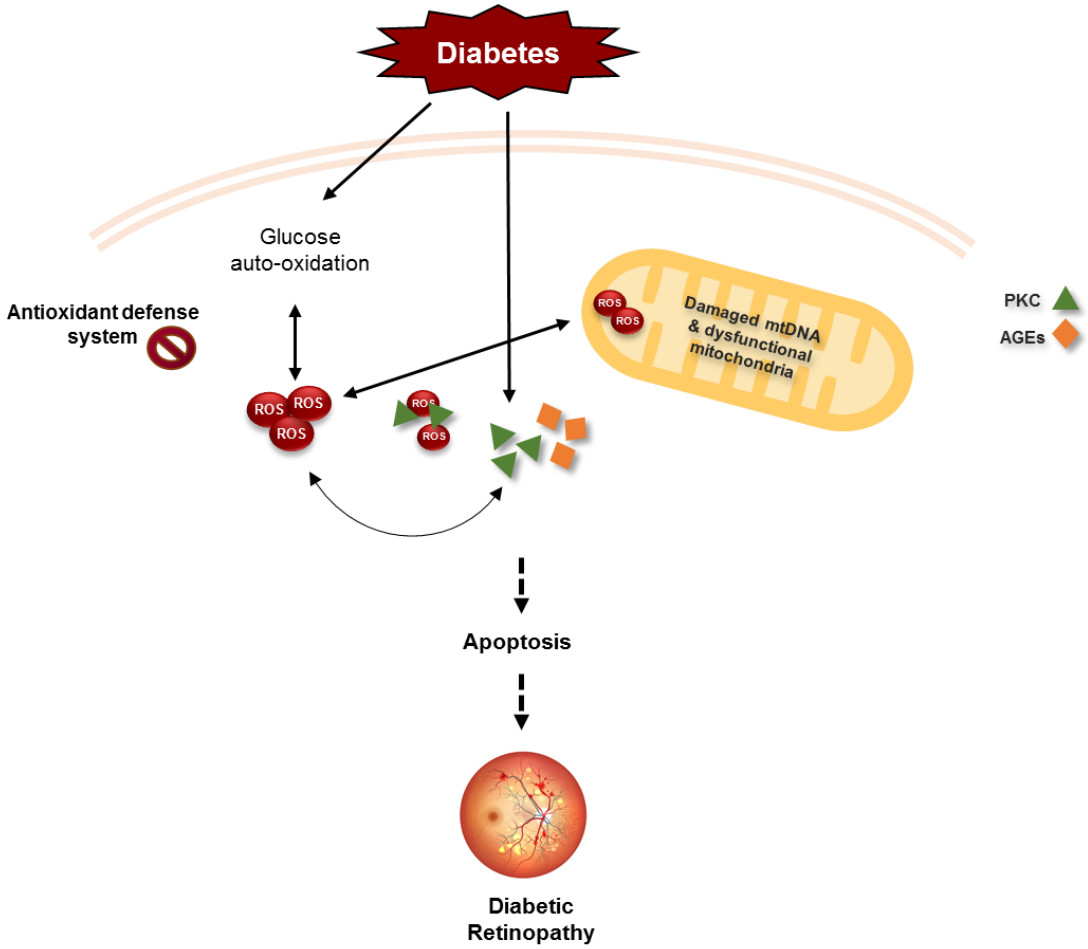

Fig. 1.1. Common intersecting pathways underlying DR microvascular complications. Diabetic environment increases the production of ROS and also metabolic abnormalities leading to capillary cell apoptosis and ultimately development of diabetic retinopathy. PKC, AGEs and the production of inflammatory mediators feed the metabolic abnormalities and continuous ROS production as well as oxidative damage to mitochondria, accelerating apoptosis. Adapted from (17).

1.2.3. Neurodegeneration in DR

However, even though DR was for many years seen as solely a microvascular disease caused by significant alterations in the retinal vasculature and blood barrier of the retina, recent evidence suggests that neurodegeneration occurs prior the microvascular complication onset, through deficits in the neural retina (5,26).

It is thought that alteration in the levels of various neurodegenerative metabolites' and neurodegenerative factors as well as a decrease in neurotrophic factors damage the retinal neurons in early stages of the disease (27).

Apoptosis markers were identified in higher levels in diabetic retinas. Increased levels of pro-apoptotic protein Bax (Bcl-2-associated X protein) was found in diabetic retinas by several studies (28). Other resesarchers have shown a correlation between TUNEL (terminal deoxynucleiotidyl transferase nick end labeling)-positive cells and increased Caspase 3 levels in neuronal retinas of diabetic rats (29–31). In recent studies, clinical tools like multifocal and flash electroretinography (ERG), contrast sensitivity, color vision and short-wavelength automated perimetry indicate that neurons are vulnerable to damage, shortly after the onset of diabetes (32). Degeneration of retinal neurons has been reported on amacrine and ganglion cells (33,34). Studies in animal models further show photoreceptors' death (35,36) and abnormalities in horizontal and bipolar synaptic terminals (36,37).

In the retina, glia and neurons share a close interaction with retinal vasculature to maintain a normal retinal function. It has been shown that apoptosis of neurons and activation of glial cells may cause oxidative stress and initiate vasoregretion (38), here suggesting a link between neurodegeneration and microvascular changes in diabetic retinopathy (39,40)

1.2.4. Prevention and treatment methods

The prevention methods for DR combine glucose and blood pressure control to normal levels, considerably retarding the progression of the disease. Further prevention and treatment methods usually apply to more severe forms of DR, relying on retinal laser photocoagulation to slow the formation of new vessels and the progression of vision loss (41). More advanced retinal disease, such as late stages of proliferative DR and macular edema, that combine vitreous haemorrhages and detachment of the retina upon new vessel formation, benefits from intravitreal anti-VEGF injections, vitrectomy, focal laser and argon laser treatment (42,43).

1.3. The retina functional architecture

The retina is a layered structure that includes both sensory neurons and intricate neural circuits that respond to light and perform the first stages of image processing before traveling through the optic nerve into the brain (44).

It is composed of vascular cells (pericytes and endothelial cells), microglia, macro glial cells (Müller cells, astrocytes) and neurons (17).

There are, essentially, five major neuronal cell classes distributed between the nuclear layers of the retina. Rod and Cone photoreceptors are integrated in the Outer Nuclear Layer (ONL) followed by horizontal, bipolar and amacrine cells that share the Inner Nuclear Layer (INL) and ganglion cells that, along with a subtype of amacrine cells, is found in the Ganglion Cell Layer (GCL) (Fig. 1.2). All cells communicate with each other electrically, through gap junctions and chemically, using neurotransmitters (45,46).

In between the nuclear layers, the Outer Plexiform Layer (OPL) and the Inner Plexiform Layer (IPL) assure the communication between neuronal cell populations of different layers through

synapses (Fig. 1.2). The plexiform layers can also be divided into strata, depending on the connections that take place in each one. The IPL is divided in 5 strata, whereas the OPL is traditionally divided in 3 (45). Strata 1 and 2 of the IPL comprise synapses between OFF-bipolar cells and retinal ganglion and amacrine cells as strata 3-5 contain synaptic connections between ON-bipolar cells and retinal ganglion and amacrine cell bodies (47).

ON- and OFF-type cells are so called depending on the stimulation. ON-cells are stimulated by a spot of light brighter than the background, occurring an ON-discharge. When the cells are stimulated by light darker than the background, OFF-cells are activated and an OFF-discharge occurs (47,48).

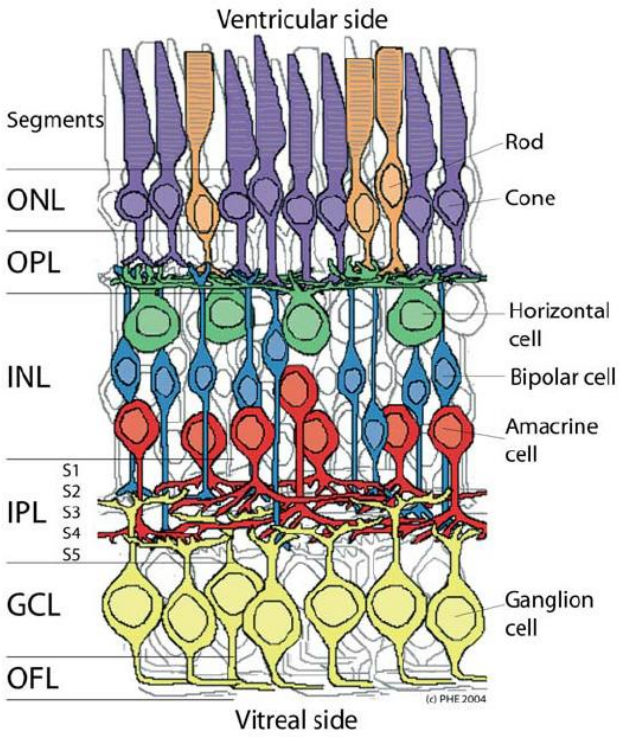

Fig. 1.2. Schematic enlargement of the neuronal retina. Outer Nuclear Layer (ONL), containing the photoreceptors rodes and cones; the Inner Nuclear Layer (INL), containing the horizontal, bipolar and amacrine cells and the Ganglion Cell Layer (GCL) containing the ganglion cells; and the plexiform layers: Outer Plexiform Layer (OPL), containing the presynaptic terminals of the photoreceptors, bipolar and horizontal cells and Inner Plexiform Layer (IPL), containing the presynaptic terminals of amacrine, bipolar and ganglion cell bodies (in Webvision: Simple Anatomy of the Retina).

1.3.1. Processing of visual information

Photoreceptors rods and cones are the first response to photons each having specific roles in the retina. Rods show an elevated sensitivity to light and are therefore responsible for dim-light vision. Cones, although less sensitive to light than rods, exhibit a higher sensitivity to a specific light wave consequently engaging bright-light, high acuity color vision (49,50).

The processing of the visual information begins with the conversion of light into depolarizing spikes of neurotransmitter glutamate by photoreceptors into glutaminergic ON-center bipolar cells in

the OPL and hyperpolarizing spikes into OFF-center bipolar cells, mediated by horizontal cells (Fig. 1.3) (47,50).

Bipolar cells can be divided into two major classes, rod and cone bipolar cells and further divided into depolarizing bipolar cells (the ON-type) and hyperpolarizing bipolar cells (the OFF-type). Rod bipolar cells are ON bipolar cells and contact primarily with rod photoreceptors, whereas cone bipolar cells, which can be either ON- or OFF-type, mostly synapse with cone photoreceptors. Moreover, ON- and OFF-bipolar cells also contact with retinal ganglion and amacrine cells within the IPL (Fig. 1.3) (51,52).

When depolarized, bipolar cells release glutamate into ganglion cells but when hyperpolarized they decrease its release what increases or decreases ganglion cell firing rate, respectively (Fig. 1.3) (52).

Regarding the amacrine cells, there are more than 30 known types of these, that communicate with different neurons using different neurotransmitter, playing several roles in the retina (53). When responsible for the excitation of ganglion cells, they act in two ways, both relying on γ-aminobutyric acid (GABA) and glycine neurotransmitters: 1) direct feedforward inhibition from amacrine cells onto retinal ganglion cells, or 2) feedback inhibition, where amacrine cells are intermediates between bipolar and ganglion cells. In the end, the retinal ganglion cells send the message to the brain (54,55).

Amacrine cells are classified by the width of their connection and layer of the IPL they are in and also by the neurotransmitter they use. The AII amacrine cells are the most studied amacrine cells and participate predominantly in the vertical flow of information in the photoreceptor-bipolar-ganglion cell chain, transmitting both rod and cone-driven signals within the ON- and OFF-pathways (54,56). Other examples include the A8, A17, A19 and A20 amacrine cells, intermediates in several neuronal cell chains of the retina, not forgetting the dopaminergic amacrine cells (56).

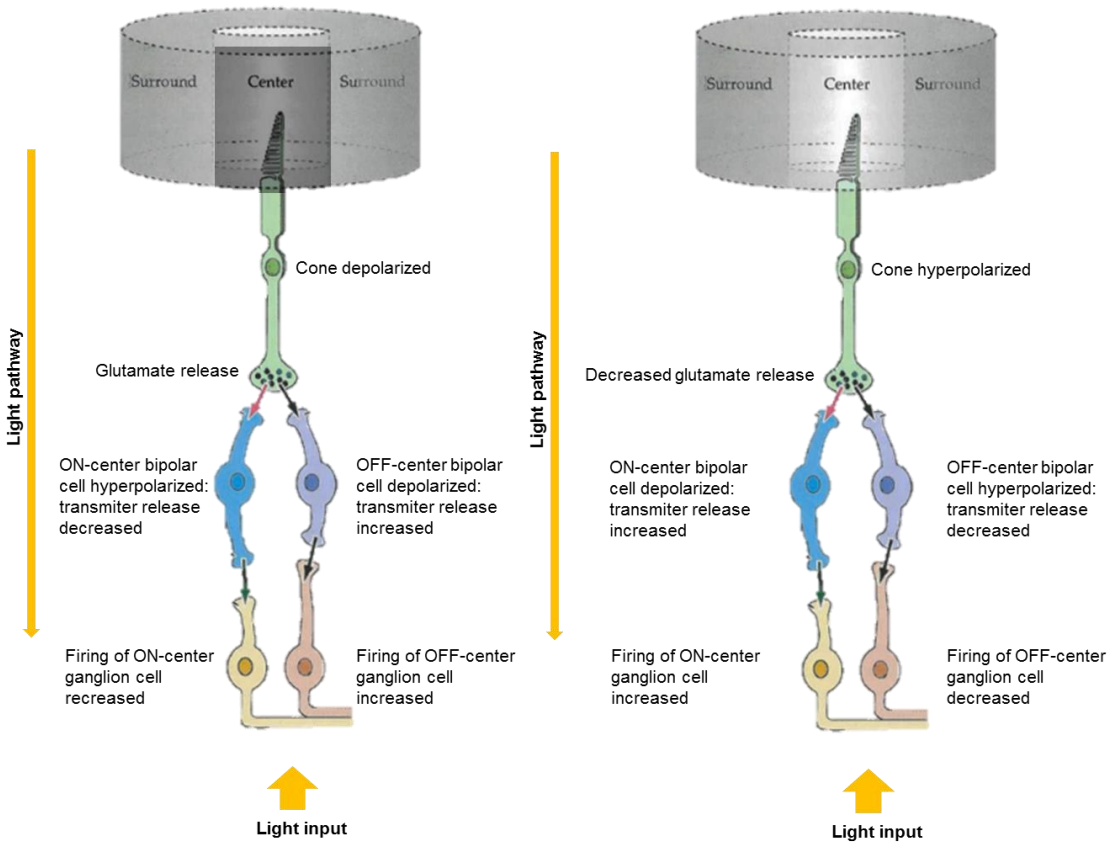

Fig. 1.3. Responses of retinal photoreceptors, bipolar and ganglion cells to darkness and illumination in the respective field surround. Depending on light availability, cone photoreceptors either hyperpolarize or depolarize, decreasing or increasing glutamate release rates, respectively, leading to hyperpolarization of depolarization of ON- and OFF-center biplar cells, thus mediating ganglion cell's firing rate and vision adaptation to light. Adapted from Webvision: Bipolar Cell Pathways in the Vertebrate Retina.

1.4. Parkinson's Disease

Parkinson's disease (PD) is the second most common neurodegenerative disease in middle-aged and elderly people. It is characterized by the loss of dopaminergic (dopamine-producing) neurons in the *substantia nigra pars compacta* of the brain and the aggregation of alpha-synuclein (aSyn) in association with other proteins such as ubiquitin in Lewy bodies (LBs) in the remaining nigral neurons, impairing optimal neuron functioning (57).

Epidemiological studies reveal that a small percentage of <10% of PD are familial cases of PD while the majority of cases are sporadic (58). This complex disease has multiple factors involved in its pathogenesis. Ageing seems to be the most potent risk for PD but other risk factors have shown to be important, such as predisposing factors, diabetes and exposure to environmental toxins like pesticides. Studies from both environmental factors and familial PD-related genes helped identifying the several pathways involved in the events leading to the death of dopaminergic neurons due to mitochondrial dysfunction, oxidative damage and protein accumulation (59).

Pathogenic mutations in the familial PD-linked genes aSyn, Parkin, DJ-1 and PINK1 as well as environmental factors have been associated with abnormalities in mitochondrial structure, function and protection system, oxidative damage, abnormal protein aggregation and protein phosphorylation compromising dopaminergic neuronal function and survival. (Fig. 1.4) (60). These mutated proteins are thought to bind to lipids and increase mitochondrial, lysosomal and vesicular membrane permeability, leading to mitochondrial dysfunction, impairment of the respiratory chain, decrease ubiquitin proteasome system (UPS) activity, increased calcium influx, ion homeostasis disruption and activation of Caspase 3 (Fig. 1.4). This cycle of events leads to cell death, by release of the apoptosis machinery (61,62).

The main manifestations of PD are motor changes such as resting tremor, bradykinesia, postural instability and cogwheel rigidity and, especially in early stages, symptomatic relief is available through dopamine (DO) restoring therapies. Moreover, non-motor manifestation such as constipation, rapid eye movement sleep (REM sleep) behaviour disorder, depression, cognitive disturbances and visual impairment have been rising awareness (63).

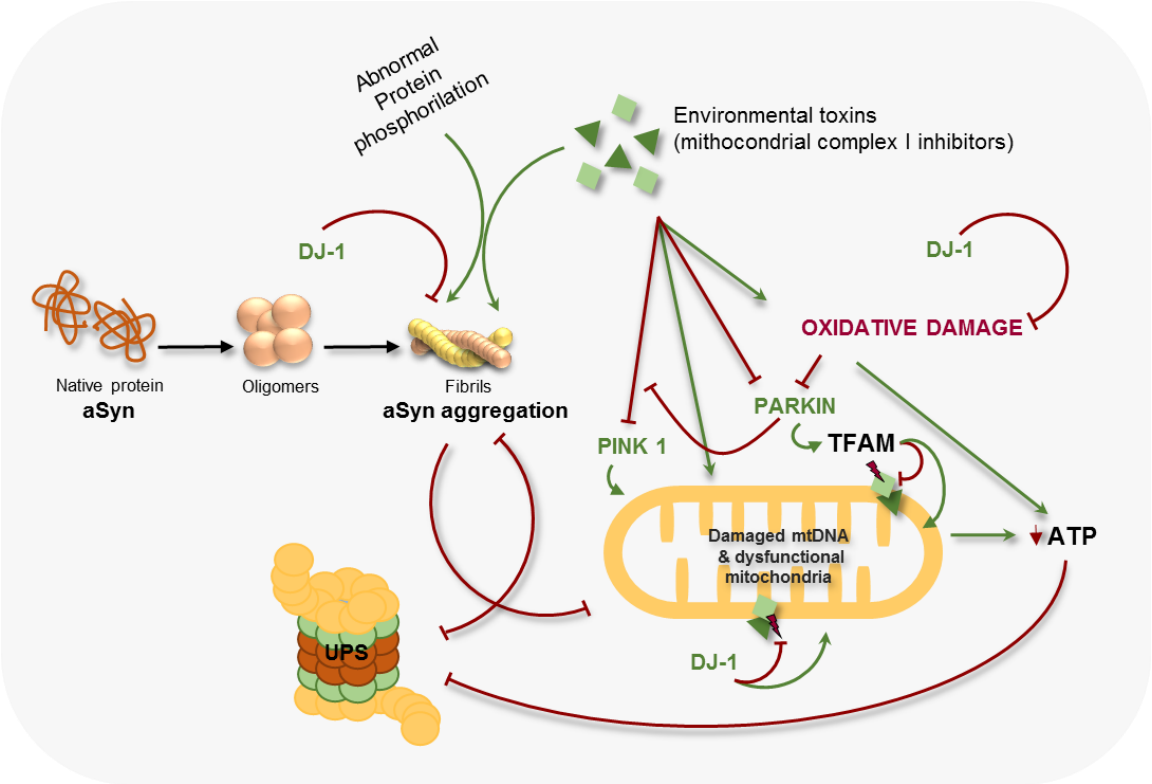

Fig. 1.4. Common intersecting pathways underlying PD pathogenesis. aSyn undergoes aggregation due to pathogenic mutations which in turn compromise ubiquitin proteasome function (UPS) and cause mitochondrial dysfunction. Mitochondrial dysfunction and oxidative damage lead to a decrease in ATP which may compromise the UPS function promoting abnormal protein aggregation. Parkin increases mitochondrial biogenesis by activating mitochondrial transcription factor A (TFAM) and blocks PINK1-induced mitochondrial dysfunction, while pathogenic mutations in the protein and oxidative damage severely compromise its protective function. DJ-1 protects against oxidative stress, functions as a chaperone to block aSyn aggregation and protects against

mitochondrial dysfunction. PINK1, when not compromised by pathogenic mutations, seems to protect against mitochondrial dysfunction. Adapted from (64).

1.4.1. Visual impairment in PD

Decreased visual acuity, reduced colour vision, deficits in vision-spatial orientation and contrast sensitivity are commonly found in patients with PD (65).

The pathological changes that have been reported in the eye in PD refer mostly to the retina and include cell loss related to reductions in retinal dopamine, with a visible thinning of the retinal fiber layer observed (66,67). Dopamine is a key neuromodulator in the brain and is highly present in the retina, as a chemical messenger for light adaptation, modulating photoreceptor activity, organizing ganglion and bipolar cell receptive fields and coupling horizontal cells and the amacrine lateral system (68). It is synthetized and released by the dopaminergic amacrine cells, upon light input and circadian clock, and activates D1 and D2 dopamine receptors distributed throughout the retina. When reaching the horizontal cells it uncouples their gap junctions blocking the communication between cells. Similar occurs for the amacrine cells themselves, considering that dopamine is thought to lead to the uncoupling of gap junctions of AII amacrine cells. In this way dopamine controls the light signal that reaches the ganglion cells, decreasing their sensitivity which is important to avoid saturation to light stimulation (54,69). Therefore, dopamine release reduction would be catastrophic.

In the brain, dopamine reduction in subcortical regions involved in eye movement, like basal ganglia and *substancia nigra pars reticulata*, could also be implicated in visual impairment of PD patients (70).

1.5. The synuclein family

The synucleins (syn) are a family of small and highly conserved proteins, very closely related: aSyn, beta-synuclein (bSyn) and gamma-synuclein (gSyn), that are encoded by the SNCA, SNCB and SNCG genes, respectively (Fig. 1.5). The first 42 aminoacids are identical between the synucleins but studies show that aSyn and bSyn and more closely related to each other (71).

These proteins are divided in three domains: residues between 1 and 60 make up the N-terminal which contains four lysine-rich repeats highly conserved motif similar to the lipid-binding motifs in lipoproteins that form a α-helice in the presence of lipids, allowing lipid-binding capacity to these proteins; residues between 61 and 95 form the central domain which has a high hydrophobic aminoacid content responsible for the amyloidogenic properties of the protein and, finally, residues 96-140 make up the C-terminus which is thought to confer chaperone-like activity to the synucleins (Figure 1.5) (72).

1.5.1. aSyn

aSyn is a 14kDa protein that has been the center of focus in a group of neurodegenerative disorders called α-synucleinopathies, which includes both familial and sporadic PD, PD dementia (PDD), Dementia with Lewy bodies (DLB), multiple system atrophy (MSA), among others (73).

aSyn is located in the central nervous system (CNS), predominantly in the presynaptic terminals of neurons, where synaptic vesicles constantly approach in order to release their neurotransmitter content, being later on recycled to clear the active zone (74). Even though its role in the brain is not fully known, it has been speculated that aSyn is involved in synaptic signaling and membrane trafficking, being suggested to play a role in both exo- and endocytosis of synaptic vesicles (74).

Regarding the role of aSyn on synapses, its role in the assembly of the soluble N-ethylmaleimide-sensitive factor (NSF) attachment protein receptor (SNARE) complex is suggested. The SNARE complex is an assembly of plasma membrane proteins, namely syntaxin and synaptopsome-associated protein 25 (SNAP-25), with vesicle-associated membrane protein 2 (VAMP2), that bind vesicles to the plasma membrane, undergo fusion and stimulate neurotransmitter release (75). Upon binding to synaptic vesicles during docking and priming, aSyn undergoes conformation changes folding into an amphipathic a-helix. As a result, this synuclein promotes the SNARE complex assembly by bounding to the SNARE-protein synaptobrevin-2/VAMP2 during synaptic exocytosis (73,75,76).

Moreover, aSyn may play a complementary role in endocytosis, facilitating membrane retrieval in order to maintain the membrane structure and facilitate further neurotransmitter release although the exact mechanisms are not fully understood (77). aSyn was described as being able to sense membrane curvature and stabilize it by binding its N-terminal region as well as residues between 65-97 region to lipid membranes and applying a double anchor mechanism by which aSyn tethers two vesicles to one another or to the plasma membrane, facilitating exo- and endocytosis (74).

1.5.1.1 aSyn toxicity

In its native state, aSyn is thought to predominantly exist as an unfolded monomer in equilibrium between cytosolic and membrane-bound states. However, duplication and triplication of the SNCA gene, post-translational modifications such as Ser129 and Ser87 phosphorylation (Figure 2), truncation and glycation as well as disease related mutations are thought to change this protein's aggregation dynamics (78). All known clinical mutations, such as A30P, E46K, H50Q, G51D, A53T and A53E are present in the N-terminal, emphasizing the importance of this domain in the aggregation of aSyn (Fig. 5).

Evidence suggests that the principle mechanism behind α-synucleinopathies is the misfolding of aSyn into aggregates in intracellular bodies, beginning with the formation of relatively soluble oligomers that can self-assemble into insoluble fibrils, resulting in the formation of deposits (79). This leads to neuroinflammation, neurodegeneration and cell death (80).

Increased aSyn levels are thought to disrupt neurotransmitter release through a decrease in size and mobility of the synaptic-vesicle recycling-pool (81). Overexpression of aSyn stabilizes the

SNARE complex in the membrane, inhibiting vesicle fusion and, therefore, neurotransmitter release (82) such as dopamine release (83).

Not only can aggregated aSyn interfere with neurotransmitter release but it can also affect its synthesis. Dopamine synthesis consists on the conversion of tyrosine into dopamine in two steps: tyrosine is firstly converted into L-3,4-dihydroxyphenylalanine (L-DOPA), mediated by phosphorylated tyrosine hydroxylase (TH), following L-DOPA conversion into dopamine by DOPA decarboxylase (DDC) (84). However, aSyn binds to the dysphosphorilated TH, maintaining its inactive form and, subsequently, causing a decrease in its enzymatic activity and dopamine synthesis (85).

Overall, this protein has been found to interact with mitochondria, mitochondria-endoplasmic reticulum (mitochondria-ER) and ER-Golgi networks and with the ubiquitin proteasome system (86).

Mitochondria are essential for the synthesis of adenosine triphosphate (ATP), regulation of calcium, lipid metabolism and, overall, neuronal survival (87). ATP is synthesized *via* oxidative phosphorylation complexes, which are present in the inner membrane of mitochondria: ubiquinone oxidoreductase Complex I, succinate dehydrogenase Complex II, ubiquinol–cytochrome c oxidoreductase Complex III, cytochrome c oxidase Complex IV and ATP synthase Complex V mitochondrial (88). Mitochondrial complex I is responsible for catalyzing the first step of the electron transport chain which is the main source of ROS (89).

Studies revealed that aggregated aSyn binds to the inner membrane of mitochondria, altering its normal function by associating with complex I (90). This events lead to cytochrome c release and a consequent increase of Ca^{2+} uptake and ROS levels which ultimately leads to cell death (91). Furthermore, wild type aSyn and A53T mutant are proposed to promote an up-regulation of mitophagy, the delivery of damaged and dysfunctional mitochondria to the lysosome, culminating in an abnormal mitochondrial activity, increased ROS levels and further mitochondrial degradation levels (92–94). However, is not only aSyn that promotes ROS levels to rise. Increased ROS, and consequently oxidative stress, is suggested to promote aSyn aggregation, creating a never ending cycle of degeneration (95).

Moreover, mitochondria communicates with the ER to regulate several cellular processes (96). Alterations in this mitochondria-ER communication can cause deregulation of Ca^{2+} homeostasis resulting in protein misfolding, metabolic alterations and apoptosis (97). ER stress, which is usually caused by the accumulation of misfolded proteins within the ER, is associated with the development of several neurodegenerative diseases. By either interacting with ER chaperones or affect ER function while compromising ER membranes integrity and exposing portions for the ER lumen to the cytosol, Insoluble aSyn aggregates could generate ER stress (98). Actually, aSyn was reported to inhibit trafficking in the ER-Golgi network in yeast models, increasing protein accumulation in the ER, cell toxicity and cell loss and exacerbating ER stress (99). Moreover, similar to what was seen in yeast cells, vesicle accumulations due to trafficking impairment have been observed in neurons before Lewy body formation (100). Furthermore, vesicle accumulations are often found in proximity to Lewy bodies in later stages of disease (101).

Ultimately aSyn is degraded both by the UPS and by the autophagy/lysosomal pathway (ALP). However, some mutations such as the A30P and A53T may cause a failure in the release of aSyn and clogging of the autophagy translocation machinery thus accumulating aSyn (102).

1.5.2. bSyn and gSyn

bSyn is slightly smaller than aSyn but shares some of the synuclein features, including the location, being mainly found in the CNS (Fig. 1.5). Even though it is not as prone to aggregate as aSyn due to the lack of 11 aminoacids in its NAC domain, studies suggest that when exposed to toxins such as metal ions and pesticides, bSyn tends to fibrillate (103). Furthermore, when co-expressing with aSyn, it leads to an increase in cytotoxicity in yeast and forms heterodimers in both yeast and cell lines (104).

gSyn is the least conserved and the smallest of the three proteins (Fig. 1.5) (71). This synuclein is a putative marker for breast cancer (105). In the nervous system, it can be found mainly in the peripheral nervous system (PNS), including in primary sensory neurons, sympathetic neurons and motor neurons (106) but can also be found in other tissues such as ovarian and breast cancer (71). Although its function is likewise not known, exogenous expression of the protein potentiates the metastatic ability of breast tumours (107).

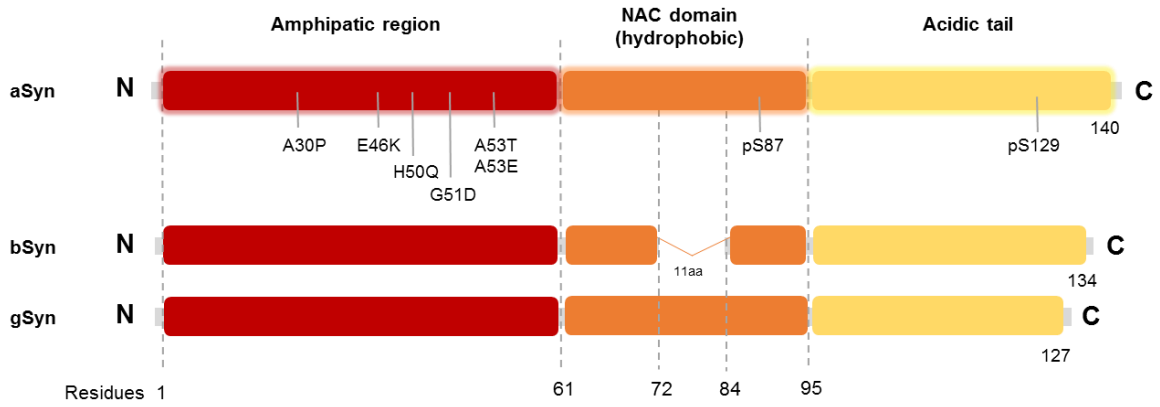

Fig. 1.5. Schematic structure of synuclein proteins. aSyn, bSyn and gSyn share high homology. The N-terminal region is highly conserved between the three proteins. Major differences are observed in the acidic C-terminal, with bSyn and gSyn having a shorter size when compared to aSyn (adapted from (108)).

1.5.3. Synucleins in the eye

All the members of the synuclein family can be found ocular tissues. aSyn and bSyn are both located in synapse-rich IPL of the retina showing similar distribution patterns although bSyn is also found in the INL. gSyn, on the other hand, can be found in the GCL which is mainly composed of ganglion cells (109).

To date, few have dedicated to the task of describing in detail the exact neuronal population where these proteins are located.

A study conducted by Martínez-Navarrete et al. in several animal models, namely in rodent (rat and mouse), bovine, and primate (human and monkey) retinas, not only reports the presence of aSyn in the presynaptic terminals of retinal neurons in the IPL (110), in agreement with the findings of Surguchov et al. (76), but also in the OPL due to the colocalization with synaptophysin (110), a synaptic-vesicle transmembrane protein involved in the regulation of vesicular exocytosis in the CNS, that can be found in both plexiform layers of the retina (111). The same group claims that aSyn was further localized in the somata and dendrites of both GABAergic and glycinergic amacrine cells and showed high levels in the RPE in all vertebrate tested (110).

gSyn localization as well as physiological and pathological role are very poorly known. However, this synuclein was found by Martínez-Navarrete et al in cultured bovine retinal pigment epithelium (RPE) cells (110). Moreover, studies in rodent and human retinas, using suitable markers for ganglion cells, such as Brn-3 and Thy1-1 family proteins, were able to detect colocalization between these markers and gSyn antibody. gSyn was even suggested as a specific marker for that neuronal population (112). This synuclein was also implicated in glaucoma and even though a lot is yet to describe about its role in eye disease, has been found in the optic nerve of glaucomatous patients, in a subset of glial cells identified as possibly reactive astrocytes, which did not happen for healthy controls (106). Furthermore, in Alzheimer's disease (AD) patients, a study revealed a decrease in gSyn levels, with no differences occurring in the levels of the other two synucleins, though the reasons behind this event remain unknown (109).

1.6. Common pathophysiology between PD and DR

Recent evidence points to a common pathophysiology in the visual impairment of PD patients and in DR, as an effect of a disruption in the dopaminergic system in both diseases. Dopamine is an essential neuromodulator in the brain and is highly present in the retina. In addition to regulating motor, cognition, and retinal function, dopamine present in the retina modulates light-adapted vision through the activation of selective receptors and retinal pathways (113,114). In fact, studies suggest that injecting the diabetic mice with dopamine-restoring and dopamine-activating drugs already used in PD can restore dopamine levels in dopaminergic amacrine cells and significantly improve retinal function (115).

Moreover, another study in a rodent PD model suggested that the administration of antidiabetic drugs proved to have a neuroprotective effect on retinal and nigrostriatal neurons in PD patients. This further suggests a common pathophysiology between these two pathologies (116).

Moreover, there is a resemblance between the diabetic retina and the environment underlying aSyn aggregation and, subsequently, PD. Hyperglycemia activates several pathways that, along with the impairment of the antioxidant defence system, result in an excessive bioavailability of ROS (20) that damages the mitochondrial membrane and mtDNA, compromising the mitochondrial machinery, namely the electron transport chain resulting in a continuous and increasing ROS production that leads to release of the apoptosis machinery (23). Likewise, in PD, increased oxidative stress and

inflammation processes as well increased glucation potentiate aSyn aggregation, a hallmark of PD (117). On the other way around, aSyn is believed to bind to the inner mitochondrial membrane, where it associates with mitochondrial complex I, culminating in increased ROS production, Ca^{2+} levels and release of cytochrome c, leading to cell death (90,91).

The synuclein family members, which play a major role in PD due to the formation of aggregates in brain tissues and consequent relation with neurodegeneration, are also highly expressed in the retina (118). Triple knockout of aSyn, bSyn and gSyn in mice leads to altered synapse structure and physiology and age-dependent neuronal dysfunction and decreased survival. Importantly, these animals developed retinal dysfunction and age dependent blindness, a strong indicative that synucleins play an important role in retina function (119).

Furthermore, aSyn aggregation was, as previously mentioned, also described in other degenerative diseases such as AD (120) but also in ageing retinas (121). Although LBs are the hallmark lesions of PD, aSyn-positive LBs also occur frequently in the brains of many AD patients (122). Also, within ageing, progressive accumulation of potentially toxic protein aggregates and the dysfunction of the ubiquitin proteasome system, eventually contribute to neuronal degeneration (121,123).

Altogether these data suggest a possible role of the synucleins in DR's pathology.

1.7. $Ins2^{Akita}$ as a diabetic model

The most commonly used diabetes animal models include rodents, dogs and primates with diabetes induced by chemical toxins such as streptozotocin. Streptozotocin enters the pancreatic β-cells via a glucose transporter, glucose transporter 2 (GLUT2), and causes alkylation of DNA. DNA damage induces later on the formation of superoxide radicals. Consequently, hydrogen peroxide and hydroxyl radicals are also generated. As a result of the streptozotocin action, β-cells are destroyed (124).

Still, due to the creation of strain-dependent resistance to streptozotocin, studies have been developed in order to describe a better model for early diabetic retinal complications in diabetes.

The $Ins2^{Akita}$, a C57BL/6 mutant heterozygous mouse, is a relatively recent and improved model for type 1 diabetes complications' studies, such as DR. It consists of a point mutation in the insulin 2 gene, which replaces a cysteine with tyrosine at the seventh amino acid of the A chain of the insulin 2 gene product (125,126). This spontaneous mutation causes a conformational change in the protein, leading to its accumulation in the ER of pancreatic β-cells, triggering the unfolded protein response and consequently β-cell death. Loss of β-cells in the pancreas results in systemic hypoinsulinemia and hyperglycaemia, which are significant after only 4 weeks with significant as well as significantly less weight (Fig. 1.6) (126). Importantly, these mice develop diabetes complications including diabetic neuropathy (126–128).

Although the $Ins2^{Akita}$ mice show a few signs of proliferative DR like indices of neovascularization and new capillary bed formation (129), this model is particularly strong in retinal pathologies

characteristic of early, nonproliferative DR, such as increased frequency of apoptotic retinal neurons, microaneurysms, vascular damage, and increased vascular leakage, accompanied by vision loss (126,130,131).

When compared to other models, such as the streptozotocin(STZ)-induced diabetic rats, the Ins2^{Akita} mice mimic several outcomes of diabetes established in the STZ-model, namely retinal complications such as increased vascular permeability, increased acellular capillaries and vascular inflammation (Fig. 1.6) (126). Moreover, increased levels of apoptosis markers such as Caspase 3 was reported in both models (Fig. 1.6) (126,132). However, the Ins2^{Akita} model shows some earlier the other models such as the acute STZ-model. Thinning of the inner layers of the retina were reported in the Ins2^{Akita} model after little more than 5 months of diabetes onset, more than two months earlier than in STZ mice, suggesting a degeneration and loss of horizontal, bipolar and amacrine cells (Fig. 1.6) (133,134).

Overall, the Ins2^{Akita} has several advantages over other models. This heterozygotic mouse model breeds well, presents stable insulin-deficient diabetes that can be maintained at a noncatabolic state without exogenous insulin and shows a mechanism of diabetes onset that does not involve systemic immunologic alterations making it possible to evaluate the metabolic impact on the retina (126).

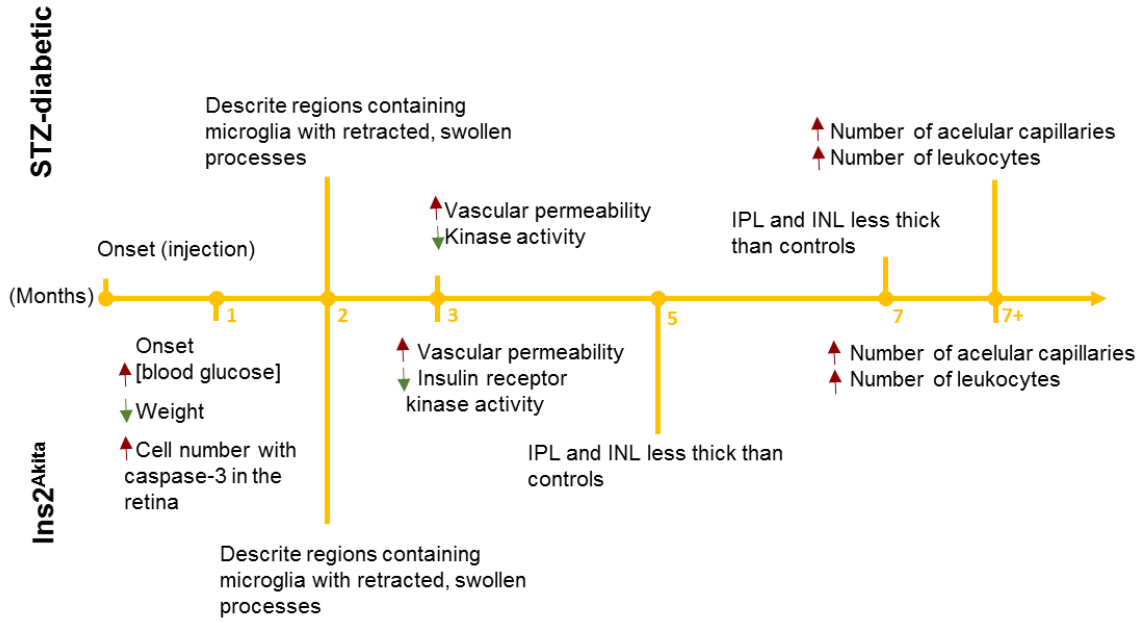

Fig. 1.6. Diabetes progression and molecular markers in the STZ and Ins2^{Akita} diabetic retinopathy model. The Ins2^{Akita} mice present several retinal complications. By one month these mice show a higher blood glucose concentration and higher levels of Caspase 3 in the retina and considerably less weight than controls. By 2 months old swollen processes in the retina are noticed and shortly after increased vascular permeability. Thinning of the Inner Nuclear and Inner Plexiform Layers of the retina are considerably increased in the Ins2^{Akita} model after little more than 5 months of diabetes onset, suggesting a degeneration and loss of horizontal, bipolar and amacrine cells. By 7 months old, increased acellular capillaries and vascular inflammation occur.

1.8. Scientific question and aims

Diabetes is a chronic disease responsible for significant macro- and microvascular complications such as Diabetic Retinopathy. Recently, DR was described as a neurodegenerative disease, where degeneration of neurons occurs prior to the microvascular onset. PD, the second most common neurodegenerative disease in the world, and DR are proposed to share a common pathophysiology in visual impairment due to the disruption of the dopaminergic system as well as to a similar hostile environment that, in PD, culminates in aSyn aggregation, toxicity and neuronal death. aSyn is the main focus not only in PD but also in other neurodegenerative diseases and can be found in ocular tissues. Its precise location in the retina and pathophysiological role are not fully described though it is suggested that it is crucial for vision to occur.

The aim of this study is to do a description of the synucleins distribution pattern in the retina and to establish a correlation between the synucleins profile and the progression of diabetic retinopathy, using a type 1 diabetes mice model, the $Ins2^{Akita}$, as well as Wild Type controls in different stages of the disease.

2. Material and Methods

2.1. Sample handling

C57Bl6/WT (WT) and C57Bl6/Ins2^{Akita} (Ins2^{Akita}) mice of matching ages 6, 9 and 12-months old were euthanized and their brains, eyes and kidneys removed. All animal procedures were performed according to the FELASA (Federation of European Laboratory Animal Science Associations) recommendations for laboratory animal research and wellfair guidelines, approved by the CEDOC-NMS|FCM-UNL rodent facility. This facility is certified by the Portuguese Directorate-Gereral of Animal Wellfare.

The retinas destined for protein extraction and consequent Western blot (WB) analysis were immediately dissected in Phosphate-Buffered Saline (PBS, pH 7.2; Gibco, Grand Island, New York, USA) with phosphatase (Phosphostop, Roche Diagnosis GmbH, Mainhein, Germany) and protease inhibitors (cOmplete, Roche Diagnosis GmbH, Mainhein, Germany) and protein extraction protocol, in detail bellow, was followed.

All the organs destined for immunohistochemistry (IHC) were stored in 4% paraformaldehyde (PFA)/PBS at 4ºC for 48 hours and then transferred into a solution of 30% sucrose/PBS. In the case of the eyes, this was done through a sucrose gradient, remaining in a solution of 10% sucrose/PBS for 1h at RT shaking, then in a solution of 20% sucrose/PBS shaking for another hour at room temperature (RT) and finally put in a solution of 30% sucrose/PBS at 4ºC, shaking at 4ºC *overnight* (O/N).

2.2. Cryosections of the Ins2^{Akita} and Wild type mice retinas

The eyes used for IHC were embedded in a cryo embedding media (Tissue Tek, Sakura Finetek, Torrance, California, USA) in the plastic mold and the eye oriented with the optic nerve pointing right from viewers point. The sample was then frozen at -80°C until used.

The sectioning was performed in the Cryostat Leica CM3050 S, with an object temperature (OT) of -20°C and camera temperature (CT) of -22°C, as suggested in literature. The sections were 10 µm thick.

The sectioning was sequential, containing each portion of the eye (6-8 sections), so that every slide is representative.

Superfrost Plus Microscope Slides (Thermofisher scientific, Braunschweigh, Germany), containing the cryosections were dried for 12 hours at RT and then stored at -20°C until needed.

2.3. Localization of the synucleins in the Wild Type and Ins2^{Akita} mice retinas and colocalization with specific markers

Immunohistochemistry allows the visualization of the localization and distribution of specific tissue components by the interaction of target antigens with antibodies tagged with a label.

For that purpose, frozen retina sections were thawed at room temperature (RT) for 2 hours and rehydrated with PBS 1x for 30 min. The cryo embedding media was washed three times for 15 minutes each with PBS-0,25% Triton (PanReac AppliChem, Barcelona, Spain) (PBS-T) and the slides blocked for 1 hour with blocking solution 1% Bovine Serum Albumin (BSA; (NZYTech, Lisboa, Portugal)/3% Goat serum (Sigma-Aldrich, Saint-Louis, Missouri, USA)/PBS-T. Primary antibodies were diluted in PBS-T and incubated O/N at 4°C. The slides were, once again, washed with PBS-T (3 washes of 15min) and secondary antibody, diluted in PBS-T, was incubated for 1 hour. Mounting media Fluoromount-G™ containing DAPI (4',6-diamidino-2-phenylindole; Southern biotech, Birmingham, USA) was added to the slides and, after dried, the slides were stored at 4°C. Moreover, controls using exclusively secondary antibodies were performed.

The slides were imaged in the Zeiss Z2 widefield fluorescent microscope (Carl Zeiss MicroImaging GmbH, Germany) with the 20x or 40x objective and in the confocal microscope Zeiss LSM710. Confocal microscope images were analysed with the ImageJ – Fiji image analysis software (135), obtaining maximum intensity projection images and orthogonal view of the colocalization sites. This software was also used to calculate colocalization percentages between antibodies' signals in the IPL region as well as the amount of cell bodies. For quantifications, three different images of each independent animal were used.

Colocalization results were obtained addressing the Mander's colocalization coefficients for channel 1 (M1) and channel 2 (M2), being M1 the percentage of green dye molecules that share their location with a red dye molecule and M2 the percentage of red dye molecules that share their location with a green dye molecule.

The antibodies specification and dilutions used are listed in Table 2.1 and 2.2.

Table 2.1. Description of primary antibodies used for IHC.

Antibody	Reference	Species	Dilution (in PBS-T)
aSyn	Cell signalling (2629S)	Rabbit	1:200
bSyn	Abcam (ab76111)	Rabbit	1:200
gSyn	Abcam (ab55424)	Rabbit	1:200
Syntaxin 1A	Sigma (S0664)	Mouse	1:200
Synaptopysin	Sigma (S5768)	Mouse	1:200
PKC-α	Santa Cruz (sc-8393)	Mouse	1:200
Calbindin	Sigma (C9848)	Mouse	1:200
TH	Abcam (ab112)	Rabbit	1:500

Table 2.2. Description of secondary antibodies used for IHC.

Antibody	Reference	Dilution (in PBST-T)
Alexa Fluor Goat anti-rabbit 488	Invitrogen, A11008	1:1000
Alexa Fluor Goat anti-mouse 594	Invitrogen, A11005	1:1000

2.4. Soluble protein from whole retina extraction

For total protein extraction from the animals' retina, whole retina (≈30µg) was homogenized in 50µg RIPA lysis buffer with protease and phosphatase inhibitors, using a pellet pestle and centrifuged for 20 minutes at 4°C and full speed (13,200g). Supernatant was stored at -80°C.

2.5. Total soluble protein quantification from retina protein extracts

Protein quantification was done according to the bicinchoninic acid (BCA) assay (Thermo Fisher Scientific Inc., Waltham, MA, USA) protocol. The BCA Protein Assay consists of the reduction of Cu^{2+} to Cu^{1+} by protein in an alkaline medium which is then detected by the bicinchoninic acid, developing colour. The intense purple-colored reaction is then quantified. The protocol was followed according to the manufacturer's instructions with the following observations: due to the small amount of each sample, 10µL of sample and standard were used.

2.6. Assessment of the levels of the synucleins and other markers of interest

Protein sample buffer (200mM Tris-HCl pH 6.8, 6% 2-mercaptoethanol, 8% sodium dodecyl sulfate (SDS), 40% glycerol, 0.4% bromophenol blue) was added to each sample with a total protein concentration of 15 µg/µL. Protein extracts from whole retina were analyzed by Western blot in order to determine the levels of the synucleins and other markers of interest. The samples were denatured at 100°C for 10 min and then loaded in a 12% acrylamide gel. After running, the proteins were transferred into a nitrocellulose membrane (Bio-Rad, USA) using the Trans-Blot® Turbo™ Transfer System (Bio-Rad, Hercules, CA, USA), through a 7 min transfer. The nitrocellulose membranes were divided in two, between the 35 kDa and 25 kDa bands, in order to incubate the membrane with both β-actin, which was used as loading control, and the synucleins and other markers.

The membranes were then blocked with 5%BSA/Tris-buffered Saline – Tween 20 (5% BSA/TBS-T) (w/v) for 1 hour and incubated O/N with the primary antibody diluted in 5%BSA/TBS-T. The membranes were afterwards washed with TBS-T three times for 15 min each and incubated with the secondary antibody diluted in 5%BSA/TBS-T for 1 hour at RT. After washing with TBS-T, the membranes were analyzed in the Chemidoc Touch (Bio-Rad, Hercules, CA, USA) using the Pierce™ ECL Western Blotting Substrate (Thermo Fisher Scientific, Waltham, MA, USA).

The antibodies' specification and dilution used are listed in Tables 2.2 and 2.3.

The images acquired were treated using the Image Lab Software (Bio-Rad, Hercules, CA, USA) for quantification of the protein levels and comparison between diabetic animals and controls.

Table 2.3. Description of primary antibodies used for Western Blot.

Antibody	Reference	Species	Dilution (in 5%BSA-TBST)
aSyn	Cell signalling (2629S)	Rabbit	1:1000
bSyn	Abcam (ab76111)	Rabbit	1:1000
Syntaxin 1A	Sigma (S0664)	Mouse	1:1000
Synaptopysin	Sigma (S5768)	Mouse	1:1000
SNAP25	111 002	Rabbit	1:1000
PSD95	Milipore (04-1066)	Rabbit	1:1000
Rab3a	Sicgen (AB10032-200)	Goat	1:1000
Caspase 3	Cell Signaling /Izasa (8G10)	Rabbit	1:1000
β-actin	Sigma, A-5441	Mouse	1:10000

Table 2.4. Description of secondary antibodies used for Western Blot.

Antibody	Reference	Dilution (in 5%BSA-TBST)
Donkey anti-rabbit	GE Healthcare (NA934V)	1:5000
Sheep anti-mouse	GE Healthcare (NA931V)	1:5000
Donkey anti-goat	Santa Cruz (sc-2620)	1:5000

In order to incubate other antibodies in the same membranes, membranes were stripped using a stripping solution (glycine, 10% SDS, ddH_2O; pH 2.0) during 45 min, followed by three washes with TBS 1x and three washes with TBS-T, for 10 min each. Membranes were again blocked and incubated with new primary antibodies, following WB protocol.

2.7. Statistical Analysis

To perform the statistical analysis, the Prism 7 (GraphPad Software Inc., La Jolla, CA, USA) was used. The analysis of the colocalization between proteins was performed using a two-way ANOVA, comparing ages and WT and $Ins2^{Akita}$ samples. Statistical analysis of protein levels was performed using parametric t-test and non-parametric Mann-Whitney test, comparing the mean between two groups, WT and $Ins2^{Akita}$ mice. P value ≤ 0.05 was considered statistically significant. Results are shown as mean ± standard deviation.

3. Results

3.1. Characterization of the WT and Ins2^{Akita} population

The Ins2^{Akita} is a mouse model for type 1 diabetic complications' studies, such as diabetic retinopathy. When compared to controls, these animals present hyperglycemia and a smaller weight (126).

Before sample collection, the animals used for this study were weighted and glycaemia levels measured in order to characterize the mice population and to criticize possible variations in the results (Fig. 3.1 and 3.2).

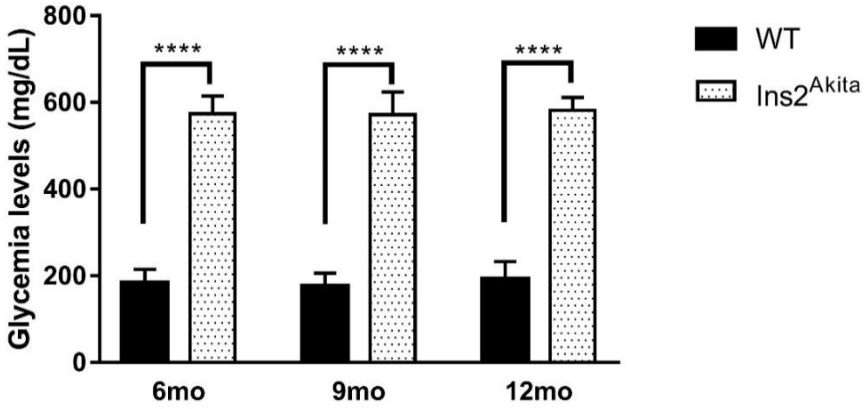

Fig. 3.1. Glycemia levels of WT and Ins2^{Akita} mice sacrificed between September 2016 and August 2017. N=23 for 6 months old, N=23 for 9 months old and N=18 for 12 months old WT and N=19 for 6 months old, N=15 for 9 months old and N=8 for 12 months old Ins2^{Akita}. Data are presented as Mean ± SD. ****p<0.001 Ins2^{Akita} compared with WT; T-test.

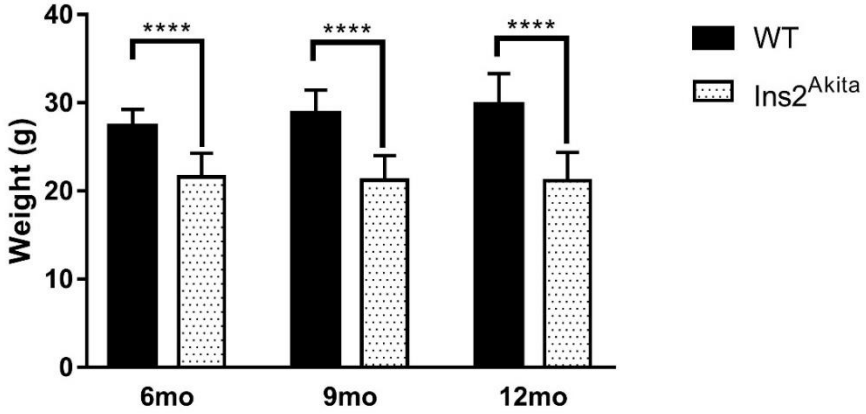

Fig. 3.2. Weight levels of WT and Ins2^{Akita} mice sacrificed between September 2016 and August 2017. N=23 for 6 months old, N=23 for 9 months old and N=18 for 12 months old WT and N=19 for 6 months old, N=15 for 9 months old and N=8 for 12 months old Ins2^{Akita}. Data are presented as Mean ± SD. ****p<0.001 Ins2^{Akita} compared with WT; T-test.

Weight and glycemia levels measurment revealed a consistency in both parameters between WT animals of all ages and between Ins2^{Akita} animals of all ages. Ins2^{Akita} mice show significantly higher levels of glycemia (183.16 ± 33.80 vs 576.31 ± 42.19) and significantly lower weight than WT mice (28.55 ± 2.84 vs 21.76 ± 3.70, p<0.001) (Fig. 3.1 and 3.2).

With diabetes, thinning of the INL was described in Ins2^{Akita} mice (126) as well as other models such as the STZ mice (133). The area of the INL in the central retina was measured and compared between WT and Ins2^{Akita} retinas of all ages (Fig. 3.3).

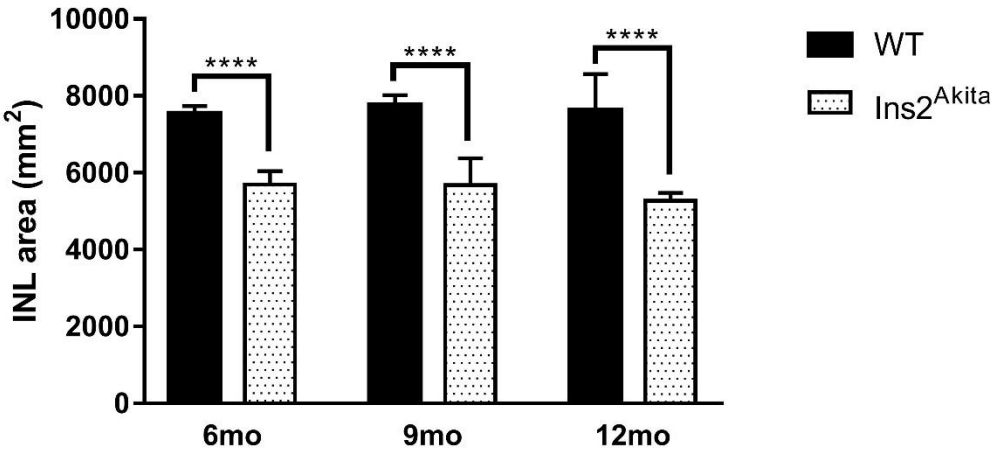

Fig. 3.3. INL area (mm^2) of WT and Ins2^{Akita} mice. N=5 to 6 and 9-months old group; N=3 to 12-months old group. Data are presented in Mean ± SD. ****p<0.001 Ins2^{Akita} compared with WT; Mann-Whitney test.

Regarding the area of the INL, results show that the INL of 6, 9 and 12-months old Ins2^{Akita} retinas is significantly thinner than controls (7676.33 ± 94.78 vs 5546.76 ± 196.31, P<0.001), not showing any differences with ageing (Fig. 3.3).

Overall, these results show that the Ins2^{Akita} mice model we used in our study is reproducing the halmarks previously described by Barber and colaborators (126).

3.2. Evaluation of synucleins profile in WT and Ins2^{Akita} retinas

3.2.1. The synucleins in the retina

The localization of the synucleins in the retina is of major importance as its location may dictate or at least influence its function.

In order to localize aSyn in the retinal cell populations of WT or Ins2^{Akita} mice of different ages (6, 9 and 12-months old) and, therefore, different disease stages, IHC was performed according to protocol (Fig. 3.4).

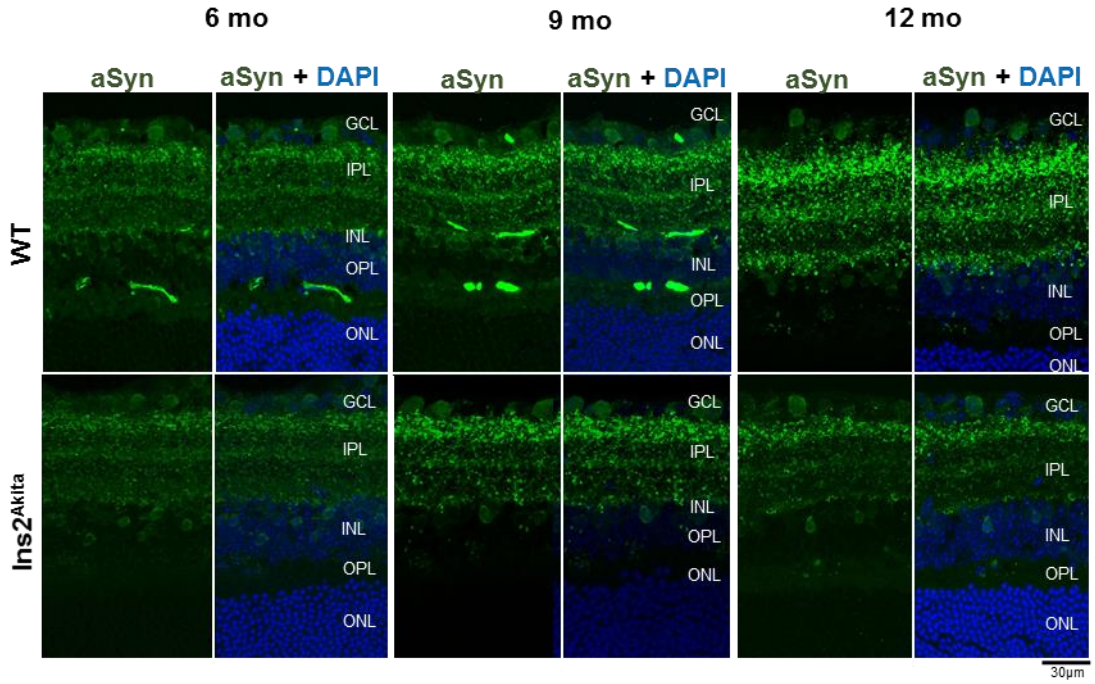

Fig. 3.4. Immunohistochemistry for aSyn in retinal sections of WT and Ins2^{Akita} mice of 6, 9 and 12-months old. N=5 to 6 and 9-months old group; N=4 to 12-months old group. Nucleus are stained with DAPI (blue) and aSyn stained with Alexa Fluor 488 GAR (Green). GCL, ganglion cell layer; IPL, inner plexiform layer; INL, inner nuclear layer; OPL, outer plexiform layer; ONL, outer nuclear layer. Confocal images obtained with a 40x objective.

aSyn is localized in the IPL and to be stratified in strata 1, 3 and 5 (s1, s3 and s5) in both WT and Ins2^{Akita}, being more intense in s5 which is where the ON bipolar and ON ganglion cells as well as amacrine cells communicate (Fig. 3.4). Also, aSyn is localized in cell bodies of the GCL and INL (Fig. 3.4). Aiming to detect differences within ageing and diabetes, the number of cell bodies containing aSyn in both layers was counted (Fig. 3.5 and 3.6).

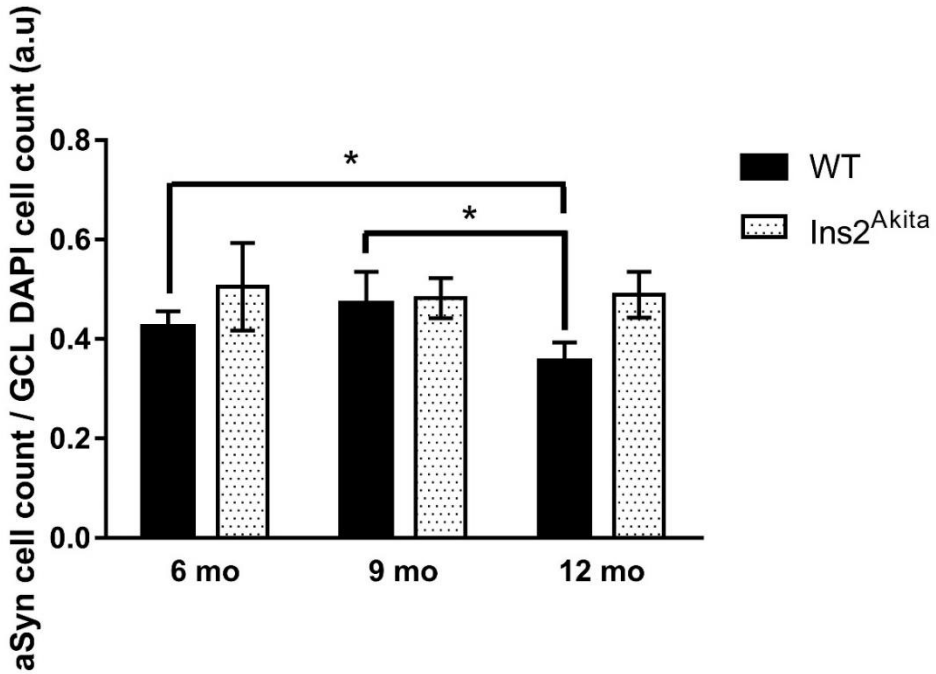

Fig. 3.5. Quantification of the amount of cell bodies containing aSyn in the GCL of 6, 9 and 12-months old WT and Ins2^{Akita} mice retinas. N=4 to 6 and 9-months old group; N=3 to 12-months old group. Data are presented as Mean ± SD, considering the number of cell bodies containing aSyn per area. *p<0.05 Ins2^{Akita} compared with WT; Mann-Whitney Test.

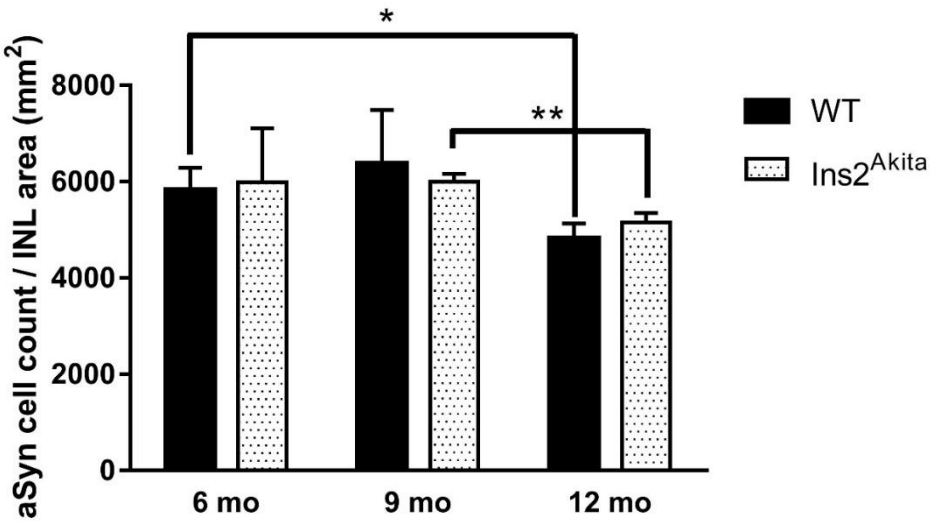

Fig. 3.6. Quantification of the amount of cell bodies containing aSyn in the INL of 6, 9 and 12-months old WT and Ins2^{Akita} mice retinas. N=3 to each group. Data are presented as Mean ± SD considering the number of cell bodies containing aSyn per mm^2. *p<0.05; **p<0.005 Ins2^{Akita} compared with WT; Mann-Whitney test.

Regarding the amount of cell bodies containing aSyn in the GCL, there are no differences between WT and Ins2^{Akita} retinas of all ages. With ageing however, there is a significant decrease in

the amount of cells expressing aSyn by 12 months old WT retinas when comparing to 6 months old samples and a decrease by 12 months old Ins2^{Akita} when compared to 9 months old Ins2^{Akita} retinas (Fig. 3.5).

In the INL the same is observed. The amount of cell bodies with aSyn appears to be similar between WT and Ins2^{Akita} retinas and between Ins2^{Akita} retinas of all ages (6, 9 and 12-motnhs old). With ageing, the amount of cell bodies with aSyn is considerably lower in 12 months old WT retinas than in 6 and 9-months old controls (Fig. 3.6).

bSyn localization in the retinal cell populations of WT and Ins2^{Akita} mice of different ages was also evaluated, in 6, 9 and 12-months old animal retinas (Fig. 3.7).

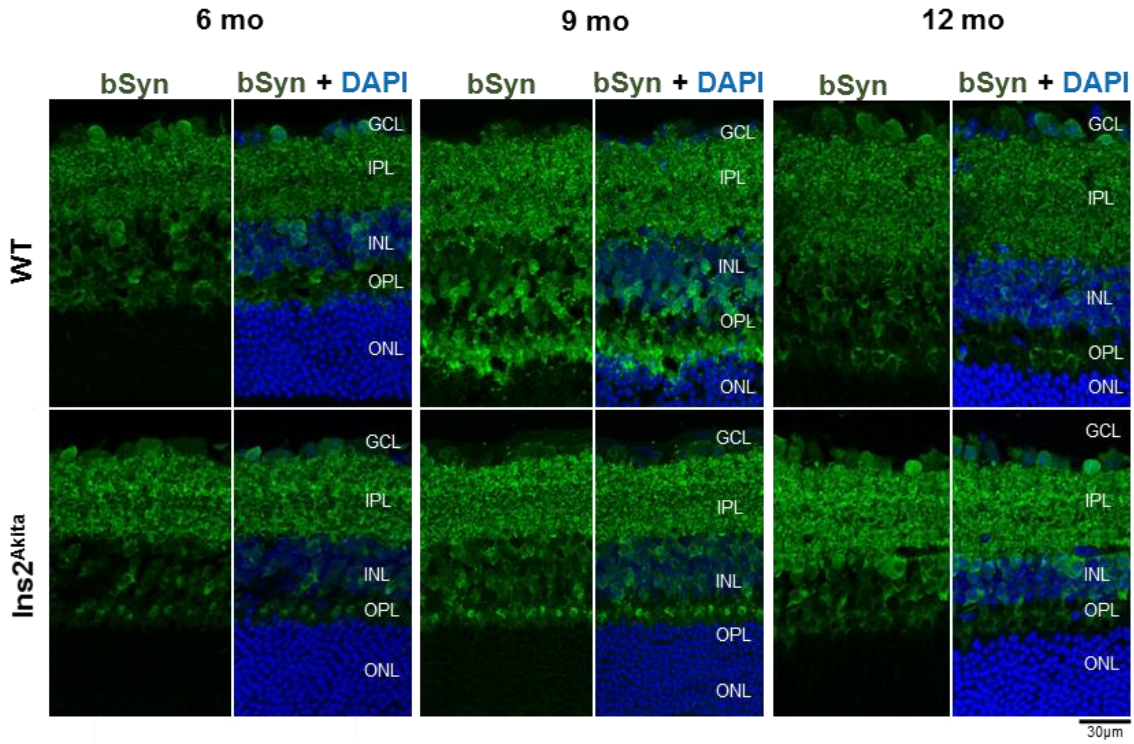

Fig. 3.7. Immunohistochemistry for bSyn in retinal sections of WT and Ins2^{Akita} mice of 6, 9 and 12-months old. N=5 to 6 and 9-months old group; N=4 to 12-months old group. Nucleus are stained with DAPI (blue) and bSyn stained with Alexa Fluor 488 GAR (Green). GCL, ganglion cell layer; IPL, inner plexiform layer; INL, inner nuclear layer; OPL, outer plexiform layer; ONL, outer nuclear layer. Confocal images obtained with a 40x objective.

bSyn is localized in the IPL, similarly to aSyn, however less stratified. Furthermore, bSyn is expressed in the OPL and in cell bodies in the INL and GCL (Fig. 3.7). Considering bSyn distribution with ageing and diabetes progression, between images there appear to be no striking differences with ageing nor between WT and Ins2^{Akita} retinas (Fig. 3.7). However, in order to conclude if there are in fact differences, a quantification, similar to what was done for aSyn, must be done.

Regarding gSyn, its localization in the retina was also determined in 6, 9 and 12-months old animals (Fig. 3.8).

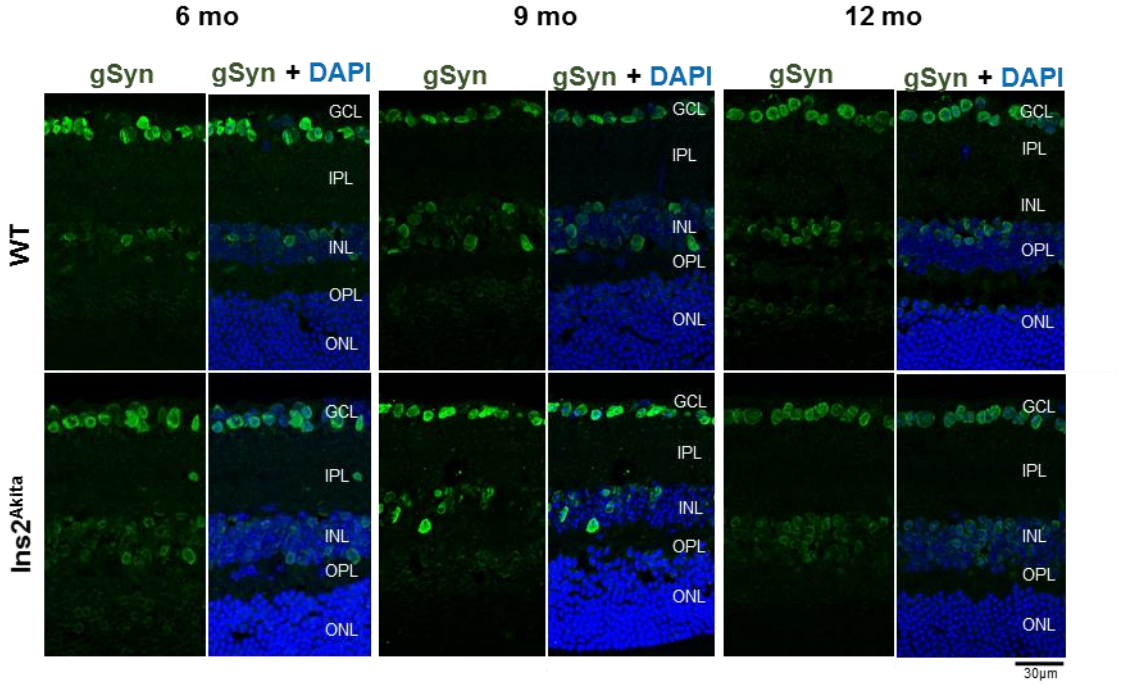

Fig. 3.8. Immunohistochemistry for gSyn in retinal sections of WT and Ins2^{Akita} mice of 6, 9 and 12-months old. N=5 to 6 and 9-months old group; N=4 to 12-months old group. Nucleus are stained with DAPI (blue) and gSyn stained with Alexa Fluor 488 GAR (Green). GCL, ganglion cell layer; IPL, inner plexiform layer; INL, inner nuclear layer; OPL, outer plexiform layer; ONL, outer nuclear layer. Confocal images obtained with a 40x objective.

gSyn, unlike aSyn and bSyn, is not present in the IPL. It presents a localization both in the GCL and in the INL of the retina of WT and Ins2^{Akita} of all ages (Fig. 3.8). The images obtained suggest that there might be an increased number of cell bodies of the INL containing gSyn in aged retinas, both in healthy but specially in diseased animals (Fig 3.8), but that will need quantification analysis for confirmation.

aSyn and bSyn protein levels were also assessed and compared between WT and Ins2^{Akita} samples of different ages (6, 9 and 12-months old) and between ages in WT and Ins2^{Akita} samples (Fig.3.9).

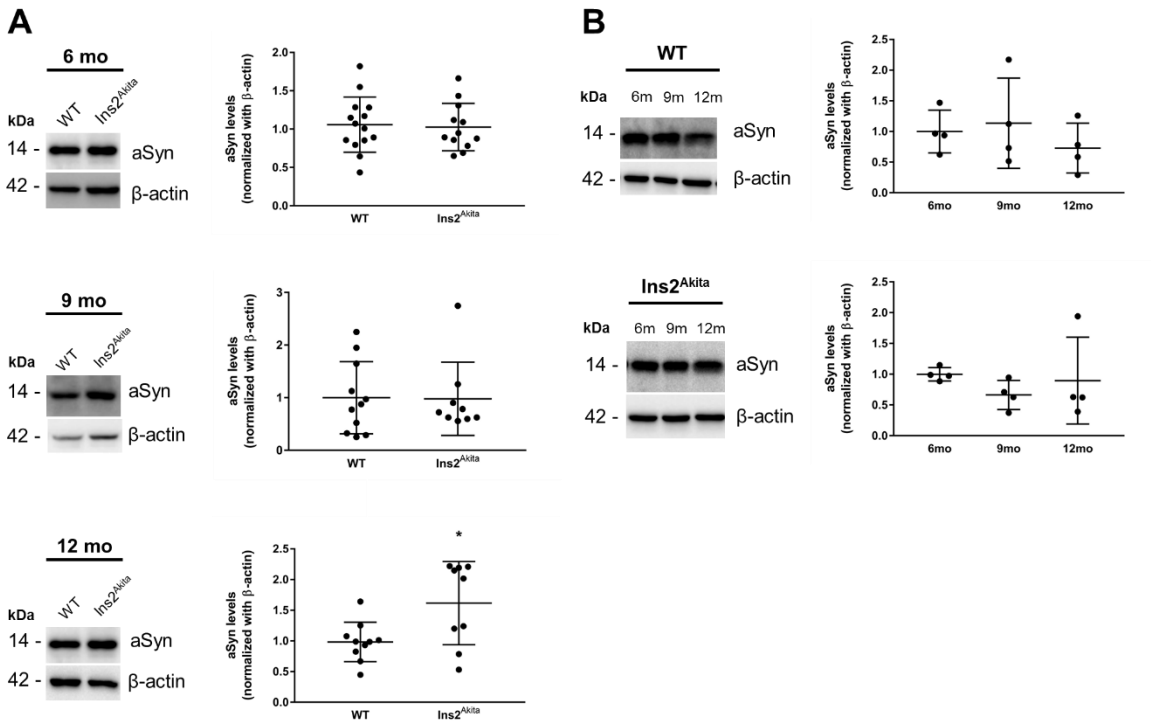

Fig. 3.9. Assessment of aSyn levels in 6, 9 and 12-months old WT and Ins2^{Akita} protein extracts from whole retina. A) Western blot for the comparison of aSyn protein levels between WT and Ins2^{Akita} mice of different ages (6, 9, and 12 months old). Data are presented as Mean ± SD. *p<0.05 Ins2^{Akita} compared with WT; T-test. B) Western blot for the comparison of aSyn protein levels between ages (6, 9 and 12-months old) in WT and Ins2^{Akita} mice. Data are presented as Mean ± SD.

aSyn levels are similar between WT and Ins2^{Akita} samples by 6 and 9-months old. However, by 12-months old, its levels are significantly increased in the Ins2^{Akita} samples (Fig. 3.9 A). Interestingly, also by 12 months old Ins2^{Akita} samples, there are to be two distinct groups with no distinct pattern, meaning that there is no explanation for this separation considering glycemia levels, weight and cages. Nevertheless, these differences do not seem to be biologically significant. aSyn levels do not seem to be affected with ageing nor disease progression since there are no significant differences between ages in WT and Ins2^{Akita} samples (Fig. 3.9 B).

bSyn was the next to be evaluated, compared between WT and Ins2^{Akita} samples of different ages (6, 9 and 12-months old) and between ages in WT and Ins2^{Akita} samples (Fig.3.10).

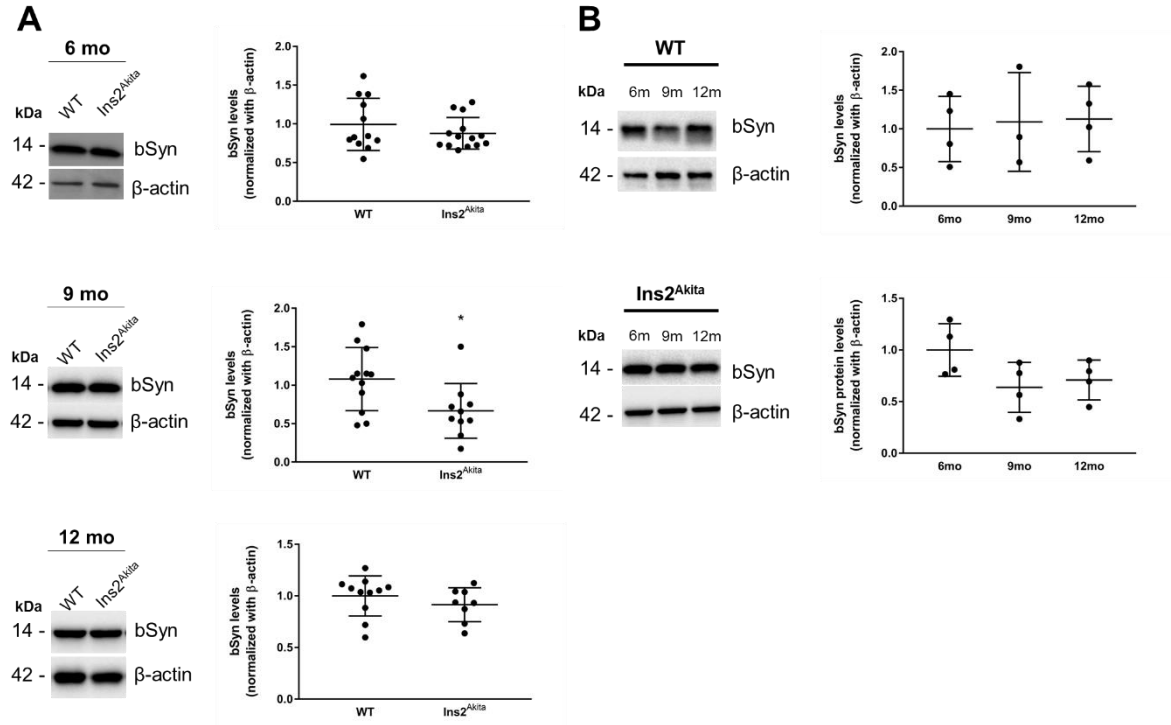

Fig. 3.10. Assessment of bSyn levels in 6, 9 and 12-months old WT and Ins2^{Akita} protein extracts from whole retina. A) Western blot for the comparison of bSyn protein levels between WT and Ins2^{Akita} mice of different ages (6, 9, and 12 months old). Data are presented as Mean ± SD. B) Western blot for the comparison of bSyn protein levels between ages (6, 9 and 12-months old) in WT and Ins2^{Akita} mice. Data are presented as Mean ± SD.

bSyn levels are similar between WT and Ins2^{Akita} samples by 6 and 12 months old. However, by 9 months old, it is significantly decreased in the Ins2^{Akita} samples. It is possible that, with ageing, we might be looking at a recovering from this difference (Fig. 3.10 A).

bSyn does not seem to be affected with ageing (Fig. 3.10 B).

It was not possible to assess the levels of gSyn as no signal was obtained for this protein using WB assay.

Overall, these results show that aSyn and bSyn are localized in the IPL the retina and that all three synucleins are localized in the cell bodies of the INL and GCL. bSyn is further localized in the OPL of retinas. The results also show that by 12 months old, both WT and Ins2^{Akita}, show a decreased number of cell bodies with aSyn in both the INL. Regarding GCL, there was a decreased number of cell bodies with aSyn with ageing in WT but not in Ins2^{Akita} mice. Furthermore, aSyn levels are increased by 12 months old Ins2^{Akita} when compared to WT samples of the same age, whereas bSyn decrease by 9 months old Ins2^{Akitas} when compared to controls.

3.2.2 Are aSyn and bSyn presynaptic proteins in the retina?

The IPL is composed of the synaptic terminals of bipolar, amacrine and ganglion cells. Previously, the results obtained indicated that aSyn and bSyn are expressed in the IPL of these mice retinas. In order to specify these proteins location in this layer, synaptic markers were used.

Synaptophysin is an integral membrane glycoprotein that occurs in presynaptic vesicles of neurons, thought to play several roles in synaptic function, including exocytosis, synapse formation, biogenesis and endocytosis of synaptic vesicles (136–140). Although no direct contact between aSyn and Synaptophysin is established, both proteins are involved in trafficking of synaptic vesicles, interacting with several other proteins (141). aSyn colocalization with Synaptopysin in the IPL was quantified and the profile of presynaptic marker Synaptophysin with ageing and diabetes evaluated through Western Blot (Fig. 3.11).

aSyn and Synaptophysin colocalized in s1, s3 and s5 of the IPL of WT and $Ins2^{Akita}$ mice retinas of all ages (6, 9 and 12-months old) (Fig. 3.11 A). Regarding the quantification of the colocalization of both proteins in the IPL, the percentage of aSyn that colocalizes with Synaptophysin and the percentage of Synaptophysin that colocalizes with aSyn in the IPL is similar between WT and $Ins2^{Akita}$ retinas, showing no differences with ageing as well (Fig. 3.11 B). Synaptophysin protein levels are also similar between WT and $Ins2^{Akita}$ samples of all ages (6, 9 and 12-months old), revealing no changes with diabetes nor ageing in WT mice (Fig. 3.11 C).

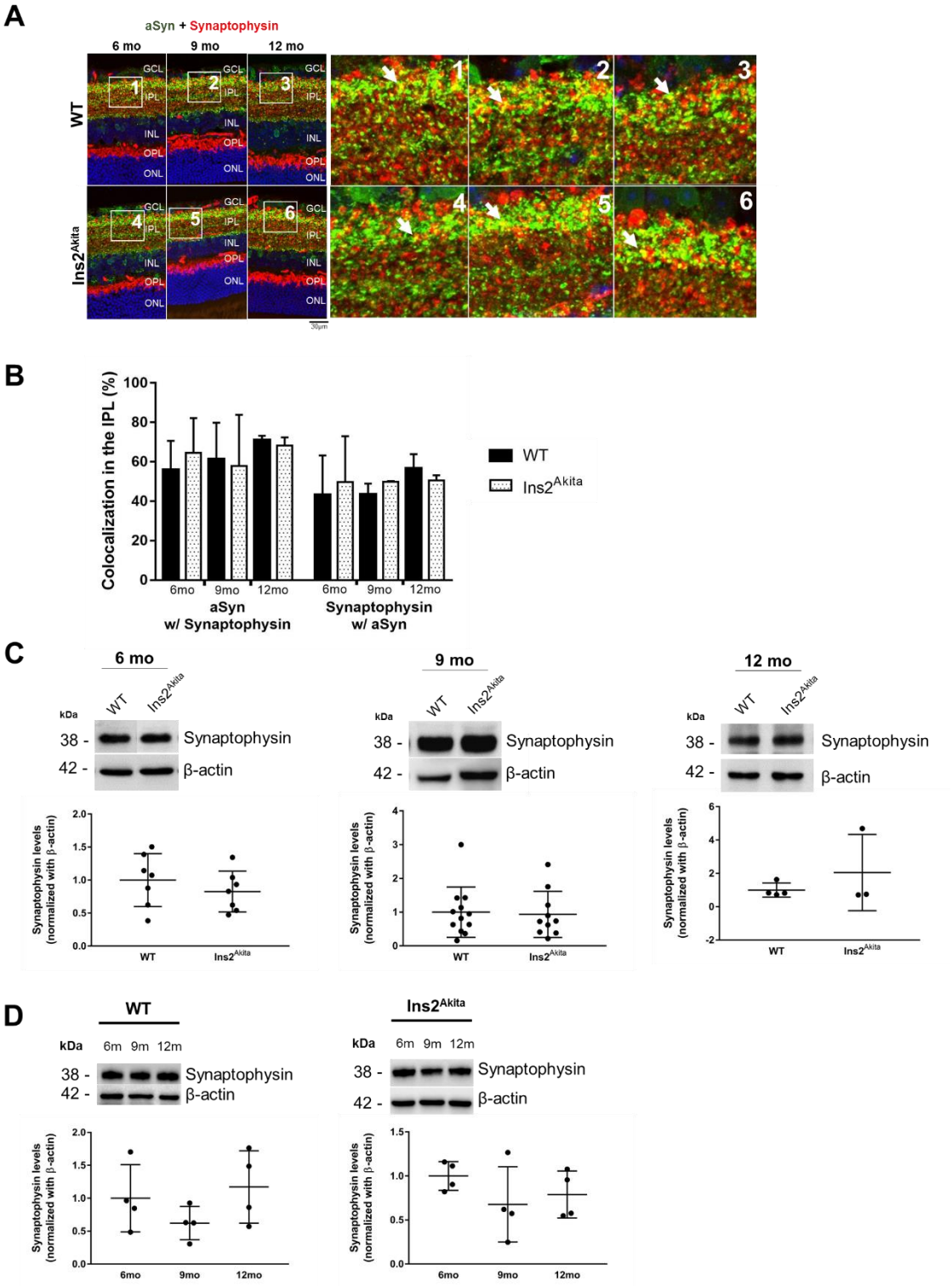

Fig. 3.11. Evaluation of the profile of presynaptic marker Synaptophysin with ageing and diabetes and its colocalization with aSyn in the same conditions. N=5 to 6 and 9-months old group; N=3 to 12-months old group. (A) Immunohistochemistry for aSyn and Synaptophysin colocalization evaluation in retinal sections of 6, 9 and 12-months old WT and Ins2^{Akita} mice. Nucleus are stained with DAPI (blue), aSyn stained with Alexa Fluor 488 GAR (Green) and Synaptophysin stained with Alexa Fluor 594 GAM (red). GCL, ganglion cell layer; IPL, inner plexiform layer; INL, inner nuclear layer; OPL, outer plexiform layer; ONL, outer nuclear layer. White

arrows indicate the colocalization sites. Confocal images obtained with a 40x objective. (B) Quantification of aSyn and Synaptophysin colocalization in the IPL of 6, 9 and 12-months old WT and Ins2^{Akita} mice retinas. N=3 to each group. Data are presented as Mean ± SD. (C) Western blot for the comparison of Synaptophysin protein levels between WT and Ins2^{Akita} mice of different ages (6, 9, and 12 months old). Data are presented as Mean ± SD. (D) Western blot for the comparison of Synaptophysin protein levels in WT and Ins2^{Akita} mice between ages (6, 9, and 12 months old). Data are presented as Mean ± SD.

The colocalization between bSyn and Synaptophysin was also evaluated (Fig. 3.12).

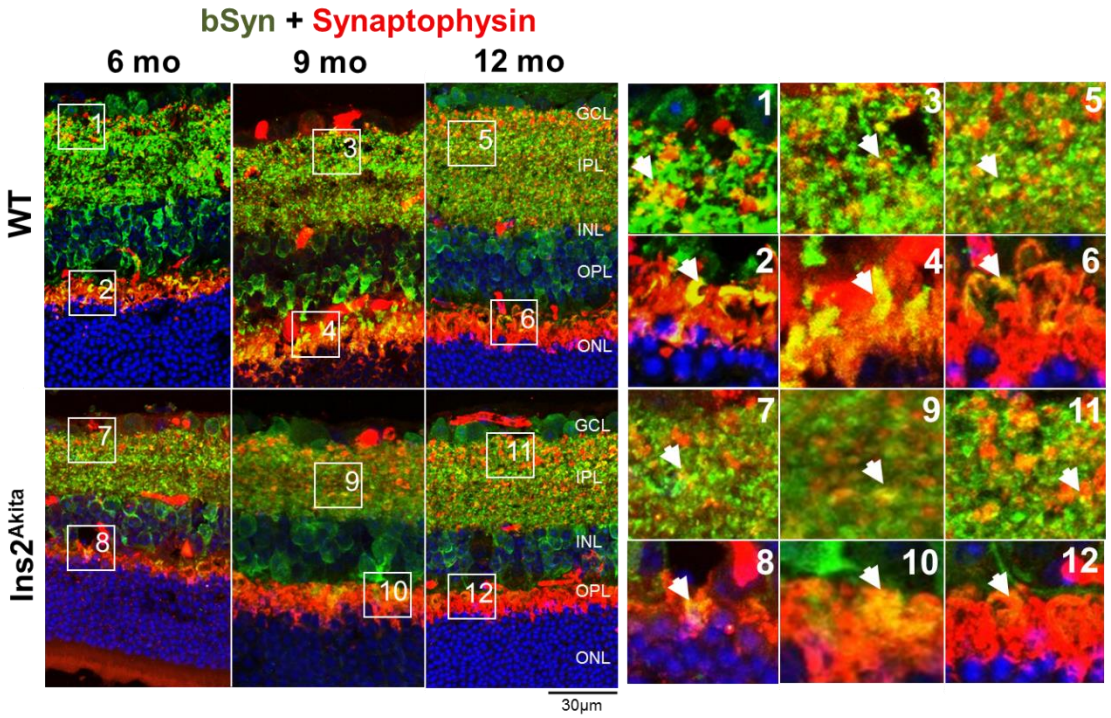

Fig. 3.12. Immunohistochemistry with colocalization between bSyn and Synaptophysin in retinal sections of WT and Ins2^{Akita} mice of 6, 9 and 12-months old. N=3 to each group. White arrows indicate the colocalization sites. Nucleus are stained with DAPI (blue), bSyn stained with Alexa Fluor 488 GAR (Green) and Synaptophysin stained with Alexa Fluor 594 GAM (red). GCL, ganglion cell layer; IPL, inner plexiform layer; INL, inner nuclear layer; OPL, outer plexiform layer; ONL, outer nuclear layer. Confocal images obtained with a 40x objective.

bSyn and Synaptophysin colocalize both in the IPL and OPL of WT and Ins2^{Akita} mice retinas of all ages. In the IPL, this colocalization seems to be specifically happening between s3 and s5 (Fig. 3.12). For more conclusions to be drawn, quantification of the colocalization between bSyn and Synaptophysin in the IPL must be performed.

Syntaxin 1A is a specific presynaptic marker for amacrine cells, being of special importance for the trafficking of synaptic vesicles as part of the SNARE complex (142). The colocalization between aSyn and Syntaxin 1A, as well as the profile of presynaptic marker Syntaxin 1A with ageing and diabetes were evaluated (Fig. 3.13).

aSyn and Syntaxin 1A colocalize in the IPL of WT and Ins2^{Akita} mice retinas of all ages, specially in s1, s3 and s5 due to aSyn described stratification (Fig. 3.13 A). Moreover, aSyn and Syntaxin 1A colocalize in cell bodies of the INL of WT and Ins2^{Akita} retinas of all ages, corresponding to amacrine cells of the INL (Fig. 3.13 A). Interestingly, by 9 and 12-months old Ins2^{Akita} retinas, these two proteins also colocalize in cell bodies of the GCL, where few amacrine cells exist (Fig. 3.13 A, 7 and 8).

Considering the quantification of aSyn colocalization with Syntaxin 1A in the IPL, it is considerably increased between 6 and 9-months old WT samples (46.12 ± 8.59 vs 72.36 ± 2.33), but to drastically decrease by 12 months old when compared to 9 months old samples (44.86 ± 8.82). Similarly, in Ins2^{Akita} samples, the percentage of aSyn that colocalizes with Syntaxin 1A significantly decreases between 9 and 12-months old samples (83.33 ± 4.49 vs 53.75 ± 4.42) (Fig. 3.13 B). Regarding the percentage of Syntaxin 1A that colocalizes with aSyn in the IPL, it is significantly increased in 9 months old Ins2^{Akita} samples, when compared to 9 months old controls (59.56 ± 0.74 vs 90.83 ± 2.18). It is also significantly increased by 9 months old WT when compared to 6 months old controls (59.56 ± 0.74 vs 32.03 ± 5.11). Between Ins2^{Akita} samples, it is considerably decreased by 12 months old when compared to 9 months old samples (53.53 ± 4.79 vs 90.83 ± 2.1) (Fig. 3.13 B).

Regarding Syntaxin 1A protein levels, it is significantly decreased by 6 months old Ins2^{Akita} samples when compared to controls (0.67 ± 0.05 vs 1 ± 0.17 vs) and by 9 months old (0.45 ± 0.27 vs 1 ± 0.66), seeming to recover by 12 months old where the levels appear to be similar between conditions (Fig. 3.13 C).

Ageing also seems to affect this protein. In controls, its levels are significantly higher by 9 months old when compared with younger and older WT mice (6 and 12-months old WT mice) (1.65 ± 0.21 vs 1 ± 0.22 and 1.65 ± 0.21 vs 1.08 ± 0.27). In Ins2^{Akita} samples there are no differences between ages (Fig. 3.13 D).

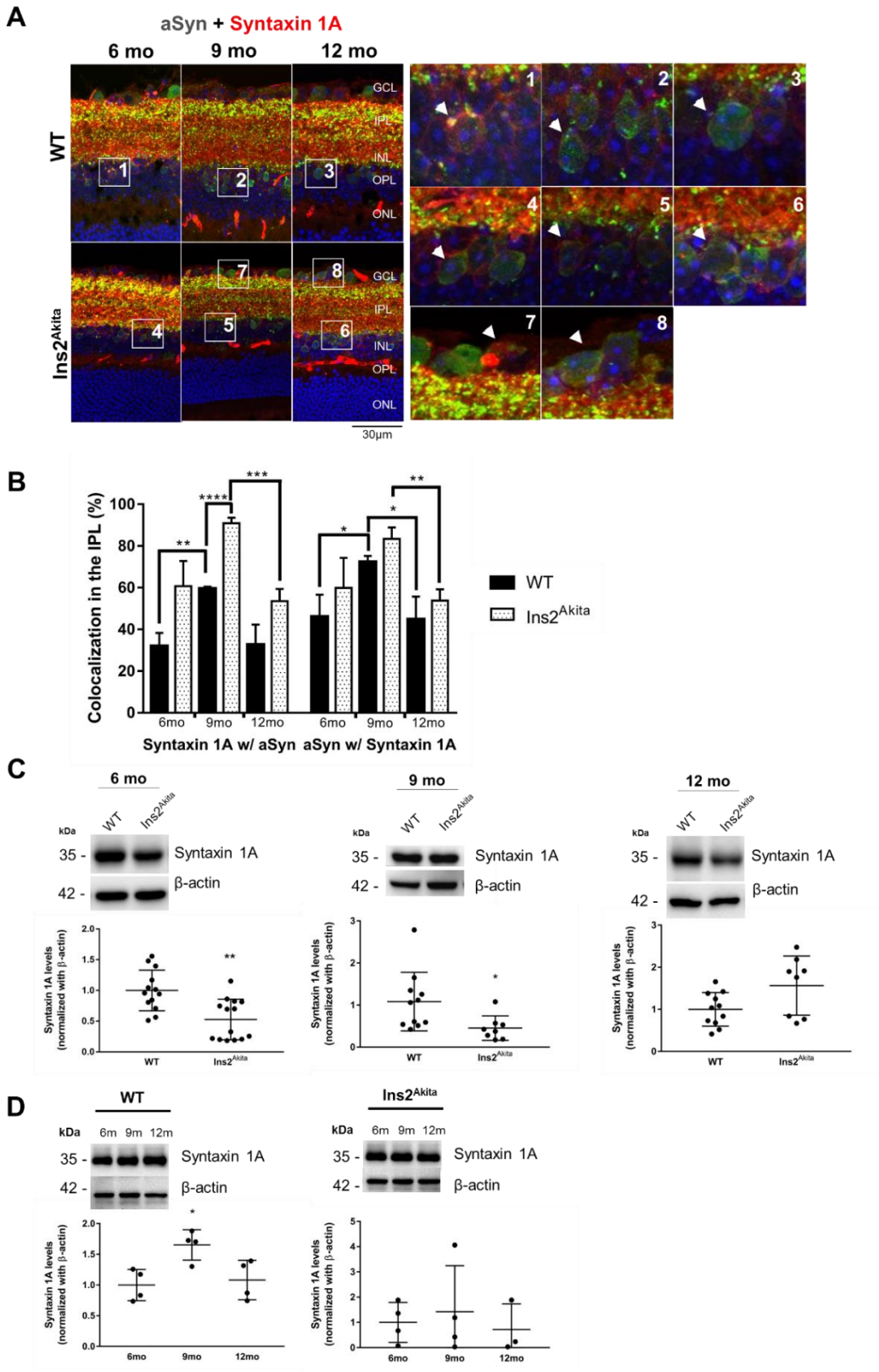

Fig. 3.13. Evaluation of the profile of presynaptic marker Syntaxin 1A with ageing and diabetes and its colocalization with aSyn in the same conditions. N=5 to 6 and 9-months old group; N=3 to 12-months old group. (A) Immunohistochemistry for aSyn and Syntaxin 1A colocalization evaluation in retinal sections of 6, 9

and 12-months old WT and Ins2^{Akita} mice. Nucleus are stained with DAPI (blue), aSyn stained with Alexa Fluor 488 GAR (Green) and Syntaxin 1A stained with Alexa Fluor 594 GAM (red). GCL, ganglion cell layer; IPL, inner plexiform layer; INL, inner nuclear layer; OPL, outer plexiform layer; ONL, outer nuclear layer. White arrows indicate the colocalization sites. Confocal images obtained with a 40x objective. (B) Quantification of aSyn and Syntaxin 1A colocalization in the IPL of 6, 9 and 12-months old WT and Ins2^{Akita} mice retinas. N=3 to each group. Data are presented as Mean ± SD. *p<0.05, **p<0.005, ***p<0.0005, ****p<0.001 ; Mann-Whitney test. (C) Western blot for the comparison of Syntaxin 1A protein levels between WT and Ins2^{Akita} mice of different ages (6, 9, and 12 months old). Data are presented as Mean ± SD. *p<0.05, **p<0.005 Ins2^{Akita} compared with WT; T-test. (D) Western blot for the comparison of Syntaxin 1A protein levels in WT and Ins2^{Akita} mice between ages (6, 9, and 12 months old). Data are presented as Mean ± SD. *p<0.05 9 months old WT compared with 6 and 12-months old WT; T-test.

The colocalization between bSyn and Syntaxin 1A was also evaluated (Fig. 3.14).

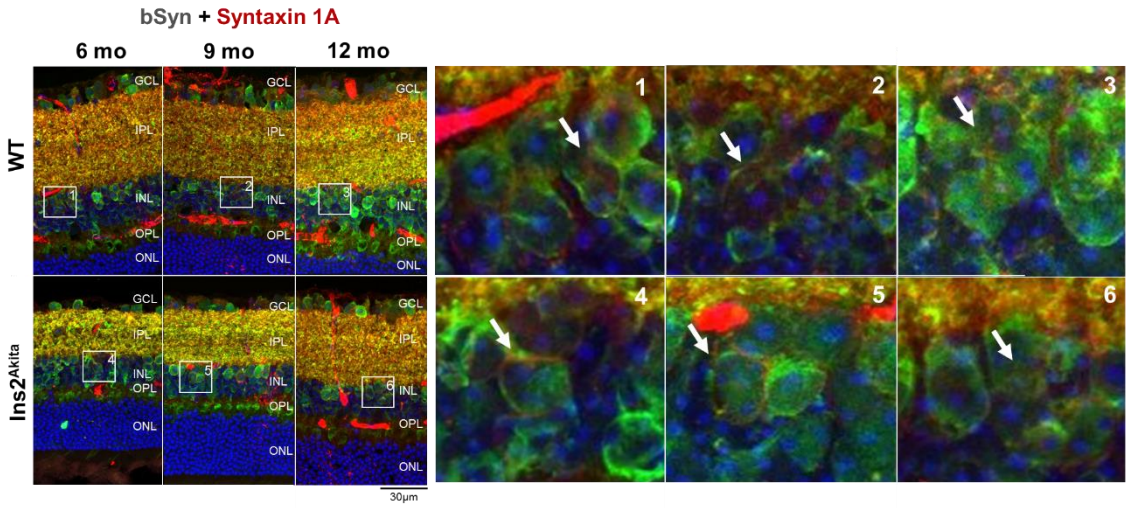

Fig. 3.14. Immunohistochemistry with colocalization between bSyn and Syntaxin 1A in retinal sections of WT and Ins2^{Akita} mice of 6, 9 and 12-months old. N=3 to each group. White arrows indicate the colocalization sites. Nucleus are stained with DAPI (blue), bSyn stained with Alexa Fluor 488 GAR (Green) and Syntaxin 1A stained with Alexa Fluor 594 GAM (red). GCL, ganglion cell layer; IPL, inner plexiform layer; INL, inner nuclear layer; OPL, outer plexiform layer; ONL, outer nuclear layer. Confocal images obtained with a 40x objective.

bSyn and Syntaxin 1A colocalize both in the IPL as well as the INL of WT and Ins2^{Akita} mice retinas of all ages. In the IPL, this colocalization seems to be similarly distributed between strata (Fig. 3.14). However, quantification analysis can be more detailed information.

Overall these results show that both aSyn and bSyn are presynaptic proteins in the retina and that both are located in amacrine cells and their terminals. Furthermore, the quantification of the colocalization between aSyn and Syntaxin 1A in the IPL indicated that the colocalization between both proteins decreases by 12 months old for both WT and Ins2^{Akita} samples.

3.2.3 Colocalization between the synucleins

Next, it was evaluated if the members of the synuclein family can be expressed in the same neuronal cell types of the retina, since colocalization might implicate some form of synergistic or antagonistic relation between them. IHC was performed in 6, 9 and 12-months old WT and Ins2^{Akita} mice retinas and the colocalization of aSyn and bSyn and aSyn and gSyn evaluated and, when between aSyn and bSyn in the IPL, quantified (Fig. 3.15 and 3.16, respectively).

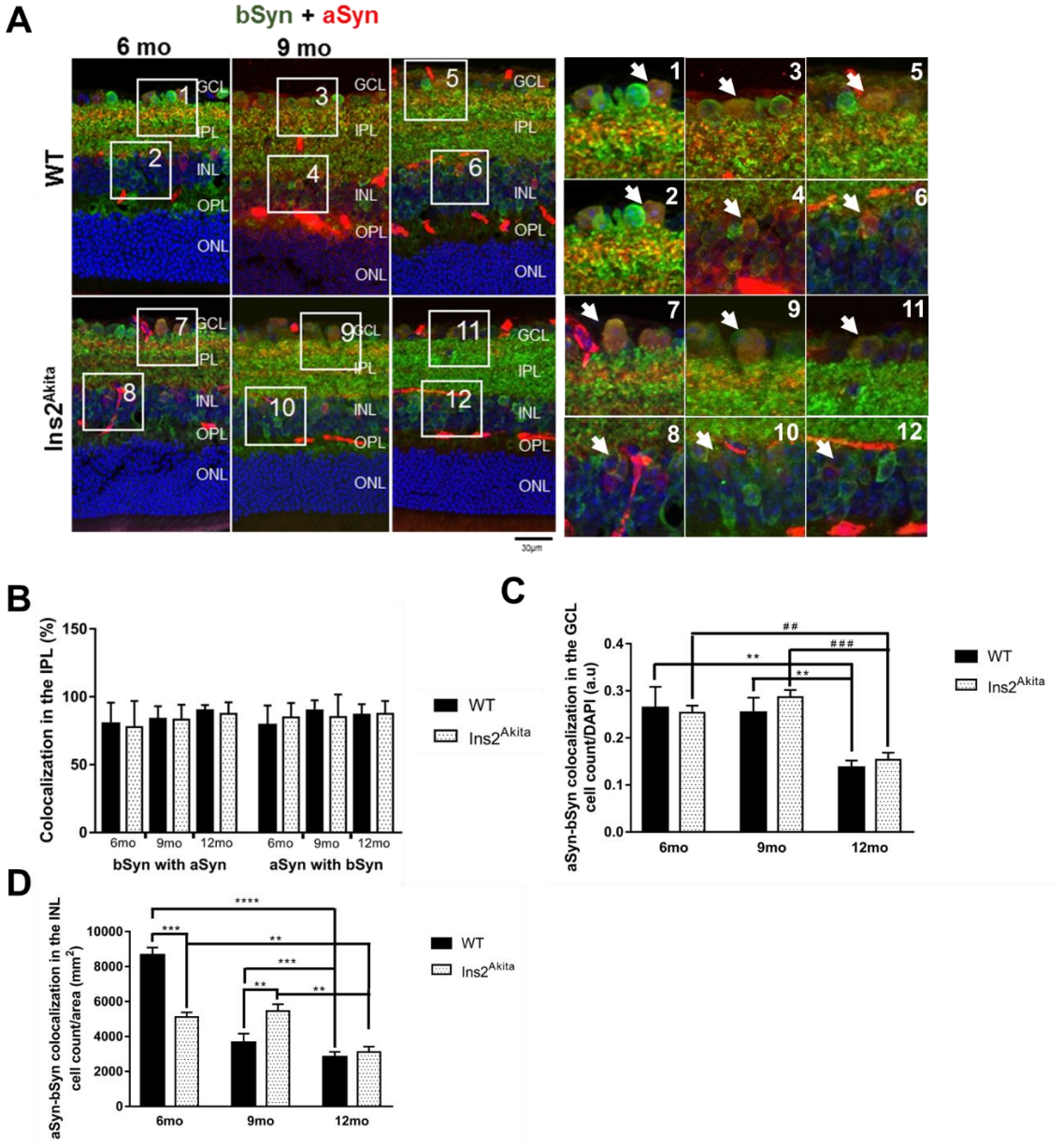

Fig. 3.15. Evaluation of the colocalization of aSyn and bSyn in retinal sections of WT and Ins2^{Akita} mice of 6, 9 and 12-months old. N=5 to 6 and 9-months old group; N=4 to 12-months old group. A) Confocal imaging of the colocalization of aSyn and bSyn in 6, 9 and 12-months old WT and Ins2^{Akita} retinas. Nucleus are stained with DAPI (blue), bSyn stained with Alexa Fluor 488 GAR (Green) and aSyn stained with Alexa Fluor 594 GAM (red). GCL, ganglion cell layer; IPL, inner plexiform layer; INL, inner nuclear layer; OPL, outer plexiform layer; ONL, outer nuclear layer. White arrows indicate the colocalization sites. Confocal images obtained with a 40x

objective. B) Quantification of the colocalization of aSyn and bSyn in the IPL of 6, 9 and 12-months old retinas. N=5 to 6 and 9-months old group; N=4 to 12-months old group. Data are presented as Mean ± SD. C) Quantification of the colocalization of aSyn and bSyn in the GCL of 6, 9 and 12-months old retinas. N=3 to each group. Data are presented as Mean ± SD. **p<0.005 12 months old WT when compared to 6 and 9-months old WT; ##p<0.005 12 months old $Ins2^{Akita}$ when compared to 6 and 9-months old $Ins2^{Akita}$. D) Quantification of the colocalization of aSyn and bSyn in the INL of 6, 9 and 12-months old retinas. N=3 to each group. Data are presented as Mean ± SD. **p<0.005, ***p<0.0005, ****p<0.001 ; T-test.

The results indicate that aSyn and bSyn colocalize in the IPL but also in the GCL and INL (Fig. 3.15 A). In the INL, it looks like by 12 months old $Ins2^{Akita}$ retinas, colocalization is less evident (Fig. 3.15 A). Considering the quantification of aSyn and bSyn colocalization in the IPL, results show that there are no differences between WT and $Ins2^{Akita}$ retinas (Fig. 3.15 B). Regarding aSyn and bSyn colocalization in the GCL, there seem to be no differences between WT and $Ins2^{Akita}$ retinas. However, with ageing, it is significantly decreased by 12 months old WT mice when compared to 6 and 9-months old controls (0.13 ± 0.01 vs 0.26 ± 0.03 and 0.13 ± 0.01 vs 0.25 ± 0.02). The same happens for $Ins2^{Akita}$ samples where aSyn and bSyn colocalization is significantly decreased by 12 months old WT mice when compared to 6 and 9-months old controls (0.15 ± 0.01 vs 0.25 ± 0.01 and 0.15 ± 0.01 vs 0.28 ± 0.01) (Fig. 3.15 C).

Regarding aSyn and bSyn colocalization in the INL, it is significantly lower in the $Ins2^{Akita}$ retinas by 6 months old when compared to controls (5510 ± 219.69 vs 8657 ± 354) but to be significantly higher by 9 months old (5450 ± 325.67 vs 3643.67 ± 425.74). By 12 months old, there seem to be no differences between WT and $Ins2^{Akita}$ samples (Fig. 3.15 D). Furthermore, it is significantly lower in the 12 months old WT when compared to other control ages (6 and 9-months old)(2823.67± 243.05 vs 8657 ± 354 and 2823.67± 243.05 vs 3643.67 ± 425.74), as well as significantly lower in the 12 months old $Ins2^{Akita}$ samples, when compared to the other ages (6 and 9-months old)(3110 ± 253.11 vs 5110 ± 219.69 and 3110 ± 253.11 vs 5450 ± 325.67)(Fig. 3.15 D).

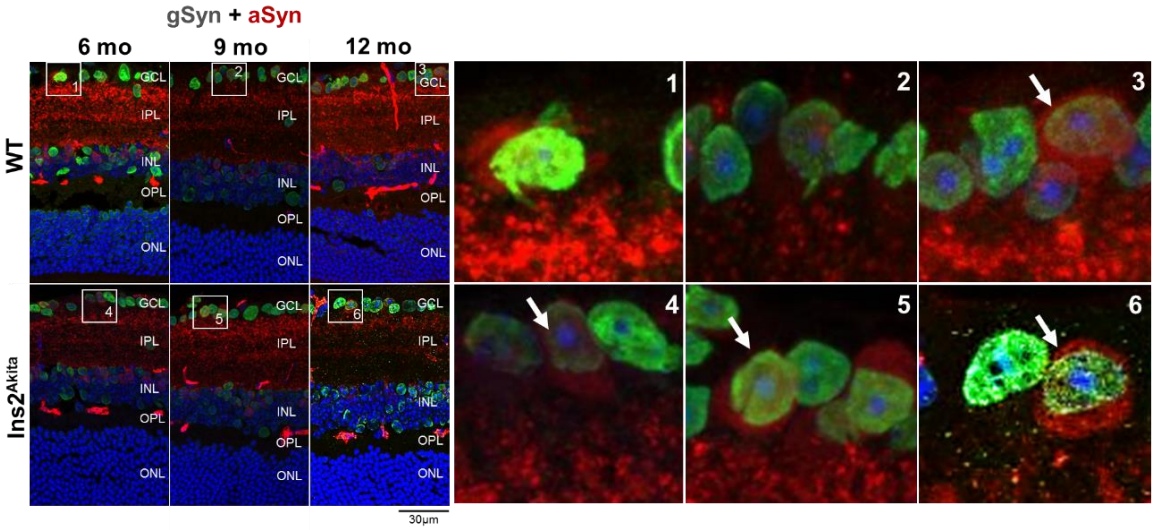

Fig. 3.16. Immunohistochemistry with colocalization between aSyn and gSyn in retinal sections of WT and Ins2^{Akita} mice of 6, 9 and 12-months old. N=5 to 6 and 9-months old group; N=4 to 12-months old group. Nucleus are stained with DAPI (blue), gSyn stained with Alexa Fluor 488 GAR (Green) and aSyn stained with Alexa Fluor 594 GAM (red). GCL, ganglion cell layer; IPL, inner plexiform layer; INL, inner nuclear layer; OPL, outer plexiform layer; ONL, outer nuclear layer. White arrows indicate the colocalization sites. Confocal images obtained with a 40x objective.

Considering aSyn colocalization with gSyn, it is observed in the GCL. Although no quantification was done, images suggest that the colocalization is more evident by 12 months old WT and by Ins2^{Akita} samples (Fig. 3.16).

Overall, these results show that aSyn colocalizes with both bSyn and gSyn. aSyn and bSyn not only colocalize in the IPL, with no differences between WT and Ins2^{Akita} of all ages, but also in the INL and GCL, where their colocalization is decreased in late stages of the disease (12 months old).

3.2.3. The synucleins and specific retinal neuronal markers

As previously described, the retina is composed of several layers, each hosting different neuronal cell populations. To further and more accurately evaluate the localization of the synucleins in the retina, specific neuronal cell markers were used and their colocalization with the synucleins analyzed.

Previous results showed that aSyn was localized in the presynaptic terminals of amacrine cells, further being localized in amacrine cell bodies in the INL. As mentioned, dopaminergic amacrine cells are extremely important due to their ability to produce and release dopamine: a system that, when disrupted in the brain leads to motor features (143). TH is a specific marker for dopaminergic amacrine cells, considering its role as a mediator in the production of dopamine (84). The colocalization between aSyn and TH was determined and the number of dopaminergic amacrine neurons containing aSyn quantified in order to evaluate these cells behaviour with ageing and diabetes progression and a possible relation with aSyn (fig. 3.17).

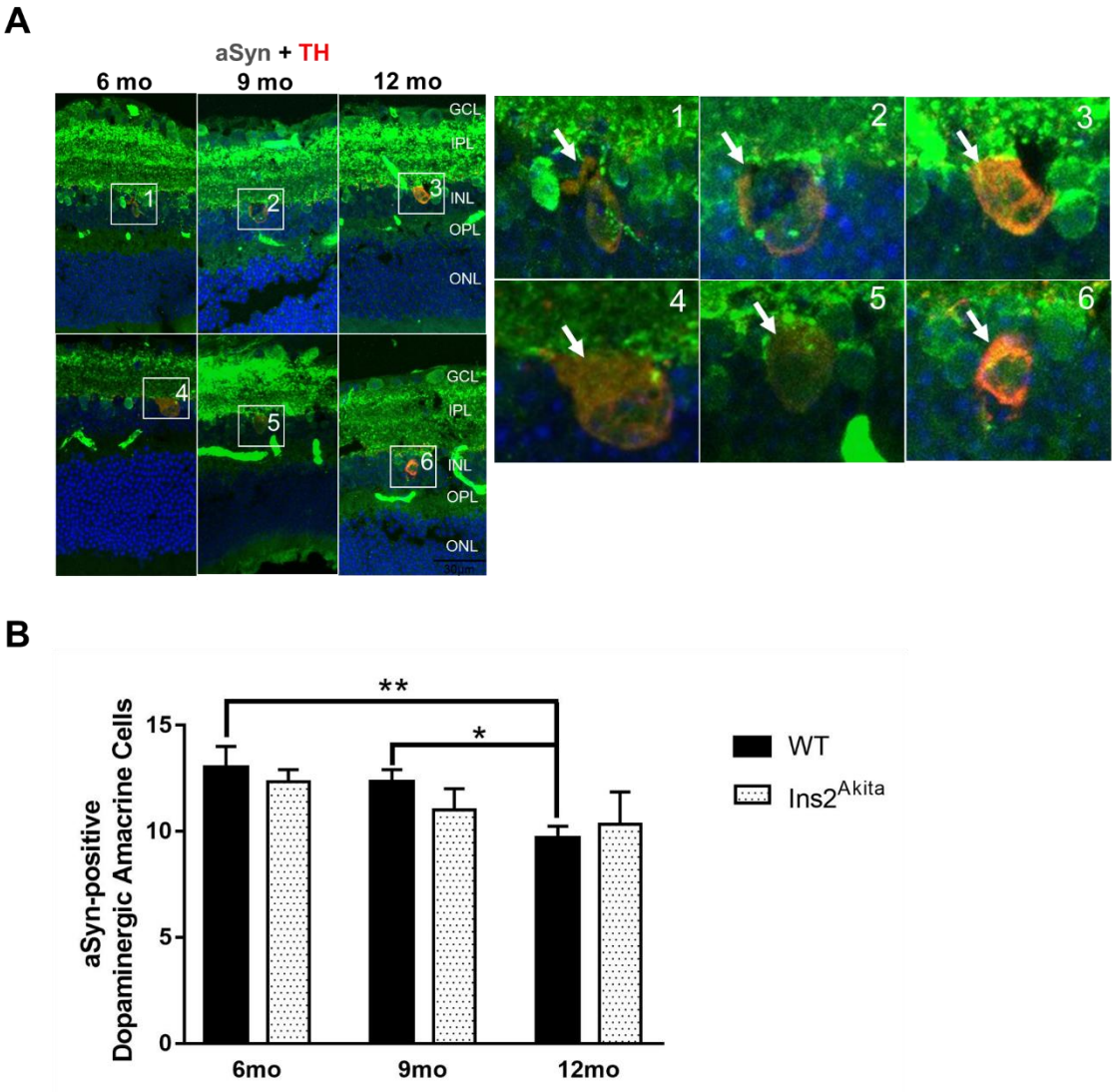

Fig. 3.17. Evaluation of the profile of dopaminergic amacrine cells with ageing and DR and the colocalization of TH with aSyn in the same conditions. N=3 to each group. (A) Immunohistochemistry for aSyn and TH colocalization evaluation in retinal sections of 6, 9 and 12-months old WT and Ins2^{Akita} mice. Nucleus are stained with DAPI (blue), aSyn stained with Alexa Fluor 488 GAR (Green) and TH stained with Alexa Fluor 594 GAM (red). GCL, ganglion cell layer; IPL, inner plexiform layer; INL, inner nuclear layer; OPL, outer plexiform layer; ONL, outer nuclear layer.Confocal images obtained with a 40x objective. (B) Quantification of aSyn and TH colocalization in cell bodies of the INL/TH-positive cell bodies in the INL of 6, 9 and 12-months old WT and Ins2^{Akita} mice retinas. N=3 to each group. Data are presented as Mean ± SD. * p>0.05 9 months old WT compared to 12 months old WT; ** p>0.005 6 months old WT compared to 12 months old WT; Mann-Whitney test.

aSyn and TH colocalize in the INL in both WT and Ins2^{Akita} retinas of all ages (6, 9 and 12-months old) (Fig. 3.17 A). The images analysed, within a total of 3N to each group, demonstrated that aSyn and TH may colocalize in 100% of cases. There is a tendency for these cells to significantly decrease in number with ageing in healthy animals, considering that the number of dopaminergic cells are

significantly higher by 6 months old than by 12 months old (13 ± 0.81 vs 9.66 ± 0.47) and significantly higher by 9 months old than by 12 months old (12.33 ± 0.47 vs 9.66 ± 0.47)(Fig. 3.17 B). However, between WT and Ins2^{Akita} and between Ins2^{Akita} samples there seem to be no differences (Fig. 3.17 B).

PKC-α is an abundant protein in retinal bipolar cells, due to its role in the activation of these cells (144). Therefore, it is a specific marker for this neuronal cell population retina, which are the most direct pathway between the photoreceptors and ganglion cells. It's colocalization with the synucleins was evaluated (Fig. 3.18 – 3.20) and a match found for bSyn (3.19).

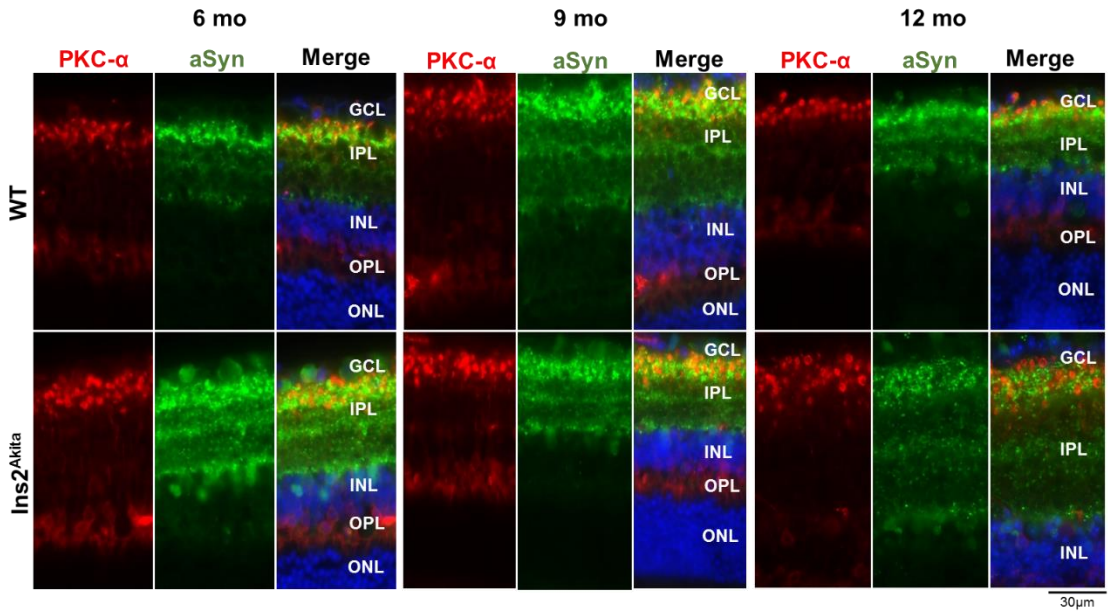

Fig. 3.18. Immunohistochemistry with colocalization between aSyn and PKC-α in retinal sections of WT and Ins2^{Akita} mice of 6, 9 and 12-months old. N=3 to each group. Nucleus are stained with DAPI (blue), aSyn stained with Alexa Fluor 488 GAR (Green) and PKC-α stained with Alexa Fluor 594 GAM (red). GCL, ganglion cell layer; IPL, inner plexiform layer; INL, inner nuclear layer; OPL, outer plexiform layer; ONL, outer nuclear layer. White arrows indicate the colocalization sites. Fluorescence microscope Zeiss Z2 images obtained with a 40x objective.

aSyn and PKC-α seem to colocalize in the IPL, although no colocalization seems to occur in the INL where bipolar cells are. However, confocal analyzis shows that there is no colocalization between aSyn and PKC-α in WT and Ins2^{Akita} retinas of all ages (Fig. 3.18).

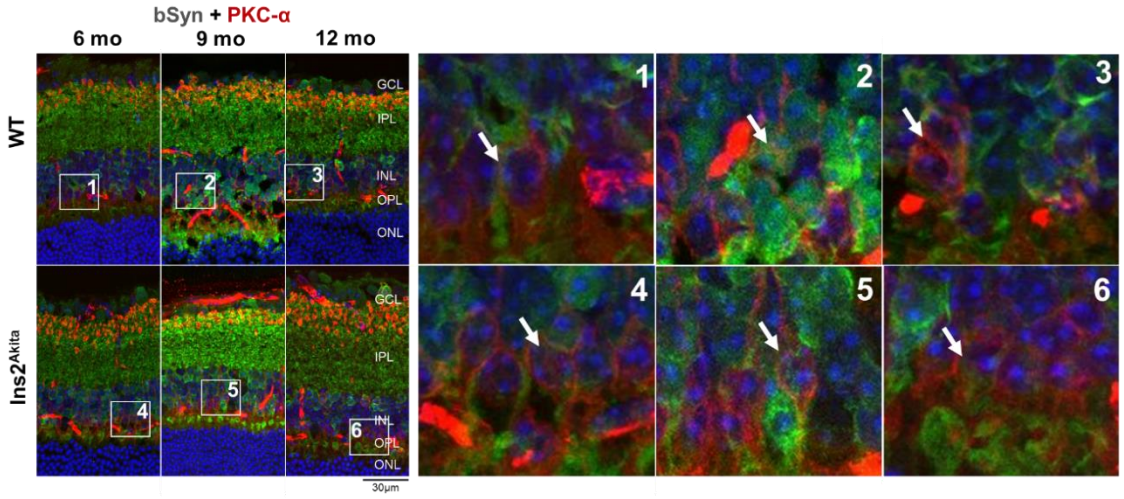

Fig. 3.19. Immunohistochemistry with colocalization between bSyn and PKC-α in retinal sections of WT and Ins2^{Akita} mice of 6, 9 and 12-months old. N=5 to 6 and 9-months old group; N=3 to 12-months old group. Nucleus are stained with DAPI (blue), bSyn stained with Alexa Fluor 488 GAR (Green) and PKC-α stained with Alexa Fluor 594 GAM (red). GCL, ganglion cell layer; IPL, inner plexiform layer; INL, inner nuclear layer; OPL, outer plexiform layer; ONL, outer nuclear layer. White arrows indicate the colocalization sites. Confocal images obtained with a 40x objective.

bSyn and PKC-α do colocalize in the IPL and in the INL (Figure 3.18). The images obtained show no clear differences in bSyn and PKC-α colocalization between WT and Ins2^{Akita} retinas of all ages (Fig. 3.19).

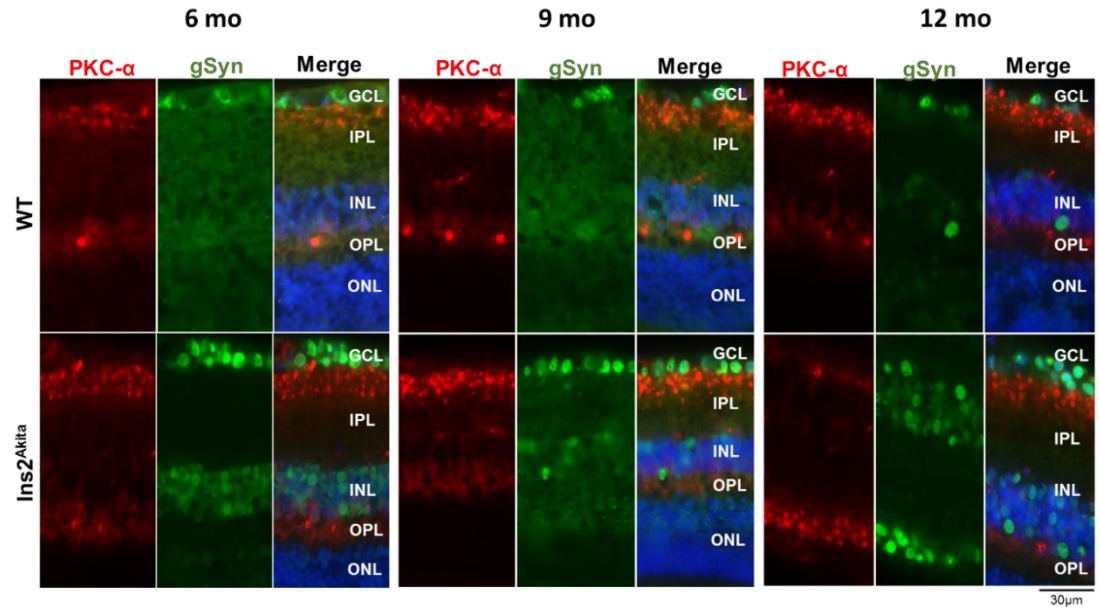

Fig. 3.20. Immunohistochemistry with colocalization between gSyn and PKC-α in retinal sections of WT and Ins2^{Akita} mice of 6, 9 and 12-months old. N=3 to each group. Nucleus are stained with DAPI (blue), gSyn stained with Alexa Fluor 488 GAR (Green) and PKC-α stained with Alexa Fluor 594 GAM (red). GCL, ganglion cell layer; IPL, inner plexiform layer; INL, inner nuclear layer; OPL, outer plexiform layer; ONL, outer nuclear

layer. White arrows indicate the colocalization sites. Fluorescence microscope Zeiss Z2 images obtained with a 40x objective.

gSyn and PKC-α do not colocalize in WT and Ins2^{Akita} retinas of 6, 9 and 12-months old (Fig. 3.20). These results were confirmed in the confocal microscope.

Calbindin is a specific marker for horizontal cells, which allow the interactions between photoreceptors and bipolar cells (47,50,145). It's colocalization with the synucleins was evaluated (Fig. 21-23) and a match found for gSyn (Fig. 3.22).

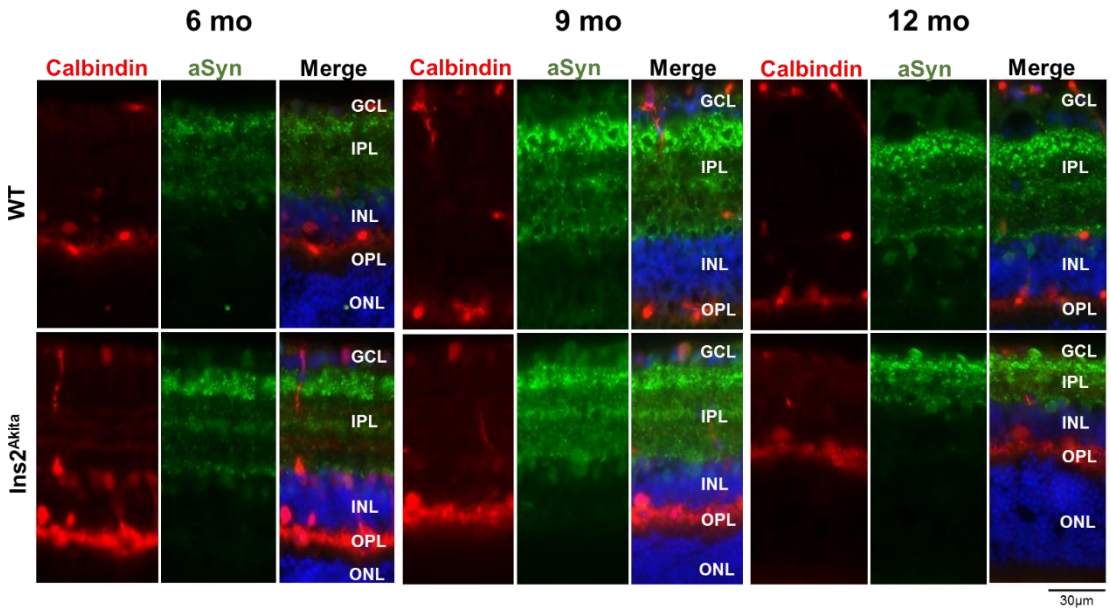

Fig. 3.21. Immunohistochemistry with colocalization between aSyn and Calbindin in retinal sections of WT and Ins2^{Akita} mice of 6, 9 and 12-months old. N=3 to each group. Nucleus are stained with DAPI (blue), aSyn stained with Alexa Fluor 488 GAR (Green) and Calbindin stained with Alexa Fluor 594 GAM (red). GCL, ganglion cell layer; IPL, inner plexiform layer; INL, inner nuclear layer; OPL, outer plexiform layer; ONL, outer nuclear layer. Fluorescence microscope Zeiss Z2 images obtained with a 40x objective.

aSyn and Calbindin do not colocalize in WT and Ins2^{Akita} retinas of 6, 9 and 12-months old (Fig. 3.21). These results were confirmed in the confocal microscope.

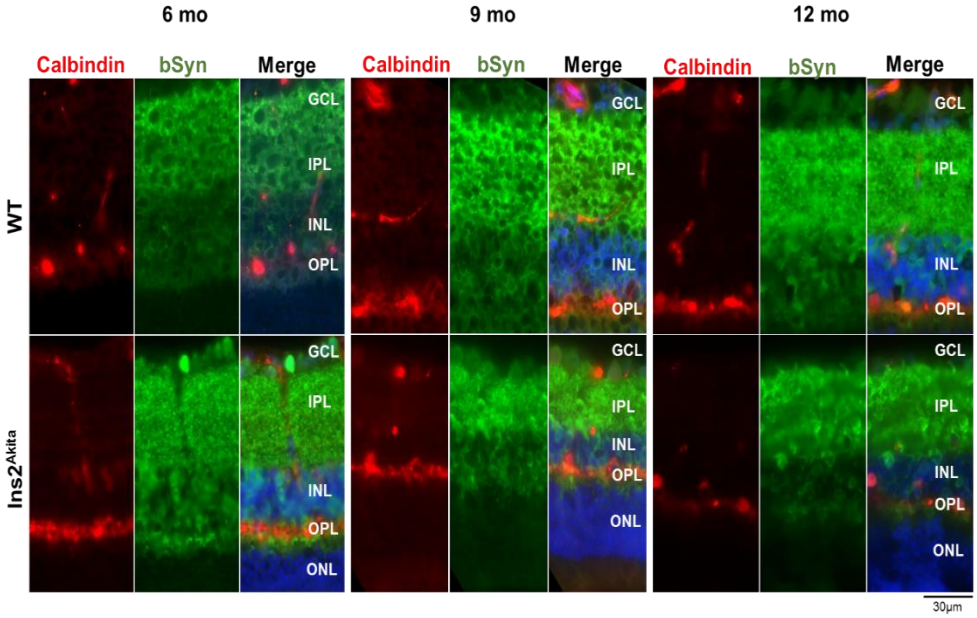

Fig. 3.22. Immunohistochemistry with colocalization between bSyn and Calbindin in retinal sections of WT and Ins2^{Akita} mice of 6, 9 and 12-months old. N=3 to each group. Nucleus are stained with DAPI (blue), gSyn stained with Alexa Fluor 488 GAR (Green) and Calbindin stained with Alexa Fluor 594 GAM (red). GCL, ganglion cell layer; IPL, inner plexiform layer; INL, inner nuclear layer; OPL, outer plexiform layer; ONL, outer nuclear layer. Fluorescence microscope Zeiss Z2 images obtained with a 40x objective.

bSyn and Calbindin do not colocalize in WT and Ins2^{Akita} retinas of 6, 9 and 12-months old (Fig. 3.22). These results were confirmed in the confocal microscope.

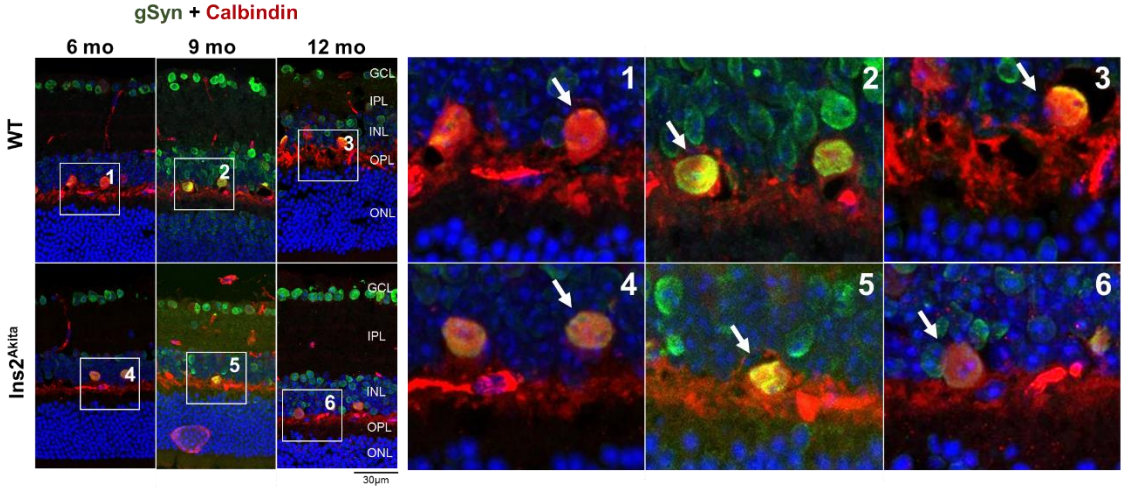

Fig. 3.23. Immunohistochemistry with colocalization between gSyn and Calbindin in retinal sections of WT and Ins2^{Akita} mice of 6, 9 and 12-months old. N=5 to 6 and 9-months old group; N=3 to 12-months old group. Nucleus are stained with DAPI (blue), gSyn stained with Alexa Fluor 488 GAR (Green) and Calbindin stained with Alexa Fluor 594 GAM (red). GCL, ganglion cell layer; IPL, inner plexiform layer; INL, inner nuclear layer; OPL, outer plexiform layer; ONL, outer nuclear layer. Confocal images obtained with a 40x objective.

gSyn and Calbindin colocalize in the INL, from 6 to 12-months old WT and Ins2^{Akita} mice retinas. The images, acquired using the same parameters, seem to reveal that, by 9 months old, the colocalization is stronger both in WT and Ins2^{Akita} than in younger and older retinas. However, in order to conclude so, some form of quantification must be made (Fig. 3.23).

Overall, the results obtained suggest that aSyn is localized in the dopaminergic amacrine cells, that seem to be decreased in number with ageing. bSyn and gSyn were also localized in different neuronal populations, namely bipolar and horizontal cells, respectively.

3.3. Synaptic markers in the retina

A diabetic environment in the retina leads to a series of events that affect several pathways and the proteins involved. Therefore, the levels of markers of interest, that might be affected in the retina with ageing and diabetes, were assessed.

In the brain aSyn functions as a presynaptic protein that, in its native state, is involved in synaptic signaling and membrane trafficking (74). However, overexpression of aSyn, oligomerization and gain of toxicity might not only affect the homeostasis of several cellular organelles but also affect neurotransmitter synthesis and release, namely the normal function of the SNARE complex (82). Considering aSyn presynaptic location in the retina and the resemblance of Parkinson's and diabetic environment, synapse-associated proteins were analysed in order to evaluate the impact of diabetic retinopathy in synapses. The levels of SNAP-25, one of the proteins involved in the SNARE complex, were assessed (Fig. 3.24).

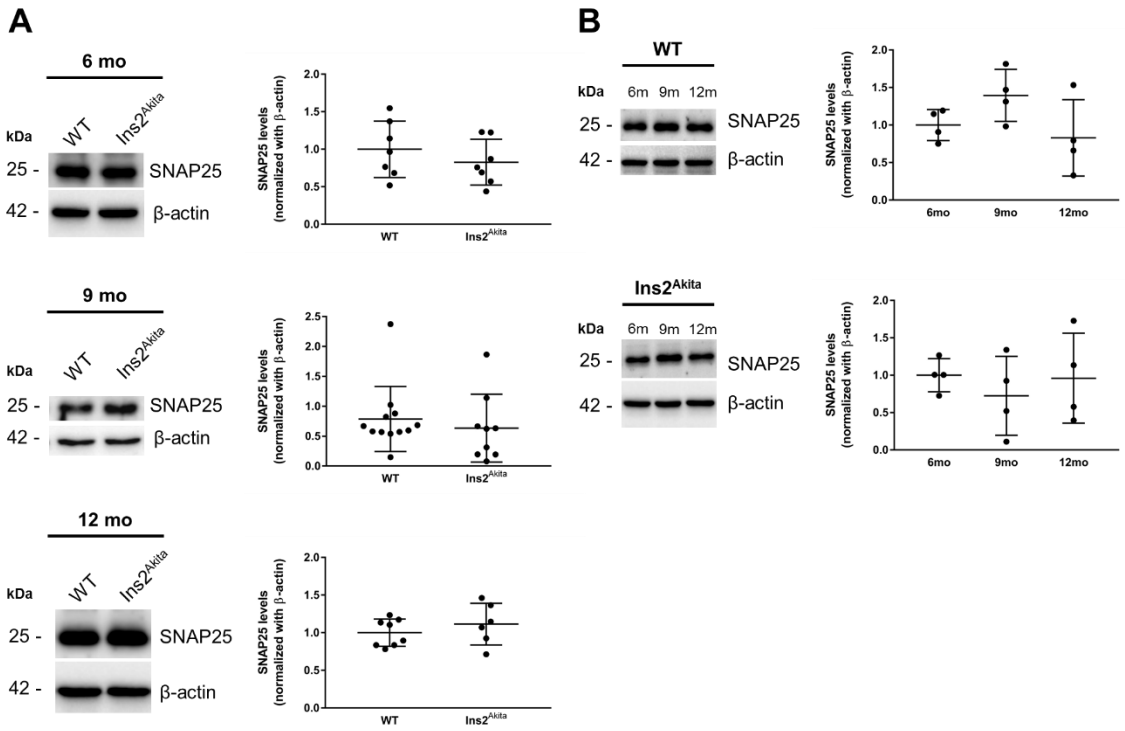

Fig. 3.24. Assessment of SNAP-25 levels in 6, 9 and 12-months old WT and Ins2^{Akita} protein extracts from whole retina. A) Western blot for the comparison of SNAP-25 protein levels between WT and Ins2^{Akita} mice of different ages (6, 9, and 12 months old). Data are presented as Mean ± SD. B) Western blot for the comparison of SNAP-25 protein levels between ages (6, 9 and 12-months old) in WT and Ins2^{Akita} mice. Data are presented as Mean ± SD.

SNAP-25 protein levels are similar between WT and Ins2^{Akita} samples of 6, 9 and 12-months old (Fig. 3.20 A). Considering ageing and disease progression, there are no differences between ages for both WT and Ins2^{Akita} samples (Fig. 3.24 B).

Rab3a is a synaptic vesicle-associated protein thought to play a crucial role in delivering synaptic vesicles to Ca^{2+}-dependent release sites (82,146). It not only indirectly collaborates with aSyn in order to facilitate neurotransmitter release but it also rescues aSyn toxicity by dissociating aSyn from the plasma membrane upon Rab3a GTPase activation allowing the normal functioning of synapse release (147). Rab3a levels were assessed by western blot (Fig. 3.25).

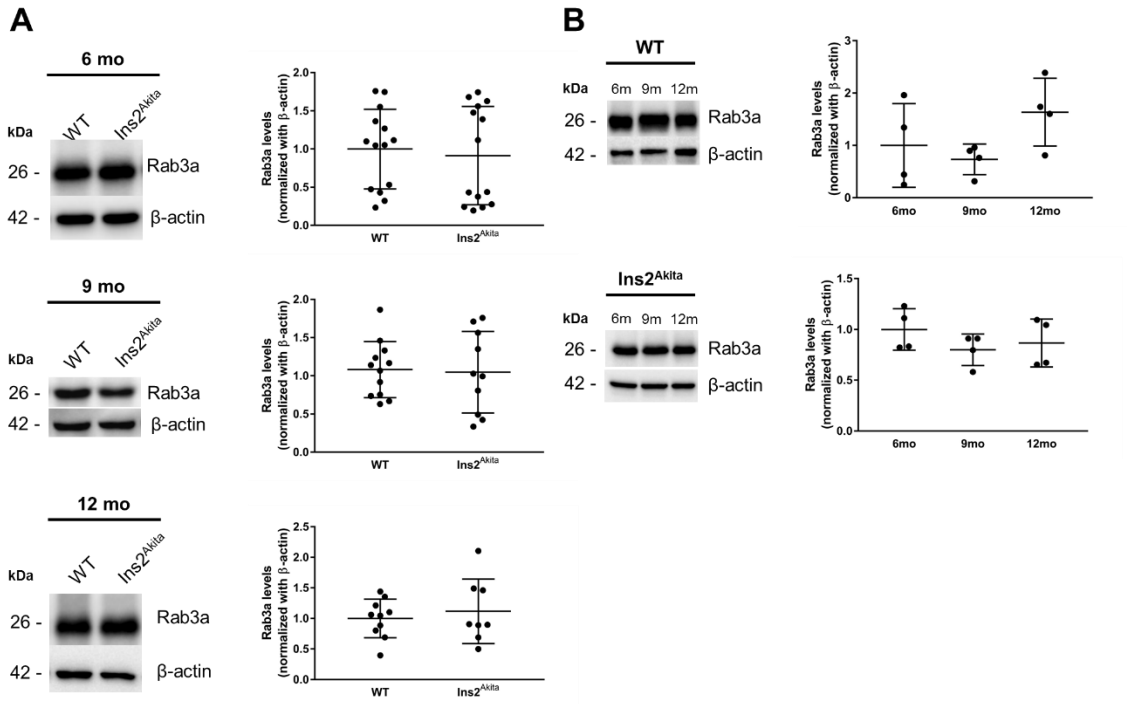

Fig. 3.25. Assessment of Rab3a levels in 6, 9 and 12-months old WT and Ins2^{Akita} protein extracts from whole retina. A) Western blot for the comparison of Rab3a protein levels between WT and Ins2^{Akita} mice of different ages (6, 9, and 12 months old). Data are presented as Mean ± SD. B) Western blot for the comparison of Rab3a protein levels between ages (6, 9 and 12-months old) in WT and Ins2^{Akita} mice. Data are presented as Mean ± SD.

Rab3a levels appear to be similar between WT and Ins2^{Akita} samples in all three ages (6, 9 and 12-months old). Interestingly, once again there seem to be two distinct groups of samples both in 6 months old WT and Ins2^{Akita} samples and the same for 9 and 12-months old Ins2^{Akita} samples (Fig. 3.25 A). With ageing, there are also no differences between ages for both WT and Ins2^{Akita} samples (Fig. 3.25 B).

The misfolding of aSyn into aggregates, resulting in toxic fibrils deposits, is thought to lead to neuroinflammation, neurodegeneration and cell death (79,80). In the retina, it is proposed that neurodegeneration occurs prior to the microvascular complication onset in DR, possibly due to aSyn toxicity. Caspases are proteolytic enzymes that are closely involved in the induction and execution phases of apoptosis. One of its members is Caspase 3, which is thought to act as an executioner of apoptosis after a longer duration of diabetes. In order to evaluate the level of cell death by apoptosis in healthy and diabetic animals, Caspase 3 levels were assessed (Fig. 3.26).

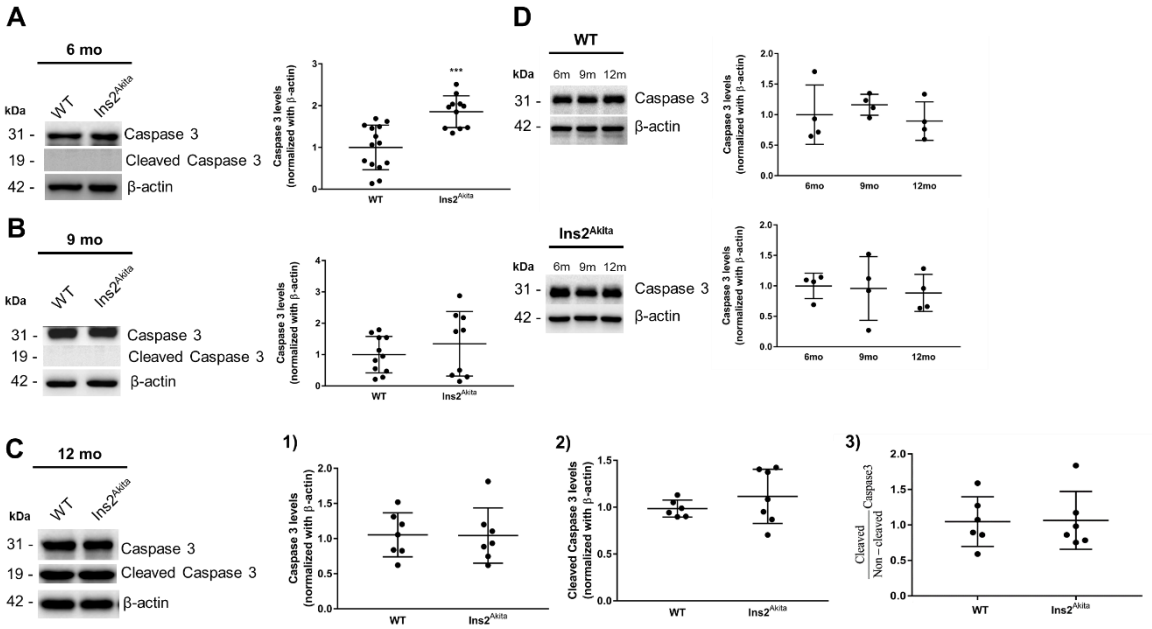

Fig. 3.26. Assessment of Caspase 3 levels in 6, 9 and 12-months old WT and Ins2^{Akita} protein extracts from whole retina. A) Western blot for the comparison of Caspase 3 protein levels between 6 months old WT and Ins2^{Akita} mice. Data are presented as Mean ± SD. **p<0.005 Ins2^{Akita} compared with WT; T-test. B) Western blot for the comparison of Caspase 3 protein levels between 9 months old WT and Ins2^{Akita} mice. Data are presented as Mean ± SD. C) Western blot for the comparison of 1) total Caspase protein levels 3, 2) Cleaved Caspase 3 protein levels and 3) the ratio cleaved/non-cleaved form of Caspase 3 protein levels, between 12 months old WT and Ins2^{Akita} mice. Data are presented as Mean ± SD. D) Western blot for the comparison of Caspase 3 protein levels between ages (6 and 9 and 12-months old) in WT and Ins2^{Akita} mice. Data are presented as Mean ± SD.

The assessment of Caspase 3 protein levels by western blot revealed that the non-cleaved form of this protein (31 kDa) is significantly higher in 6 months old Ins2^{Akita} samples (1.85 ± 0.36 vs 1 ± 0.51), showing a tendency to be similar between 9 and 12-months old WT and Ins2^{Akita} samples (Fig. 3.26 B and C). Moreover it is only by 12 months old that the cleaved and therefore active form of Caspase 3 is revealed (19kDa) showing no differences between WT and Ins2^{Akita} samples (Fig. 3.26 C). Further analysis was performed in order to understand the extension of the activation of Caspase 3 but no differences between WT and Ins2^{Akita} were seen (Fig. 3.26 C). Once again, 6 and 9-months old Ins2^{Akita} mice present two distinct groups with no explanation (Fig. 3.26 A and B). With ageing there seem to be no significant differences between WT samples and Ins2^{Akita} mice (Fig. 3.6 D). Overall, these results revealed that diabetes and ageing do not affect SNAP-25 and Rab3a levels but that diabetes increases the levels of non-cleaved Caspase 3 by 6 months old animals Ins2^{Akita} mice and to be cleaved by 12 months old although not showing differences between WT and Ins2^{Akita} animals.

4. Discussion and concluding remarks

Synucleins, and in particular aSyn, play a major pathological role in PD due to the formation of aggregates in brain tissues and consequent relation with neurodegeneration (148). Besides the brain, they are highly expressed in the retina (118) and play a role in vision since the triple knock out mice of the synucleins lead to age-dependent blindness (119). Furthermore, aSyn aggregation was found to occur in the retina in other neurodegenerative disease such as AD (120) and in aged retinas (121,123). However, the pathophysiological role of synucleins in the retina and its neurodegeneration is unexplored.

DR is the most common complication of diabetes and a leading cause of vision loss in working-age adults. Neurodegeneration is now recognized to precede vascular alterations and to occur in the early stages of DR (REF).

Several works point to a shared mechanism of neurodegeneration in PD and DR: diabetes is a risk factor for PD (149–151); aSyn is a target of glycation, a PTM potentiated by the increased levels of AGEs in diabetes which promotes aSyn toxicity and aggregation (152); a restoring dopamine drug used in PD, L-DOPA, was observed to rescue visual impairment in a DR mouse model (115); and the antidiabetic drug rosiglitazone was shown to have a neuroprotective effect on retinal and nigrostriatal neurons in a PD mouse model (116). Moreover, the environment of the diabetic eye - where it is known to occur oxidative stress, inflammation, increased levels of AGE and mitochondrial impairment - has remarkable similarities with the features that are known to be involved in aSyn aggregation in the brain of PD patients (73).

Accordingly, here we hypothesized if aSyn, bSyn and gSyn are involved in the pathological changes observed in neurodegeneration in the diabetic retina. To test our hypothesis we have performed a characterization of the distribution pattern of synucleins in a diabetic mouse model, the $Ins2^{Akita}$.

The $Ins2^{Akita}$ is a relatively recent mouse model for studying type 1 diabetic complications such as DR, that comprises signs of non-proliferative and early features of proliferative DR (126,129–131). These mice are characterized by significant hypoinsulinemia and hyperglycaemia after only 4 weeks of age as well as significantly less weight than controls (126), which was also observed in our mouse colony (Fig. 3.1 and 3.2, respectively). Furthermore these mice are described as developing diabetic neuropathy (126–128), showing an increase in cleaved Caspase 3 at an early age (126,132) and a significant thinning of the inner layers of the retina, namely the INL and IPL (133,134). Regarding the disadvantages of this model, the most critical one is the fact that the $Ins2^{Akita}$ mice do not completely mimic the outcomes of proliferative DR, limiting its usefulness to studies of initial stages of DR (126). Nevertheless, considering that neurodegeneration occurs at the very beginning of the disease, the $Ins2^{Akita}$ is a suitable model for evaluating the synucleins role in neurodegeneration in DR.

Regarding the results obtained, aSyn and bSyn were both localized in cell bodies of the GCL and INL but also in the IPL of 6, 9 and 12-months old WT and $Ins2^{Akita}$ retinas (Fig. 3.4 and 3.5).

Amacrine cells, the interneurons of the proximal retina that are divided in more than 30 subsets that communicate with different neurons using different neurotransmitters (53), are located in INL but also in cell bodies of the GCL, projecting their synapses in the IPL. Syntaxin 1A, a specific marker for amacrine cells and an important protein for neurotransmitter release considering its part in the SNARE complex (153–155), colocalized with aSyn and bSyn (Fig. 3.13 A and 3.14). Colocalization occurred in the IPL, in amacrine cell synapses, but also in the amacrine cell bodies of the INL, for 6, 9 and 12-months old WT and Ins2^{Akita}, and in cell bodies of the GCL for 9 and 12-months old Ins2^{Akita} retinas (Fig. 3.13 A and 3.14).

In the IPL, aSyn colocalization with Syntaxin 1A shows an age-associated effect, namely the increased percentage of Syntaxin 1A that colocalizes with aSyn at 9 months old animals, decreasing by 12 months old WT and Ins2^{Akita} mice (Fig. 3.13 B), which could reflect the existence of compensatory mechanisms. More interesting is the disease-associated alteration observed, namely the percentage of Syntaxin 1A that colocalizes with aSyn is increased in 9 months old Ins2^{Akita} mice when compared to controls. Overall, these results could indicate that in the 9 months old Ins2^{Akita} mice there are alterations in the synapses, which is compensated at 12 months of age. To better understand these results, further analysis will be needed, such as the evaluation of Syntaxin 1A and aSyn levels specifically in the IPL.

Interestingly, aSyn total levels are increased in the 12 months old Ins2^{Akita} mice (Fig. 3.9), while Syntaxin 1A levels are decreased in 6 and 9-month-old Ins2^{Akita} mice, as revealed by WB (Fig. 3.13 C). These results might suggest a compensatory mechanism that can be occurring in DR mice through ageing. In fact, a study using STZ model (156) as well as a study developed by Baptista and co-workers with Ins2^{Akita} mice (157), suggest that diabetes differentially affects the content of exocytotic proteins in hippocampal and retinal nerve terminals, showing that Syntaxin 1A is decreased in early stages of diabetes but tends to recover with ageing (156), as seen in our model.

Considering bSyn localization in amacrine cells, no quantifications were performed even though it would be important to do it in the future. Although less studied than aSyn, bSyn has already been reported to be involved in pathological roles, such as DLB. In DLB, mutations in the SNCB gene were found in DLB patients, raising the possibility that these alterations in the SNCB gene contribute to Lewy Body disorders (158). In yeast, bSyn was found to be toxic and to form cytosolic inclusions that are similar to those formed by aSyn, further sharing some of aSyn toxicity mechanisms, including vesicular trafficking impairment and induction of oxidative stress (104). In the brain, bSyn is not as prone to aggregate as aSyn due to the lack of a part of the Non-B-amyloid component (NAC) region (159) but studies suggest that, when exposed to toxins such as metal ions and pesticides, associated with increased ROS bioavailability, bSyn tends to fibrillate (103). In fact, increased rate of ROS generation and decline in cellular repair mechanisms will increase the oxidative stress, resulting in increased oxidized proteins that become more prone to aggregate and form fibrils (160). In the diabetic and aged retinas there seems to be iron overload that relates to increased ROS since iron can be reduced/oxidized (161). All of this considered, it is a possibility that in hostile conditions,

namely in diabetic or aged retinas, bSyn may become toxic and negatively affect these cells, leading to their impairment or even death.

Another interesting result is the colocalization of these two proteins in the IPL but also in cell bodies of both the GCL, where ganglion and amacrine cells are found, and in proximal INL, where mainly amacrine cells are found (Fig. 3.15 A). In fact, the colocalization between aSyn and bSyn might be very interesting considering two main outcomes: exacerbation or protection of aSyn toxicity by bSyn. In Tenreiro et al, when trying to investigate the cellular effects of aSyn and bSyn in yeast cells, the authors demonstrated that the cellular pathways that were affected by bSyn are similar to the ones that were affected by aSyn and demonstrated that increased expression of aSyn and bSyn followed by co-expression exacerbated cytotoxicity (104); moreover, heterodimers of aSyn and bSyn were observed to be formed in yeast and in mammalian cells (104); On the other hand, several studies suggested that increased bSyn expression has a protective effect against aSyn fibril toxicity. bSyn is thought to either compete with aSyn for binding sites at the surfaces of lipid vesicles and fibrils that otherwise would trigger the process of fibril formation, strongly supressing aSyn aggregation (162) or to directly bind aSyn creating stable nonpropagating heterodimers, similar to nonpropagating aSyn homodimers (163,164).

In the IPL, the percentage of aSyn that colocalizes with bSyn shows no significant differences between WT and $Ins2^{Akita}$ mice nor with ageing between animals (Fig. 3.15 B). On the other hand, in the GCL, it is significantly lower in aged retinas for both WT and $Ins2^{Akita}$ retinas (Fig. 3.15 C). In the INL, it significantly decreases in 6 months old $Ins2^{Akita}$ retinas, when compared to age-matched controls but to be significantly higher by 9 months old, being similar between WT and $Ins2^{Akita}$ by 12 months old (Fig. 3.15 D). By 12 months old, we might again be looking both at compensatory mechanisms but most likely at an effect of ageing itself rather than just diabetes.

Moreover, in the IPL, both aSyn and bSyn further colocalized with Synaptophysin, a presynaptic marker (Fig.3.11 A and 3.12). Our results are in agreement with published findings that placed these two synucleins in synapse-rich IPL of the retina (76,109,110). In the brain, aSyn and bSyn are located predominantly in the presynaptic terminals of neurons of the CNS and aSyn has been speculated to be involved in synaptic signaling and membrane trafficking (74), that might also be one of its roles in the retina, in healthy retinas. However, neither diabetes nor ageing seem to lead to changes in these proteins colocalization with synaptophysin.

Our findings in placing aSyn in amacrine cells are consistent with the ones reported by Martinez-Navarrete et al, that claim that aSyn was localized in the somata and dendrites of both GABAergic and glycinergic amacrine cells (110). A new and fascinating result is the localization of aSyn in the dopaminergic amacrine cells of 6, 9 and 12-months old mice (Fig. 3.17 A). As previously described, there are at least 30 known types of amacrine cells (56) of which the dopaminergic amacrine cells are of major importance. These cells produce and release dopamine cyclically, affecting all the major cell types of the outer and inner retinal layers (53,165). In our study, when comparing the number of dopaminergic amacrine cells between WT and $Ins2^{Akita}$ retinas of different ages, it is possible to infer that ageing by itself plays a greater role in the loss of dopaminergic cells than DR, considering that

the amount of these cells is significantly decreased in 12 months-old WT mice when comparing to younger control animals (Fig. 3.17 B). Also in 12 months old Ins2^{Akita} mice aSyn levels are significantly increased. In PD, toxic forms of aSyn are believed to bind to the inner mitochondrial membrane, where it associates with mitochondrial complex I, culminating in increased ROS production, Ca^{2+} levels, release of cytochrome c and activation of Caspase 3, leading to cell death (60–62,90,91). In diabetic as well as in aged retinas, several pathways are affected resulting in an excessive bioavailability of ROS (20), increased oxidative stress, damaging the mitochondria and releasing the apoptosis machinery (23,166). All of this considered, it is possible that aSyn might be playing a similar role in the retina with ageing, leading to dopaminergic amacrine cell death, if aSyn aggregation can be proved.

gSyn is so far localized by other authors in cultured bovine RPE cells and in rodent and human ganglion cells and has even been viewed as a marker of ganglion cells (112). A study further suggested that gSyn was essential for the viability of ganglion cells since the absence of gSyn leads to a decrease in ganglion cell survival (167). In the INL, gSyn was localized it in the horizontal cells (Fig. 3.23), interneurons between photoreceptor and bipolar cells (47,50), by colocalization with Calbindin, a marker for horizontal cells. Quantification analysis will be important to be performed in future studies. Nevertheless, no striking differences occur between WT and Ins2^{Akita} retinas nor with ageing. Also, gSyn protein levels were not possible to analyse due to technical difficulties associated with malfunctioning antibodies. If gSyn levels were proved to decrease with diabetes or with ageing, it would be possible that gSyn plays a similar effect on horizontal and ganglion cells as previously mentioned in the study developed by Surgucheva et al. (167), where gSyn was reported to be essential ganglion cell survival.

The colocalization between the synucleins was observed for both aSyn and bSyn and for aSyn and gSyn. aSyn and gSyn were found to colocalize in the GCL (Fig. 3.16). Although we have not quantified the amount of cell bodies that contain both proteins, it would be interesting to do so, in order to see if there are any differences between WT and Ins2^{Akita} retinas.

Altogether, these results suggest that specially aSyn and bSyn seem to be affected by DR and that DR leads to increased colocalization between these two synucleins in amacrine presynaptic terminals.

With neurodegeneration being one of our focus, apoptosis was evaluated by assessing the levels of Caspase 3, an effector of apoptosis. Our results showed that the non-cleaved and, therefore, non-activated form Caspase 3 was significantly increased in 6 months old Ins2^{Akita} mice being similar in between 9 and 12 months-old WT and Ins2^{Akita} mice. It was only by 12 months old animals that this protein was activated showing, however, not to be effected by DR (Fig. 3.26). These results do not reproduce what has been described in other studies performed in the Ins2^{Akita} mice and other models, such as the STZ, where DR led to increased Caspase 3 activation in early stages of the disease (31,126,168). There might be variations in the model itself, due to several aspects, namely differences in the conditions of the animal room related to temperature, illumination, number of animals per cage, microbiota, among others.

However, neurodegeneration is occurring in the retina of our DR mouse model, as the measurement of the thickness of the INL suggest that this layer, containing horizontal, bipolar and amacrine cells, is thinner in diabetic animals, when compared to controls (Fig. 3.3), as it was previously described (133,134).

The results obtained lead us to new questions regarding the usefulness of this model for DR studies. The main disadvantages when using these animals relied in the time needed to obtain aged diabetic animals (12 months old $Ins2^{Akita}$ mice) and the high variability between animals. Furthermore, the inconsistency between what is described to happen in this model and the actual outcomes obtained is a challenge. Still, taking in account the advantages and disadvantages that this model presents over other diabetes mice models such as the STZ mice, we still think that $Ins2^{Akita}$ might be a suitable model for this study. However, it would be interesting to see if the effects observed in these animals, also happen in other DR models as well as to evaluate further effects of DR in the retina, namely in the synucleins and their pathologic role.

Overall, the results here obtained provide a more accurate description of the synucleins distribution in the retina. aSyn and bSyn are in fact presynaptic proteins in the cells whose synapses compose the IPL of the retina. These two proteins are further localized in cell bodies of the GCL and in amacrine cells of the INL. DR seems to be increasing the colocalization of aSyn and bSyn. To understand if this reflects a functional or pathological role further studies will be needed.

Interestingly, aSyn is localized in a particular subset of amacrine cells, namely the dopaminergic amacrine cells, where, with ageing, this synuclein could be leading to dopaminergic amacrine cell death considering the significant decrease in these cells amount in aged retinas and the increased levels of aSyn in aged $Ins2^{Akita}$ mice.

Neurodegeneration, which is strongly suggested to occur by evaluation of the thickness of the INL and observation of a significant thinning of this layer in $Ins2^{Akita}$ mice of all ages, can be involving more neuronal populations rather than just amacrine cells. bSyn was observed in the IPL but also in the OPL of retinas and in bipolar cells by colocalization with PKC-α, a marker for bipolar cells. Lastly, gSyn was found mainly in cell bodies of the GCL but also in the INL and, more specifically, in horizontal cells. The detailed neuronal damage occurring in retinal neurodegeneration associated with diabetes remains ill-defined. Nevertheless, degeneration of retinal neurons was reported in amacrine and ganglion cells (33,34), and abnormalities reported in horizontal and bipolar synaptic terminals in rodent models (36,37). Even though the pathophysiological role of the synucleins in the retina and DR is almost unexplored, they seem to be somehow involved in several important processes in the retina. Interestingly, each synuclein is localized in a neuronal population previously described as being affected in DR.

Several of the results obtained are worth of further studies. One of the most promising results is the eventual degeneration of dopaminergic amacrine cells with ageing, in which aSyn could be involved. However, in order to prove so, aSyn aggregation and toxicity would have to be evaluated. The use of specific antibodies for aggregated aSyn, such as the 5G4 antibody, combined with Syntaxin 1A and the use of a positive control, namely a model for induced aggregated-aSyn such as

the Thy-1 mice (169) for testing the same antibody, could be a valuable analyses for this study. This strategy could also be used to evaluate aSyn aggregation in other neuronal populations. Evaluating the localization of bSyn and gSyn in dopaminergic amacrine cells would also be a valuable step. Moreover, other neuronal populations might be affected by DR or ageing, being of great interest understanding which cells are experiencing impairment or even decreased survival as well as understanding the role of the synucleins in such pathways. By evaluating the profile of apoptosis-related markers, such as pro-apoptotic protein Caspase 3 (170), anti-apoptotic proteins such as prohibitin (171), Bcl-2 and Bcl-xl (172,173) or even evaluating cell proliferation/cease by using markers such as ki-67 (174), are an idea.

aSyn and bSyn colocalization and localization in amacrine cells should also be dissected due to a possible negative synergy between both proteins. Both aSyn and bSyn represent a possible risk in DR considering their broad location on the retina and their aptitude to aggregate and become toxic in pathological conditions.

Also, considering the disease-associated effects on synapses observed for amacrine cells when there is an increased interaction with aSyn, a deeper evaluation of the changes occurring at these levels should be performed by synaptossomes. Moreover, it would be interesting to look for similar results in other rodent models, such as the STZ and Zucker mice. Other models, such as the Zebrafish, might also be a strategy. After diabetes induction by incubation with glucose, Zebrafish displayed defected retinal vessels as well as increased levels of VEGF but also signs of neurodegeneration by a significant thinning of the inner retinal layers (175–177). These animals are cheap to maintain, produce hundreds of offspring at weekly intervals, develop diabetes after only two days after induction and are transparent, which makes it possible to easily visualize any alterations in its interior, namely alterations in the blood vasculature (178).

Although the exact role of the synucleins in vision and in DR pathophysiology remains unclear, this work contributed to furthering the knowledge about the synucleins in the retina, by elucidating their special distribution in normal and diabetic retina. Additionally, we here provided insights on their potential contribution in ageing and DR.

5. References

1. WHO | Diabetes. WHO. World Health Organization; 2016.
2. Gangwani RA, Lian JX, McGhee SM, Wong D, Li KK. Diabetic retinopathy screening: global and local perspective. Hong Kong Med J = Xianggang yi xue za zhi. 2016;22(5):486–95.
3. Shi Y, Hu FB. The global implications of diabetes and cancer. Lancet. 2014; 383(9933):1947–8.
4. Deshpande AD, Harris-Hayes M, Schootman M. Epidemiology of Diabetes and Diabetes-Related Complications. Phys Ther. 2008; 88(11):1254–64.
5. Duh E. Diabetic Retinopathy .. Springer, editor. Human Press; 2008; 29-40 p.
6. Standards of Medical Care in Diabetes–2006. Diabetes Care. 2005.
7. Zhu CH, Zhang SS, Kong Y, Bi YF, Wang L, Zhang Q. Effects of intensive control of blood glucose and blood pressure on microvascular complications in patients with type II diabetes mellitus. Int J Ophthalmol. 2013;6(2):141–5.
8. Hu Y, Teng W, Liu L, Chen K, Liu L, Hua R, et al. Prevalence and risk factors of diabetes and diabetic retinopathy in Liaoning province, China: a population-based cross-sectional study. PLoS One. 2015;10(3):e0121477.
9. Pirart J. Diabetes mellitus and its degenerative complications: A prospective study of 4,400 patients observed between 1947 and 1973. Diabetes Care. 1978;1(4):252–63.
10. Frank RN. Diabetic Retinopathy. N Engl J Med. 2004 Jan 1;350(1):48–58.
11. Klein R, Klein BEK, Moss SE, Davis MD, DeMets DL. The Wisconsin Epidemiologic Study of Diabetic Retinopathy. Arch Ophthalmol. 1984 Apr 1;102(4):520.
12. Klein R, Klein BE, Moss SE, Davis MD, DeMets DL. The Wisconsin epidemiologic study of diabetic retinopathy. III. Prevalence and risk of diabetic retinopathy when age at diagnosis is 30 or more years. Arch Ophthalmol (Chicago, Ill 1960). 1984;102(4):527–32.
13. Mohamed Q, Gillies MC, Wong TY. Management of Diabetic Retinopathy. JAMA. 2007 Aug 22;298(8):902.
14. Wilkinson C., Ferris FL, Klein RE, Lee PP, Agardh CD, Davis M, et al. Proposed international clinical diabetic retinopathy and diabetic macular edema disease severity scales. Ophthalmology. 2003;110(9):1677–82.
15. Klein R, Klein BE, Moss SE, Cruickshanks KJ. The Wisconsin Epidemiologic Study of Diabetic Retinopathy. XV. The long-term incidence of macular edema. Ophthalmology. 1995 Jan;102(1):7–16.
16. Kowluru RA, Abbas SN. Diabetes-induced mitochondrial dysfunction in the retina. Invest Ophthalmol Vis Sci. 2003 Dec;44(12):5327–34.
17. Kowluru RA, Mishra M. Oxidative stress, mitochondrial damage and diabetic retinopathy. Biochim Biophys Acta - Mol Basis Dis. 2015;1852(11):2474–83.
18. Stitt AW. The role of advanced glycation in the pathogenesis of diabetic retinopathy. Exp Mol Pathol. 2003 Aug;75(1):95–108.
19. Geraldes P, Hiraoka-Yamamoto J, Matsumoto M, Clermont A, Leitges M, Marette A, et al. Activation of PKC-δ and SHP-1 by hyperglycemia causes vascular cell apoptosis and diabetic retinopathy. Nat Med. 2009;15(11):1298–306.
20. Kowluru RA, Chan P-S. Oxidative Stress and Diabetic Retinopathy. Exp Diabetes Res. 2007;43603.

21. CUTLER RG. Oxidative Stress Profiling: Part I. Its Potential Importance in the Optimization of Human Health. Ann N Y Acad Sci. 2005;1055(1):93–135.

22. Kowluru RA, Kowluru A, Veluthakal R, Mohammad G, Syed I, Santos JM, et al. TIAM1–RAC1 signalling axis-mediated activation of NADPH oxidase-2 initiates mitochondrial damage in the development of diabetic retinopathy. Diabetologia. 2014;57(5):1047–56.

23. Kanwar M, Chan P-S, Kern TS, Kowluru RA. Oxidative Damage in the Retinal Mitochondria of Diabetic Mice: Possible Protection by Superoxide Dismutase. Investig Opthalmology Vis Sci. 2007;48(8):3805.

24. Madsen-Bouterse SA, Zhong Q, Mohammad G, Ho Y-S, Kowluru RA. Oxidative damage of mitochondrial DNA in diabetes and its protection by manganese superoxide dismutase. Free Radic Res. 2010;44(3):313–21.

25. Engerman RL. Pathogenesis of diabetic retinopathy. Diabetes. 1989;38(10):1203–6.

26. Tian T, Li Z, Lu H. Common pathophysiology affecting diabetic retinopathy and Parkinson's disease. Med Hypotheses. 2015;85(4):397–8.

27. Ola MS, Nawaz MI, Khan HA, Alhomida AS. Neurodegeneration and neuroprotection in diabetic retinopathy. Int J Mol Sci. 2013;14(2):2559–72.

28. Kern TS, Du Y, Miller CM, Hatala DA, Levin LA. Overexpression of Bcl-2 in vascular endothelium inhibits the microvascular lesions of diabetic retinopathy. Am J Pathol. 2010;176(5):2550–8.

29. Kerr JF, Wyllie AH, Currie AR. Apoptosis: a basic biological phenomenon with wide-ranging implications in tissue kinetics. Br J Cancer. 1972;26(4):239–57.

30. Mohr S, Xi X, Tang J, Kern TS. Caspase Activation in Retinas of Diabetic and Galactosemic Mice and Diabetic Patients. Diabetes. 2002;51(4).

31. Martin PM, Roon P, Van Ells TK, Ganapathy V, Smith SB. Death of Retinal Neurons in Streptozotocin-Induced Diabetic Mice. Investig Opthalmology Vis Sci. 2004;45(9):3330.

32. Peng P-H, Lin H-S, Lin S. Nerve fibre layer thinning in patients with preclinical retinopathy. Can J Ophthalmol / J Can d'Ophtalmologie. 2009;44(4):417–22.

33. Barber AJ, Gardner TW, Abcouwer SF. The Significance of Vascular and Neural Apoptosis to the Pathology of Diabetic Retinopathy. Investig Opthalmology Vis Sci. 2011;52(2):1156.

34. Mouse A, Hombrebueno JR, Chen M, Penalva RG, Xu H. Loss of Synaptic Connectivity, Particularly in Second Order Neurons Is a Key Feature of Diabetic Retinal Neuropathy in the Ins2. 2014 .

35. Szabadfi K, Atlasz T, Kiss P, Reglodi D, Szabo A, Kovacs K, et al. Protective effects of the neuropeptide PACAP in diabetic retinopathy.

36. Park S-H, Park J-W, Park S-J, Kim K-Y, Chung J-W, Chun M-H, et al. Apoptotic death of photoreceptors in the streptozotocin-induced diabetic rat retina. Diabetologia .. 2003;46(9):1260–8.

37. Nadal-Nicolás FM, Sobrado-Calvo P, Jiménez-López M, Vidal-Sanz M, Agudo-Barriuso M. Long-Term Effect of Optic Nerve Axotomy on the Retinal Ganglion Cell Layer. Invest Ophthalmol Vis Sci. 2015;56(10):6095–112.

38. Feng Y, Wang Y, Li L, Wu L, Hoffmann S, Gretz N, et al. Gene Expression Profiling of Vasoregression in the Retina—Involvement of Microglial Cells. PLoS One. 2011;6(2).

39. Mizutani M, Kern TS, Lorenzi M. Accelerated death of retinal microvascular cells in human and experimental diabetic retinopathy. J Clin Invest. 1996 Jun 15;97(12):2883–90.

40. Fletcher EL, Phipps JA, Ward MM, Puthussery T, Wilkinson-Berka JL. Neuronal and glial

cell abnormality as predictors of progression of diabetic retinopathy. Curr Pharm Des. 2007;13(26):2699–712.

41. Early worsening of diabetic retinopathy in the Diabetes Control and Complications Trial. Arch Ophthalmol (Chicago, Ill 1960). 1998;116(7):874–86.

42. Group ETDRS. Photocoagulation for Diabetic Macular Edema. Arch Ophthalmol. 1985;103(12):1796.

43. Early vitrectomy for severe vitreous hemorrhage in diabetic retinopathy. Two-year results of a randomized trial. Diabetic Retinopathy Vitrectomy Study report 2. The Diabetic Retinopathy Vitrectomy Study Research Group. Arch Ophthalmol (Chicago, Ill 1960). 1985;103(11):1644–52.

44. Wassle H. Parallel processing in the mammalian retina. Nat Rev Neurosci. 2004;5:747–57.

45. Melloni BJ. How the retina works. Am Fam Physician. 1971;4(2):81.

46. Masland RH. Neuronal diversity in the retina. Curr Opin Neurobiol. 2001;11(4):431–6.

47. Kuffler SW. DISCHARGE PATTERNS AND FUNCTIONAL ORGANIZATION OF MAMMALIAN RETINA. J Neurophysiol. 1953;16(1).

48. Enroth-Cugell C, Robson JG. The contrast sensitivity of retinal ganglion cells of the cat. J Physiol. 1966;187(3):517–52.

49. Busskamp V, Duebel J, Balya D, Fradot M, Viney TJ, Siegert S, et al. Genetic Reactivation of Cone Photoreceptors Restores Visual Responses in Retinitis Pigmentosa. Science (80-). 2010 ;329(5990):413–7.

50. Hoon M, Okawa H, Della Santina L, Wong ROL. Functional architecture of the retina: Development and disease. Prog Retin Eye Res. 2014;42(i):44–84.

51. Dreosti E, Esposti F, Baden T, Lagnado L. In vivo evidence that retinal bipolar cells generate spikes modulated by light. Nat Neurosci. 2011;14(8):951–2.

52. Martemyanov KA, Sampath AP. The Transduction Cascade in Retinal ON-Bipolar Cells: Signal Processing and Disease. Annu Rev Vis Sci. 2017;3(1):annurev-vision-102016-061338.

53. Kolb H. Roles of Amacrine Cells .. Webvision: The Organization of the Retina and Visual System. University of Utah Health Sciences Center; 1995.

54. Zhang D-Q, Wong KY, Sollars PJ, Berson DM, Pickard GE, McMahon DG. Intraretinal signaling by ganglion cell photoreceptors to dopaminergic amacrine neurons. Proc Natl Acad Sci U S A. 2008;105(37):14181–6.

55. Enroth-Cugell C, Robson JG. The contrast sensitivity of retinal ganglion cells of the cat. J Physiol. 1966;187(3):517–52.

56. Kolb H. Roles of Amacrine Cells. Webvision Organ Retin Vis Syst. 2005;1–47.

57. Clague MJ, Rochin L. Parkinson's Disease: A Traffic Jam? Curr Biol. 2016;26(8):R332–4.

58. Kalia L V., Lang AE. Parkinson's disease. Lancet. 2015;386(9996):896–912.

59. Jenner P. Oxidative stress in Parkinson's disease. Ann Neurol. 2003;53(S3):S26–38.

60. Schapira AH. Mitochondria in the aetiology and pathogenesis of Parkinson's disease. Lancet Neurol. 2008;7(1):97–109.

61. Höglinger GU, Carrard G, Michel PP, Medja F, Lombès A, Ruberg M, et al. Dysfunction of mitochondrial complex I and the proteasome: interactions between two biochemical deficits in a cellular model of Parkinson's disease. J Neurochem. 2003;86(5):1297–307.

62. Danzer KM, Haasen D, Karow AR, Moussaud S, Habeck M, Giese A, et al. Different Species of -Synuclein Oligomers Induce Calcium Influx and Seeding. J Neurosci. 2007;27(34):9220–32.

63. Chaudhuri KR, Schapira AH. Non-motor symptoms of Parkinson's disease: dopaminergic pathophysiology and treatment. Lancet Neurol. 2009;8(5):464–74.

64. Thomas B, Beal MF. Parkinson's disease.

65. Armstrong RA. Visual signs and symptoms of Parkinson's disease. Clin Exp Optom. 2008;91(2):129–38.

66. Armstrong RA. Visual Symptoms in Parkinson's Disease. Parkinsons Dis. 2011;2011:1–9.

67. Dacey DM. Dopamine-accumulating retinal neurons revealed by in vitro fluorescence display a unique morphology. Science. 1988;240(4856):1196–8.

68. Gastinger MJ, Singh RSJ, Barber AJ. Loss of cholinergic and dopaminergic amacrine cells in streptozotocin- diabetic rat and Ins2Akita-diabetic mouse retinas. Investig Ophthalmol Vis Sci. 2006;47(7):3143–50.

69. Vancura P, Wolloscheck T, Baba K, Tosini G, Iuvone PM, Spessert R. Circadian and dopaminergic regulation of fatty acid oxidation pathway genes in retina and photoreceptor cells. PLoS One. 2016;11(10):1–17.

70. Basso MA, Pokorny JJ, Liu P. Activity of substantia nigra pars reticulata neurons during smooth pursuit eye movements in monkeys. Eur J Neurosci. 2005;22(2):448–64.

71. Lavedan C. The synuclein family. Genome Res. 1998;8(9):871–80.

72. Kahle PJ, Haass C, Kretzschmar HA, Neumann M. Structure/function of α-synuclein in health and disease: Rational development of animal models for Parkinson's and related diseases. J Neurochem. 2002;82(3):449–57.

73. Lashuel HA, Overk CR, Oueslati A, Masliah E. The many faces of α-synuclein: from structure and toxicity to therapeutic target. Nat Rev Neurosci. 2013 J;14(1):38–48.

74. Fusco G, Pape T, Stephens AD, Mahou P, Costa AR, Kaminski CF, et al. Structural basis of synaptic vesicle assembly promoted by α-synuclein. Nat Commun. 2016;7:12563.

75. Burré J, Sharma M, Tsetsenis T, Buchman V, Etherton MR, Südhof TC. Alpha-synuclein promotes SNARE-complex assembly in vivo and in vitro. Science. 2010 24;329(5999):1663–7.

76. Surguchov A, Palazzo RE, Surgucheva I. Gamma synuclein: subcellular localization in neuronal and non-neuronal cells and effect on signal transduction. Cell Motil Cytoskeleton. 2001;49(4):218–28.

77. Vargas KJ, Makani S, Davis T, Westphal CH, Castillo PE, Chandra SS. Synucleins Regulate the Kinetics of Synaptic Vesicle Endocytosis. J Neurosci. 2014;34(28):9364–76.

78. Conway KA, Lee SJ, Rochet JC, Ding TT, Williamson RE, Lansbury PT, et al. Acceleration of oligomerization, not fibrillization, is a shared property of both alpha-synuclein mutations linked to early-onset Parkinson's disease: implications for pathogenesis and therapy. Proc Natl Acad Sci U S A. 2000;97(2):571–6.

79. Mukaetova-Ladinska EB, McKeith IG. Pathophysiology of synuclein aggregation in Lewy body disease. Mech Ageing Dev. 2006;127(2):188–202.

80. Review N, Death C, Naturally a S, Mechanism O, The IN, Of D, et al. Mechanisms of Neurodegenerative Disorders. 2010;57:8–11.

81. Scott D, Roy S. Alpha-synuclein inhibits inter-synaptic vesicle mobility and maintains recycling-pool homeostasis.

82. Chen RHC, Wislet-Gendebien S, Samuel F, Visanji NP, Zhang G, Marsilio D, et al. ??-Synuclein membrane association is regulated by the Rab3a recycling machinery and presynaptic activity. J Biol Chem. 2013;288(11):7438–49.

83. Abeliovich A, Schmitz Y, Fariñas I, Choi-Lundberg D, Ho WH, Castillo PE, et al. Mice lacking alpha-synuclein display functional deficits in the nigrostriatal dopamine system. Neuron. 2000 Jan;25(1):239–52.

84. Kumer SC, Vrana KE. Intricate regulation of tyrosine hydroxylase activity and gene expression. J Neurochem. 1996 Aug;67(2):443–62.

85. Perez RG, Waymire JC, Lin E, Liu JJ, Guo F, Zigmond MJ. A Role for a-Synuclein in the Regulation of Dopamine Biosynthesis. J Neurosci. 2002;22(8):3090–9.

86. Dehay B, Bourdenx M, Gorry P, Przedborski S, Vila M, Hunot S, et al. Targeting α-synuclein for treatment of Parkinson's disease: mechanistic and therapeutic considerations. Lancet Neurol. 2015;14(8):855–66.

87. Perier C, Vila M. Mitochondrial Biology and Parkinson's Disease.

88. Sharma LK, Lu J, Bai Y. Mitochondrial respiratory complex I: structure, function and implication in human diseases. Curr Med Chem. 2009;16(10):1266–77.

89. Turrens JF. Mitochondrial formation of reactive oxygen species. J Physiol. 2003 Oct 15;552(Pt 2):335–44.

90. Luth ES, Stavrovskaya IG, Bartels T, Kristal BS, Selkoe DJ. Soluble, Prefibrillar α-Synuclein Oligomers Promote Complex I-dependent, Ca^{2+} -induced Mitochondrial Dysfunction. J Biol Chem. 2014;289(31):21490–507.

91. Winklhofer KF, Haass C. Mitochondrial dysfunction in Parkinson's disease. Biochim Biophys Acta - Mol Basis Dis. 2010;1802(1):29–44.

92. Villacé P, Mella RM, Kortazar D. Mitochondria in the context of Parkinson's disease. Neural Regen Res. 2017 Feb;12(2):214–5.

93. Chinta SJ, Mallajosyula JK, Rane A, Andersen JK. Mitochondrial alpha-synuclein accumulation impairs complex I function in dopaminergic neurons and results in increased mitophagy in vivo. Neurosci Lett. 2011;486(3):235–9.

94. Choubey V, Safiulina D, Vaarmann A, Cagalinec M, Wareski P, Kuum M, et al. Mutant A53T a -Synuclein Induces Neuronal Death by Increasing Mitochondrial Autophagy. J Biol Chem. 2011;286(12):10814–24.

95. Paxinou E, Chen Q, Weisse M, Giasson BI, Norris EH, Rueter SM, et al. Induction of a-Synuclein Aggregation by Intracellular Nitrative Insult. J Neurosci. 2001;21(20):8053–61.

96. Paillusson S, Gomez P, Radu S, Daniel S, Paul L, Devine MJ, et al. α-Synuclein binds to the ER – mitochondria tethering protein VAPB to disrupt Ca2+ homeostasis and mitochondrial ATP production. Acta Neuropathol. 2017;134(1):129–49.

97. Guardia-Laguarta C, Area-gomez E, Schon EA, Przedborski S. A New Role for a -Synuclein in Parkinson ' s Disease : Alteration of ER – Mitochondrial Communication. Mov Disord. 2015;30(8):1026–33.

98. Smith WW, Jiang H, Pei Z, Tanaka Y, Morita H, Sawa A, et al. Endoplasmic reticulum stress and mitochondrial cell death pathways mediate A53T mutant alpha-synuclein-induced toxicity. Hum Mol Genet. 2005;14(24):3801–11.

99. Cooper AA, Gitler AD, Cashikar A, Haynes CM, Hill KJ, Bhullar B, et al. α-Synuclein Blocks ER-Golgi Traffic and Rab1 Rescues Neuron Loss in Parkinson's Models. Science (80). 2006;313(5785):324–8.

100. Hayashida K, Oyanagi S, Mizutani Y, Yokochi M. An early cytoplasmic change before Lewy body maturation: an ultrastructural study of the substantia nigra from an autopsy case of juvenile parkinsonism. Acta Neuropathol. 1993;85(4):445–8.

101. Watanabe I, Vachal E, Tomita T. Dense core vesicles around the Lewy body in incidental Parkinson's disease: an electron microscopic study. Acta Neuropathol. 1977;39(2):173–5.

102. Ebrahimi-Fakhari D, Cantuti-Castelvetri I, Fan Z, Rockenstein E, Masliah E, Hyman BT, et al. Distinct Roles In Vivo for the Ubiquitin-Proteasome System and the Autophagy-Lysosomal Pathway in the Degradation of -Synuclein. J Neurosci. 2011;31(41):14508–20.

103. Taschenberger G, Toloe J, Tereshchenko J, Akerboom J, Wales P, Benz R, et al. β-synuclein aggregates and induces neurodegeneration in dopaminergic neurons. Ann Neurol. 2013;74(1):109–18.

104. Tenreiro S, Rosado-Ramos R, Gerhardt E, Favretto F, Magalhães F, Popova B, et al. Yeast reveals similar molecular mechanisms underlying alpha- and beta-synuclein toxicity. Hum Mol Genet. 2016;25(2):275–90.

105. Ji H, Liu YE, Jia T, Wang M, Liu J, Xiao G, et al. Identification of a breast cancer-specific gene, BCSG1, by direct differential cDNA sequencing. Cancer Res. 1997;57(4):759–64.

106. Surgucheva I, McMahan B, Ahmed F, Tomarev S, Wax MB, Surguchov A. Synucleins in glaucoma: implication of gamma-synuclein in glaucomatous alterations in the optic nerve. J Neurosci Res. 2002;68(1):97–106.

107. Jia T, Liu YE, Liu J, Shi YE. Stimulation of breast cancer invasion and metastasis by synuclein gamma. Cancer Res. 1999;59(3):742–7.

108. Wales P, Pinho R, Diana FL. Limelight on Alpha-Synuclein : Pathological and Mechanistic Implications in Neurodegeneration. 2013;3:415–59.

109. Surguchov A, McMahan B, Masliah E, Surgucheva I. Synucleins in ocular tissues. J Neurosci Res. 2001;65(1):68–77.

110. Martínez-Navarrete GC, Martín-Nieto J, Esteve-Rudd J, Angulo A, Cuenca N. Alpha synuclein gene expression profile in the retina of vertebrates. Mol Vis. 2007;13:949–61.

111. Wiedenmann B, Franke WW. Identification and localization of synaptophysin, an integral membrane glycoprotein of Mr 38,000 characteristic of presynaptic vesicles. Cell. 1985;41(3):1017–28.

112. Surgucheva I, Weisman AD, Goldberg JL, Shnyra A, Surguchov A. Gamma-synuclein as a marker of retinal ganglion cells. Mol Vis. 2008;14:1540–8.

113. Jackson GR, Barber AJ. Visual Dysfunction Associated with Diabetic Retinopathy. Curr Diab Rep. 2010;10(5):380–4.

114. Witkovsky P. Dopamine and retinal function. Doc Ophthalmol. 2004;108(1):17–40.

115. Aung MH, Park HN, Han MK, Obertone TS, Abey J, Aseem F, et al. Dopamine deficiency contributes to early visual dysfunction in a rodent model of type 1 diabetes. J Neurosci .. 2014;34(3):726–36.

116. Normando EM, Davis BM, de Groef L, Nizari S, Turner LA, Ravindran N, et al. The retina as an early biomarker of neurodegeneration in a rotenone-induced model of Parkinson's disease: evidence for a neuroprotective effect of rosiglitazone in the eye and brain. Acta Neuropathol Commun. 2016;1–15.

117. Vicente Miranda H, Szegő ÉM, Oliveira LMA, Breda C, Darendelioglu E, de Oliveira RM, et al. Glycation potentiates α-synuclein-associated neurodegeneration in synucleinopathies. Brain. 2017;140(5):1399–419.

118. Surguchov A, McMahan B, Masliah E, Surgucheva I. Synucleins in ocular tissues. J Neurosci Res. 2001;65(1):68–77.

119. Greten-harrison B, Polydoro M, Morimoto-tomita M, Diao L, Williams AM. αβγ -Synuclein triple knockout mice reveal age-dependent neuronal dysfunction. 2010;107(45):19573–8.

120. Hashimoto M, Masliah E. Alpha-synuclein in Lewy body disease and Alzheimer's disease. Brain Pathol. 1999;9(4):707–20.

121. Leger F, Fernagut P-O, Canron M-H, Léoni S, Vital C, Tison F, et al. Protein aggregation in the aging retina. J Neuropathol Exp Neurol. 2011;70(1):63–8.

122. Lippa CF, Fujiwara H, Mann DM, Giasson B, Baba M, Schmidt ML, et al. Lewy bodies contain altered alpha-synuclein in brains of many familial Alzheimer's disease patients with mutations in presenilin and amyloid precursor protein genes. Am J Pathol. 1998;153(5):1365–70.

123. Shringarpure R, Davies KJA. Protein turnover by the proteasome in aging and disease. Free Radic Biol Med. 2002;32(11):1084–9.

124. Szkudelski T. The Mechanism of Alloxan and Streptozotocin Action in B Cells of the Rat Pancreas. Physiol Res. 2001;50:536–46.

125. Wang J, Takeuchi T, Tanaka S, Kubo SK, Kayo T, Lu D, et al. A mutation in the insulin 2 gene induces diabetes with severe pancreatic beta-cell dysfunction in the Mody mouse. J Clin Invest. 1999;103(1):27–37.

126. Barber AJ, Antonetti DA, Kern TS, Reiter CEN, Soans RS, Krady JK, et al. The Ins2 Akita Mouse as a Model of Early Retinal Complications in Diabetes. 2016;2210–8.

127. Schmidt RE, Green KG, Snipes LL, Feng D. Neuritic dystrophy and neuronopathy in Akita (Ins2(Akita)) diabetic mouse sympathetic ganglia. Exp Neurol. 2009;216(1):207–18.

128. Yaguchi M, Nagashima K, Izumi T, Okamoto K. Neuropathological study of C57BL/6Akita mouse, type 2 diabetic model: Enhanced expression of alphaB-crystallin in oligodendrocytes. Neuropathology. 2003;23(1):44–50.

129. Han Z, Guo J, Conley SM, Naash MI. Retinal Angiogenesis in the Ins2 Akita Mouse Model of Diabetic Retinopathy. 2012;574–84.

130. Akimov NP, Rentería RC. Spatial frequency threshold and contrast sensitivity of an optomotor behavior are impaired in the Ins2Akita mouse model of diabetes. Behav Brain Res. 2012;226(2):601–5.

131. Wright WS, Yadav AS, McElhatten RM, Harris NR. Retinal blood flow abnormalities following six months of hyperglycemia in the Ins2(Akita) mouse. Exp Eye Res. 2012;98(1):9–15.

132. Asnaghi V, Gerhardinger C, Hoehn T, Adeboje A, Lorenzi M. A role for the polyol pathway in the early neuroretinal apoptosis and glial changes induced by diabetes in the rat. Diabetes. 2003;52(2):506–11.

133. Barber AJ, Lieth E, Khin SA, Antonetti DA, Buchanan AG, Gardner TW. Neural apoptosis in the retina during experimental and human diabetes. Early onset and effect of insulin. J Clin Invest. 1998;102(4):783–91.

134. Cellerino A, Bahr M, Isenmann S. Apoptosis in the developing visual system. Cell Tissue Res. 2000;301(1):53–69.

135. Rasband WS. ImageJ. U.S. National Insitutes of Health, Bethesda, Maryland, USA. 1997.

136. Wiedenmann B, Franke WW. Identification and Localization of Synaptophysin, an Integral Membrane Glycoprote,n of Mr 38,000 Characteristic of Presynaptic Vesicles. Cell.

1985;41:1017–28.

137. Tarsa L, Goda Y. Synaptophysin regulates activity-dependent synapse formation in cultured hippocampal neurons. Proc Natl Acad Sci. 2002;99(2):1012–6.

138. Spiwoks-Becker I, Vollrath L, Seeliger MW, Jaissle G, Eshkind LG, Leube RE. Synaptic vesicle alterations in rod photoreceptors of synaptophysin-deficient mice. Neuroscience. 2001;107(1):127–42.

139. Eshkind LG, Leube RE. Mice lacking synaptophysin reproduce and form typical synaptic vesicles. Cell Tissue Res. 1995;282(3):423–33.

140. Cameron PL, Südhof TC, Jahn R, De Camilli P. Colocalization of synaptophysin with transferrin receptors: implications for synaptic vesicle biogenesis. J Cell Biol. 1991;115(1):151–64.

141. Gordon SL, Cousin MA. The Sybtraps: control of synaptobrevin traffic by synaptophysin, α-synuclein and AP-180. Traffic. 2014;15(3):245–54.

142. Liang B, Kiessling V, Tamm LK. Prefusion structure of syntaxin-1A suggests pathway for folding into neuronal trans-SNARE complex fusion intermediate. Proc Natl Acad Sci. 2013;110(48):19384–9.

143. Kalia L V, Lang AE, Shulman G. Parkinson ' s disease. Lancet. 2015;386(9996):896–912.

144. Ruether K, Feigenspan A, Pirngruber J, Leitges M, Baehr W, Strauss O. PKCα Is Essential for the Proper Activation and Termination of Rod Bipolar Cell Response. Investig Opthalmology Vis Sci. 2010;51(11):6051.

145. Mitchell CK, Rowe-Rendleman CL, Ashraf S, Redburn DA. Calbindin immunoreactivity of horizontal cells in the developing rabbit retina. Exp Eye Res. 1995;61(6):691–8.

146. Schlüter OM, Basu J, Südhof TC, Rosenmund C. Rab3 Superprimes Synaptic Vesicles for Release: Implications for Short-Term Synaptic Plasticity.

147. Dalfó E, Barrachina M, Rosa JL, Ambrosio S, Ferrer I. Abnormal α-synuclein interactions with rab3a and rabphilin in diffuse Lewy body disease. Neurobiol Dis. 2004;16(1):92–7.

148. Vargas KJ, Schrod N, Davis T, Laugks U, Lucic V, Chandra SS, et al. Synucleins Have Multiple Effects on Presynaptic Article Synucleins Have Multiple Effects on Presynaptic Architecture. CellReports. 2017;18(1):161–73.

149. Santiago JA, Potashkin JA. Shared dysregulated pathways lead to Parkinson's disease and diabetes. Trends Mol Med. 2013;19(3):176–86.

150. Xu Q, Park Y, Huang X, Hollenbeck A, Blair A, Schatzkin A, et al. Diabetes and risk of Parkinson's disease. Diabetes Care. 2011;34(4):910–5.

151. Schernhammer E, Hansen J, Rugbjerg K, Wermuth L, Ritz B. Diabetes and the risk of developing Parkinson's disease in Denmark. Diabetes Care. 2011;34(5):1102–8.

152. Vicente Miranda H, Szego ÉM, Oliveira LMA, Breda C, Darendelioglu E, De Oliveira RM, et al. Glycation potentiates α-synuclein-associated neurodegeneration in synucleinopathies. Brain. 2017;140(5):1399–419.

153. Burre J, Sharma M, Tsetsenis T, Buchman V, Etherton MR, Sudhof TC. a -Synuclein Promotes SNARE-Complex Assembly in Vivo and in Vitro. Science (80-).2010;329(5999):1663–7.

154. Shin OH. Exocytosis and synaptic vesicle function. Compr Physiol. 2014;4(1):149–75.

155. Burré J, Sharma M, Südhof TC. α-Synuclein assembles into higher-order multimers upon membrane binding to promote SNARE complex formation. Proc Natl Acad Sci .. 2014;111(40):E4274–83.

156. Gaspar JM, Baptista FI, Galvão J, Castilho ÁF, Cunha RA, Ambrósio AF. Diabetes differentially affects the content of exocytotic proteins in hippocampal and retinal nerve terminals. Neuroscience. 2010;169(4):1589–600.

157. Caba FI. Impact of diabetes on exocytosis / neurotransmitter release in the retina. 2012;

158. Ohtake H, Limprasert P, Fan Y, Onodera O, Kakita A, Takahashi H, et al. β-Synuclein gene alterations in dementia with Lewy bodies. 2007;63(5):805–11.

159. Yamin G, Munishkina LA, Karymov MA, Lyubchenko YL, Uversky VN, Fink AL. Forcing Nonamyloidogenic β-Synuclein To Fibrillate. Biochemistry. 2005;44(25):9096–107.

160. Squier TC. Oxidative stress and protein aggregation during biological aging. Exp Gerontol. 2001; 36(9):1539–50.

161. Ciudin A, Hernández C, Simó R. Iron Overload in Diabetic Retinopathy: A Cause or a Consequence of Impaired Mechanisms? Exp Diabetes Res. 2010;2010:1–8.

162. Brown JWP, Buell AK, Michaels TCT, Meisl G, Carozza J, Flagmeier P, et al. β-Synuclein suppresses both the initiation and amplification steps of α-synuclein aggregation via competitive binding to surfaces. Sci Rep. 2016;6(1):36010.

163. Tsigelny IF, Bar-On P, Sharikov Y, Crews L, Hashimoto M, Miller MA, et al. Dynamics of α-synuclein aggregation and inhibition of pore-like oligomer development by β-synuclein. FEBS J. 2007;274(7):1862–77.

164. Shaltiel-Karyo R, Frenkel-Pinter M, Egoz-Matia N, Frydman-Marom A, Shalev DE, Segal D, et al. Inhibiting α-synuclein oligomerization by stable cell-penetrating β-synuclein fragments recovers phenotype of parkinson's disease model flies. PLoS One. 2010;5(11).

165. Gastinger MJ, Singh RSJ, Barber AJ. Loss of Cholinergic and Dopaminergic Amacrine Cells in Streptozotocin-Diabetic Rat and Ins2 Akita -Diabetic Mouse Retinas. 2016;47(7).

166. Cui H, Kong Y, Zhang H. Oxidative stress, mitochondrial dysfunction, and aging. J Signal Transduct. 2012;2012:646354.

167. Surgucheva I, Shestopalov VI, Surguchov A. Effect of g-synuclein silencing on apoptotic pathways in retinal ganglion cells. J Biol Chem. 2008;283(52):36377–85.

168. Yang J-H, Guo Z, Zhang T, Meng XX, Sun T, Wu J. STZ treatment induced apoptosis of retinal cells and effect of up-regulation of calcitonin gene related peptide in rats. J Diabetes Complications. 2013;27(6):531–7.

169. Chesselet M-F, Richter F, Zhu C, Magen I, Watson MB, Subramaniam SR. A progressive mouse model of Parkinson's disease: the Thy1-aSyn ("Line 61") mice. Neurotherapeutics. 2012;9(2):297–314.

170. Martin PM, Roon P, Van Ells TK, Ganapathy V, Smith SB. Death of Retinal Neurons in Streptozotocin-Induced Diabetic Mice. Investig Opthalmology Vis Sci. 2004 Sep 1;45(9):3330.

171. Jin W. New Biomarkers in the Retina and RPE Under Oxidative Stress. In: Ocular Diseases . InTech; 2012.

172. Park H-A, Licznerski P, Alavian KN, Shanabrough M, Jonas EA. Bcl-xL Is Necessary for Neurite Outgrowth in Hippocampal Neurons. Antioxid Redox Signal. 2015 Jan 10;22(2):93–108.

173. J. Yang, X. Liu, C. N. Kim, J. Cai, D. P. Jones, X. Wang. Prevention of Apoptosis by Bcl-2: Release of Cytochrome c from Mitochondria Blocked. Science (80-). 1997;275.

174. Kohno H, Sakai T, Kitahara K. Induction of nestin, Ki-67, and cyclin D1 expression in Müller cells after laser injury in adult rat retina. Graefe's Arch Clin Exp Ophthalmol . 2006

28;244(1):90–5.

175. Jung S-H, Kim YS, Lee Y-R, Kim JS. High glucose-induced changes in hyaloid-retinal vessels during early ocular development of zebrafish: a short-term animal model of diabetic retinopathy. Br J Pharmacol. 2016;173(1):15–26.

176. Carnovali M, Luzi L, Banfi G, Mariotti M. Chronic hyperglycemia affects bone metabolism in adult zebrafish scale model. Endocrine. 2016;54(3):808–17.

177. Gleeson M, Connaughton V, Arneson LS. Induction of hyperglycaemia in zebrafish (Danio rerio) leads to morphological changes in the retina. Acta Diabetol. 2007;44(3):157–63.

178. Jörgens K, Stoll SJ, Pohl J, Fleming TH, Sticht C, Nawroth PP, et al. High Tissue Glucose Alters Intersomitic Blood Vessels in Zebrafish via Methylglyoxal Targeting the VEGF Receptor Signaling Cascade. Diabetes. 2015;64(1):213–25.